

CHEMISTRY AND KINETICS OF THE HYDRO-DESULFURIZATION OF COAL

Marvin L. Vestal and William H. Johnston

Scientific Research Instruments Corporation, Baltimore

INTRODUCTION

Most of the published data on the hydro-desulfurization of coal are unsuitable for detailed kinetic interpretation because equilibrium conditions were partially or wholly achieved. Forty years ago Snow (1) showed almost ten-fold less desulfurization with "fast" heating versus "slow" heating. The present paper describes the theoretical extension and experimental application of the non-isothermal method of Juntgen (2) to the hydro-desulfurization of ten bituminous coals ranging from 1 to 5% sulfur.

This powerful method overcomes the above difficulty by treating temperature as a controlled variable. Essentially continuous measurements of reaction products in a flow system provide experimental functions whose theoretical interpretations identify sets of chemical reactions which are responsible for desulfurization. The kinetics of desulfurization of all ten coals are accounted for satisfactorily by five chemical reaction systems. This method gives activation energies and frequency factors for each chemical reaction.

Independent or idealized experiments were also conducted to test separately these results. In addition, the kinetics of a series of back reactions were also measured including the scavenging of hydrogen sulfide by calcium oxide. In this paper, the theory is summarized, the experimental conditions are described, and the results are summarized, together with a discussion of their significance to processes for control of environmental pollution.

THEORY

The non-isothermal kinetic method circumvents the uncontrolled occurrence of chemical reactions during the time that a sample is being heated to a desired isothermal reaction temperature. This is accomplished by maintaining a constant rate of heat during the experiment. Consider a solid gas reaction in a flow system which produces a new gas as a reaction product. Under the conditions of a constant heating rate of M degrees per minute the usual Arrhenius equations, $k = k_0 \exp(-E/RT)$, can be expressed in terms of the temperature rate of evolution of the new product gas, dV/dT , and the total volume of product gas when the reaction has gone to completion, V_0 .

$$\frac{dV}{dT} = \frac{V_0 k_0}{M} \exp \left\{ - \left[\frac{E}{RT} + \frac{k_0 RT^2}{ME} \right] \right\} \quad (1)$$

where R is the usual gas constant T is the absolute temperature.

The graphical expression of this function of Equation (1) is shown in Figure 1. Three important experimental parameters are obtained from this function, the integral of evolved gas V_0 which is shown as the cross-hatch area under the graph, the temperature of the maximum T_0 , and the temperature rate of evolution of the product chemical at the temperature maximum, $(dV/dT)_{T_0}$. In order to solve this equation for the activation energy, E , and the frequency factor, k_0 , it is convenient to introduce two dimensionless parameters,

$$a = E/RT_0 \text{ and } b = T_0/V_0 (dV/dT)_{T_0} \quad (2)$$

when these dimensionless parameters are substituted in the transcendental Equation (1), we obtain the following relationship

$$a = b \exp(1 - 2/a) \quad (3)$$

which by taking logarithms may be written as

$$\ln a + 2/a = 1 + \ln b \quad (4)$$

We may immediately compute b and, therefore, $1 + \ln b$ from the experimental measurement of the curve in Figure 1. Equation (4) may then be solved graphically by plotting this equation. We can read directly the value of a corresponding to the experimentally determined value of $1 + \ln b$.

Knowing a the activation energy and frequency factors are given by:

$$E - RT_0 a \text{ and } k_0 = (M a/T_0) e^a \quad (5)$$

This derivation is given in greater detail together with extensions to reversible and for back reactions in reference (3).

EXPERIMENTAL

Ten samples of bituminous coal ranging from 1 to 5 percent sulfur were provided by the Illinois Geological Survey and the U.S. Bureau of Mines. These include coals from Illinois, Ohio, Maryland, Pennsylvania and Kentucky. A.S.T.M. analyses were done on these coals for forms of sulfur, mineral analyses, proximate analyses, and sulfur in ash and fixed carbon.

Heating was done with flow hydrogen in a furnace controlled by a linear temperature programmer. Continuous analyses were done with a special mass spectrometer designed and built for this purpose. The experimental set up is shown schematically in Figure 2.

HYDROGEN SULFIDE EVOLUTION FROM COAL

In a hydrogen atmosphere the sulfur in the coal reacts with hydrogen to produce hydrogen sulfide. A typical H_2S evolution curve for a non-isothermal experiment on coal heated in hydrogen is given in Figure 3. These results were obtained using a hydrogen flow rate of 1 litre per minute over a 250 mg sample of Illinois coal No. 4, as identified in our report, reference (3). The heating rate

was 4°C per minute. Clearly the H₂S evolution does not occur by a single process. Since sulfur exists in coal in many different forms, e.g. pyrite, sulfide, sulfate and several different types of organic sulfur, this result is expected. Each individual reaction of the form, coal + H₂ → H₂S, should yield an H₂S evolution curve similar to that shown in Figure 1. The parameters characterizing that curve T₀, V₀, and (dV/dT)_{T₀} should reflect the kinetics for the individual process. The overall H₂S evolution curve will be composed of the sum of the set of overlapping curves characterizing each of the individual reactions. In the absence of any knowledge on the individual processes an experimental result such as given in Figure 3 can be resolved into individual processes in infinitely many ways. However, if the kinetics of the individual processes are known a priori, a unique resolution of the experimental results can be achieved.

Since iron pyrite is known to be a major source of sulfur in coal, we conducted non-isothermal experiments on samples of iron pyrite obtained from the U.S. Bureau of Mines. In these experiments the back reaction of H₂S with iron was suppressed by using a very high hydrogen flow rate and a very small sample of iron pyrite. The heating rate employed was 4°C per minute. The experimental data on the non-isothermal evolution of H₂S from pyrite are shown in Figure 4. These results clearly indicate two reactions producing hydrogen sulfide; firstly the reduction to FeS and secondly to Fe.

These experimental results on pyrite may be analyzed in a straight forward manner to yield the kinetic parameters for the two reactions. The procedure used is as follows: First we sketch in two peaks of the type shown in Figure 1 which give a reasonable fit to the experimental points. The values of the parameters characterizing the curves are read off of these curves. These parameters are the temperature corresponding to each of the peaks, T₀(°K), the area of the peak, V₀, and the amplitude of the peak at T₀. From these values a dimensionless parameter b as given by Equation (2) is computed and used to graphically obtain a. The values of the activation energies E and pre-exponential factor k₀ are then computed using Equation (5). The results are then double checked by recomputing the H₂S evolution peak corresponding to these parameter values using Equation (1). The calculated peaks are then replotted with the experimental data and the accuracy of the fit is checked. By these procedures we find for the pyrite reaction E = 47 kilocalories per mole and k₀ = 2.8 × 10¹² (atm H₂)⁻¹ min⁻¹ and for the sulfide reduction E = 55 kilocalories per mole k₀ = 2.1 × 10¹³ (atm H₂)⁻¹ min⁻¹. The calculated H₂S evolution curves for these two reactions are compared with the experimental data in Figure 5. The calculated H₂S evolution for the sum of the two processes is shown in the dash line in the figure. The fit between calculation and experimental could obviously be improved by slightly adjusting the amplitudes of the two peaks. However, the amplitudes reflect the stoichiometries of the reaction while the locations and shapes of the peaks reflect the kinetics. These results suggest that the pyrite sample was not pure FeS₂ but rather initially contained a small amount of sulfide.

DESULFURIZATION KINETICS FOR ORGANIC SULFUR

The pyrite sulfur clearly accounts for most of the inorganic sulfur found in coal, but there is also generally substantial amounts of organic sulfur and it is well known that this sulfur may exist in many different kinds of bonding arrange-

ments within the coal. In an attempt to investigate behavior of the organic sulfur on a somewhat simpler, but, related system, we prepared artificially some organic sulfur-containing material. A sample of essentially mineral free charcoal was reacted with hydrogen sulfide in a stream of helium to produce a sulfurated carbon which contained approximately 2.5% sulfur. Non-isothermal measurements on the desulfurization of this material in both hydrogen and helium were carried out. The results of one such experiment are given in Figure 6. In this experiment the sample size and flow rate of hydrogen used were the same as that employed on the major series of non-isothermal experiments on coals. It is clear from the results of studies to date on the sulfurated carbon that a single simple reaction does not account for the behavior of this material. Pending the completion of the kinetic investigation on the complex sequence of reactions involved in the desulfurization of these relatively stable organic sulfur species the empirical result corresponding to the smooth curve shown in Figure 8 has been used in the analysis on the results on coal. We have designated this form of organic sulfur as Organic III.

To proceed further in our analysis of the experimental result given in Figure 3 it is necessary to consider the results on all ten coals studied. The results of non-isothermal kinetic experiments for ten coals studied under similar experimental conditions are summarized in Figures 7 and 8. Certain points in common and certain differences should be noted in these results. All of the H_2S evolution curves show a peak in the range between $380^\circ C$ and $430^\circ C$. All of the coals high in pyrite show secondary peaks very close to those found experimentally for the sample of pyrite as illustrated in Figure 5. However, in general for these coals these peaks appear to occur at slightly lower temperatures typically from $10 - 20^\circ C$. If we assume that results on the pyrite are valid for coal we would expect that the presence of the carbon should have little effect on the activation energies for these reactions. But, because of both the production of hydrogen from within the coal and the possibility of the absorption of hydrogen on the carbon surface, we might expect that the pre-exponential factor which is expressed in terms of the concentration of hydrogen in the bulk gas stream might be increased in the case of the coal by these effects increasing surface concentration of hydrogen for a given bulk gas concentration of hydrogen. A downward shift in the temperature corresponding to the peak in the H_2S evolution from pyrite of $20^\circ C$ corresponds to an increase in the pre-exponential factor of about 40%. Data obtained by us and by Powell in his earlier work on the forms of sulfur in char, as a function of carbonizing temperature, support the hypothesis that the secondary peaks in these non-isothermal results do correspond to the reaction of the pyritic and sulfide sulfurs. Similarly this work suggests that the low temperature peaks in the non-isothermal results correspond to the reaction of relatively unstable organic sulfur compounds in coal. A single reaction cannot account for the variation in the location and shape of the low temperature peak for all of these ten coals. However, we have found that two processes, one with T_0 corresponding to $380^\circ C$ and a second with T_0 corresponding to $430^\circ C$ satisfactorily account for the low temperature peak in all ten coals. The kinetic parameters for these two processes which we have designed as Organic I and Organic II are as follows: ORGANIC I, $E = 34.5$ kcal/mole, $K_0 = 3.1 \times 10^{10}$ (atm H_2) $^{-1}$ min $^{-1}$; ORGANIC II : $E = 41.5$ kcal/mole, $K_0 = 2.8 \times 10^{11}$ (atm H_2) $^{-1}$ min $^{-1}$. It is, of course, possible that more than two processes contribute to this low temperature peak, however, only the two are required to account for the experimental

results.

We will now discuss the resolution of the experimental result given in Figure 3 into individual processes. The five processes we have identified in the preceding discussion are three forms of organic sulfur, pyrite, and sulfide. This result in the individual processes were performed graphically by drawing in the peaks corresponding to the individual processes and adjusting the amplitude of the peak without changing the peak location until a best fit to the experimental data is obtained. The fit is determined by comparing the sum of all of the H_2S evolution peaks with the experimental data. The result of this analysis is shown in Figure 9. In the figure the dotted line represents the sum of the individual processes with the amplitudes shown in the figure and the agreement with the experimental points is quite satisfactory with one exception. In the region about $530^\circ C$ there appears to be a significant amount of sulfur evolution which is not accounted for by these five processes. This discrepancy occurs in most of the coals studied but is particularly prominent in coal No. 7, the Maryland coal. This discrepancy may indicate that an additional desulfurization process occurs which we have not taken into account, however, our recent experiments, in an attempt to further understand the Organic III set of reactions, have indicated that the results obtained on the artificial sample of sulfurated carbon may not be directly applicable to coal. It now appears that a proper representation of the Organic III sulfur removal may remove this discrepancy.

One additional point that should be mentioned concerning this analysis of Illinois No. 4 coal is that the total amount of sulfur evolved from the pyrite and sulfide processes appears rather lower than would be expected from the amount of iron pyrite in the coal from the ASTM analysis. However, this coal contains an unusually high calcium content. Our separate experiments on the reaction of H_2S with calcium oxide and calcium carbonate have shown that the reaction of H_2S with these materials in the temperature range above 500° is extremely fast so that nearly one half of the sulfur, which might otherwise be evolved in the pyrite and sulfur peaks, is converted to calcium sulfide and retained in the char. Similar procedures to those described above have been employed in analyzing all ten of the coals studied.

KINETICS OF DESULFURIZATION

We may summarize the chemical reactions and the rate data of coal desulfurization in hydrogen atmospheres by listing our measured kinetics parameters for the five major reactions and two back reactions, as shown in Table I.

Non-isothermal studies were also made of the removal of H_2S by calcined dolomites and limestones and the regeneration kinetics of the resulting calcium sulfide. The kinetic parameters for these rate data are shown in Table II.

The significance of these results to considerations of sulfur control can be seen by expressing them as rate constants versus temperature over the range of engineering interest. The rate constants for these reactions are shown from $400^\circ C$ to $1000^\circ C$ in Figure 10. There emerges a desulfurization band which encompasses the desulfurization reactions which account for the hydrodesulfurization of the ten bituminous coals studied.

TABLE I

CHEMICAL REACTIONS AND RATE DATA OF COAL DESULFURIZATION
IN HYDROGEN ATMOSPHERES

<u>No.</u>	<u>Reaction</u>	<u>E^{kcal}/mole.</u>	<u>k₀</u>
1	(Org-S) _I + H ₂ → H ₂ S	34.5	3.1 × 10 ¹⁰ (atm H ₂) ⁻¹ min ⁻¹
2	(Org-S) _{II} + H ₂ → H ₂ S	41.5	2.8 × 10 ¹¹ " "
3	FeS ₂ + H ₂ → H ₂ S + FeS	47	2.8 × 10 ¹² " "
4	FeS + H ₂ → Fe + H ₂ S	55	2.1 × 10 ¹³ " "
5	(C-S) + H ₂ → H ₂ S	52	~2 × 10 ¹³ " "
6	Fe + H ₂ S → H ₂ + FeS	18	6.5 × 10 ⁶ (atm H ₂ S) ⁻¹ min ⁻¹
7	Coke + H ₂ S → (C-S) + H ₂	32	2.3 × 10 ⁸ " "

TABLE II

8	CaO + H ₂ S → CaS + H ₂ O	38	4.7 × 10 ¹³ (atm H ₂ S) ⁻¹ min ⁻¹
9	CaS + H ₂ O → CaO + H ₂ S	55	1.0 × 10 ¹⁴ (atm H ₂ O) ⁻¹ min ⁻¹
10	CaCO ₃ → CaO + CO ₂	58	3.0 × 10 ¹² min ⁻¹
11	CaO + CO ₂ → CaCO ₃	17	5.0 × 10 ⁴ (atm CO ₂) ⁻¹ min ⁻¹

ACKNOWLEDGMENTS

We acknowledge support of the National Air Pollution Control Administration under Contract No. PH 86-68-65 and the cooperation and advice of Paul W. Spaite, E.D. Margolin, and Leon Stankus.

REFERENCES

1. Snow, Ind. and Eng. Chem. 24, 903 (1932).
2. (a) Juntgen, Erdol and Kohle 17, 180 (1964), (b) Juntgen and Traenckner, Brennstoff-Chem. 45, 105 (1964). See 3(b) ref. 15-22.
3. (a) Scientific Research Instruments Corporation Report No. SRIC 68-13 (1969), (b) Scientific Research Instruments Corporation Report No. SRIC 69-10 (1969).

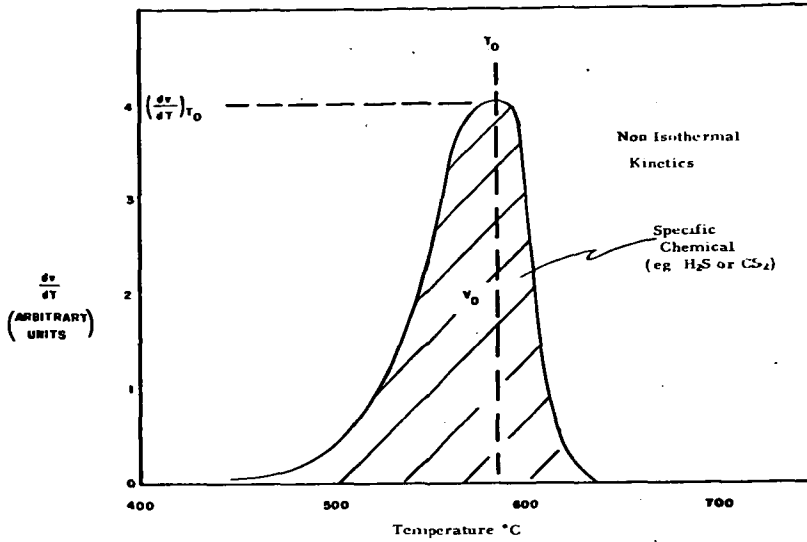


Figure 1. Typical outgassing kinetics curve vs. temperature. T_0 is temperature at peak. $(dv/dT)_{T_0}$ is peak height, v_0 is area.

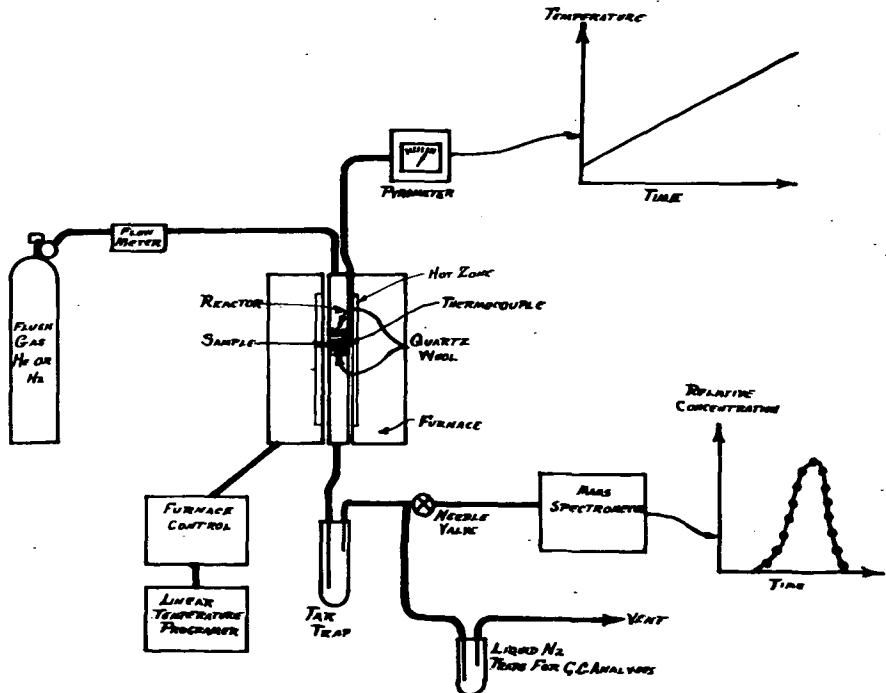


Figure 2. Schematic diagram of experimental apparatus.

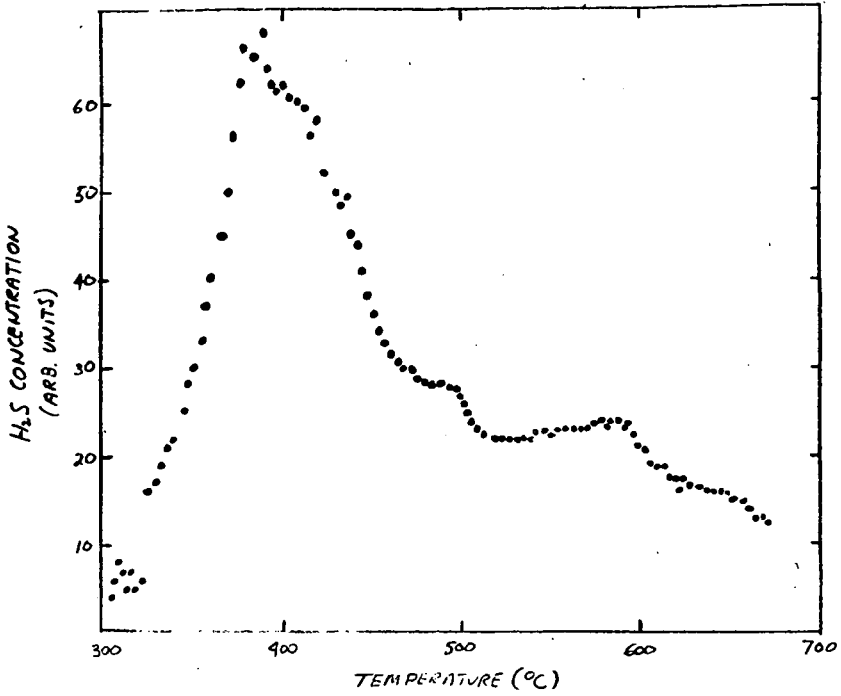


Figure 3. H₂S evolution in a non-isothermal experiment at one atmosphere of hydrogen on Illinois 5% sulfur coal, SRI No. 4.

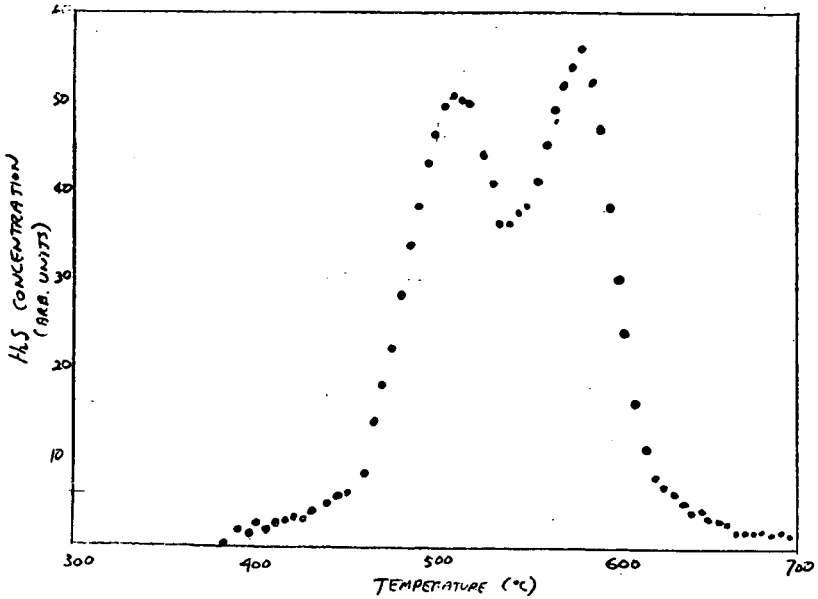


Figure 4. H₂S evolution in a non-isothermal experiment at one atmosphere of hydrogen on pyrite.

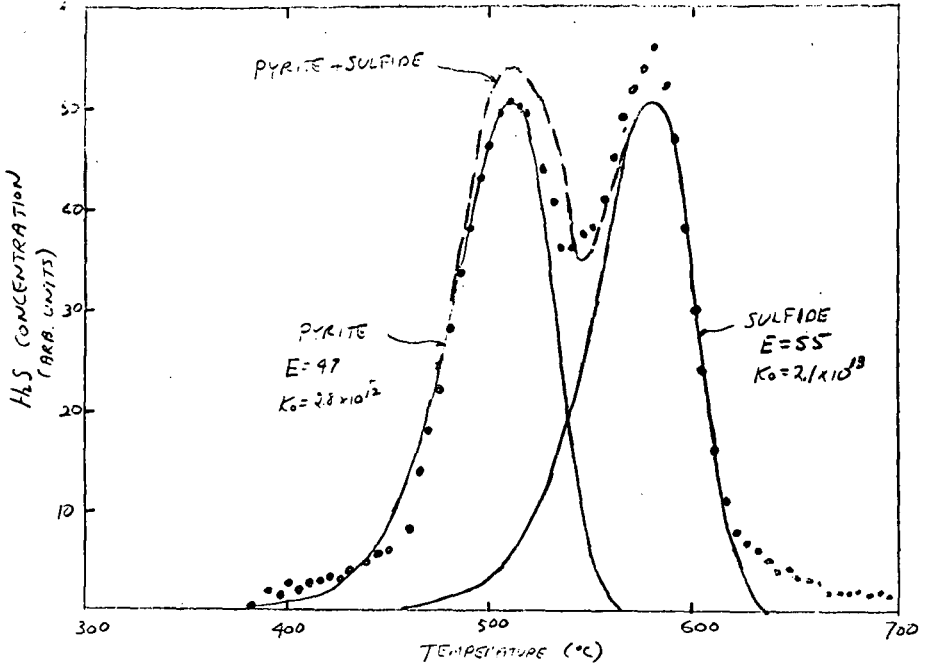


Figure 5 . Kinetic analysis of the non-isothermal measurement on pyrite.

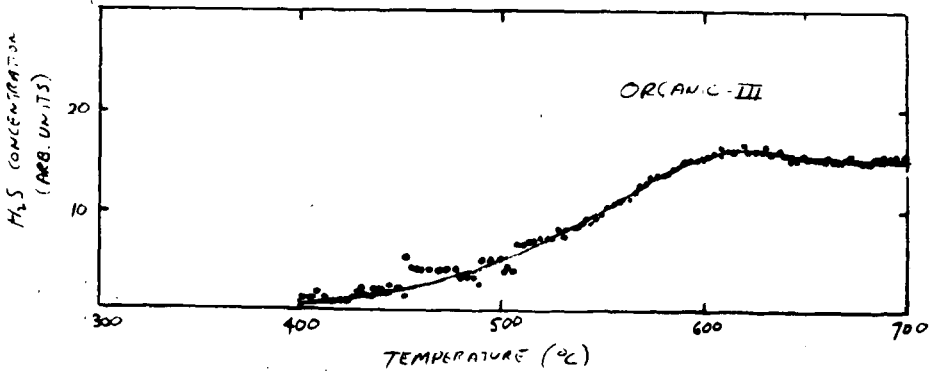


Figure 6. H₂S evolution in non-isothermal experiment at one atmosphere of hydrogen on sulfurated carbon prepared from charcoal.

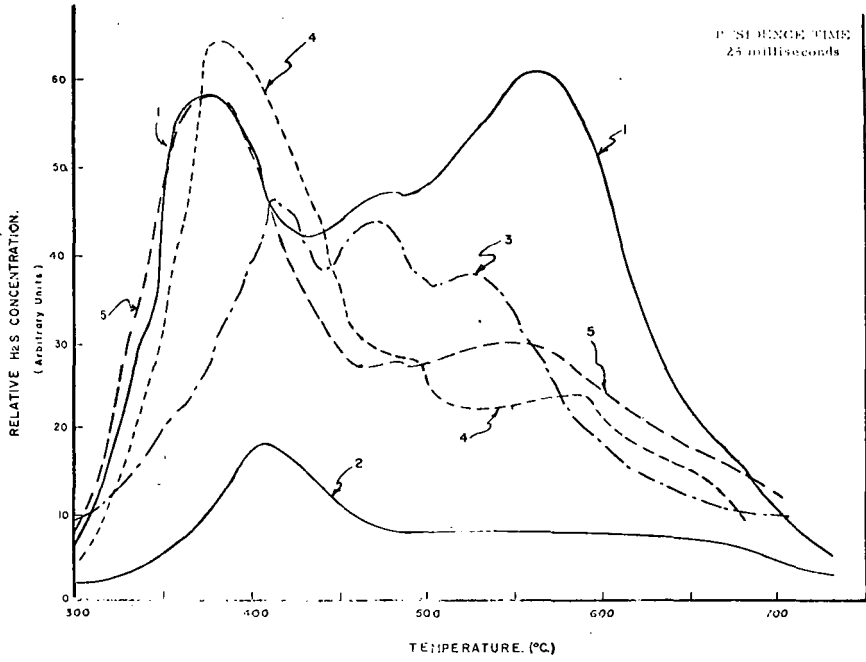


FIGURE 7. NON-ISOTHERMAL H_2S EVOLUTIONS IN H_2 FROM COALS SRI NUMBERS 1 THROUGH 5.

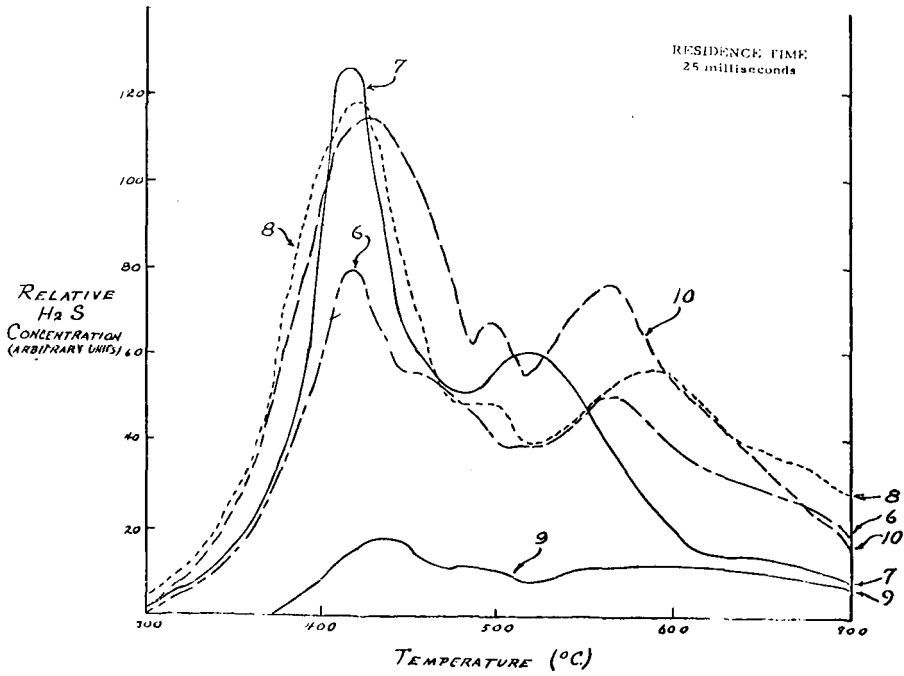


FIGURE 8. NON-ISOTHERMAL H_2S EVOLUTIONS IN H_2 FROM COALS SRI NUMBERS 6 THROUGH 10.

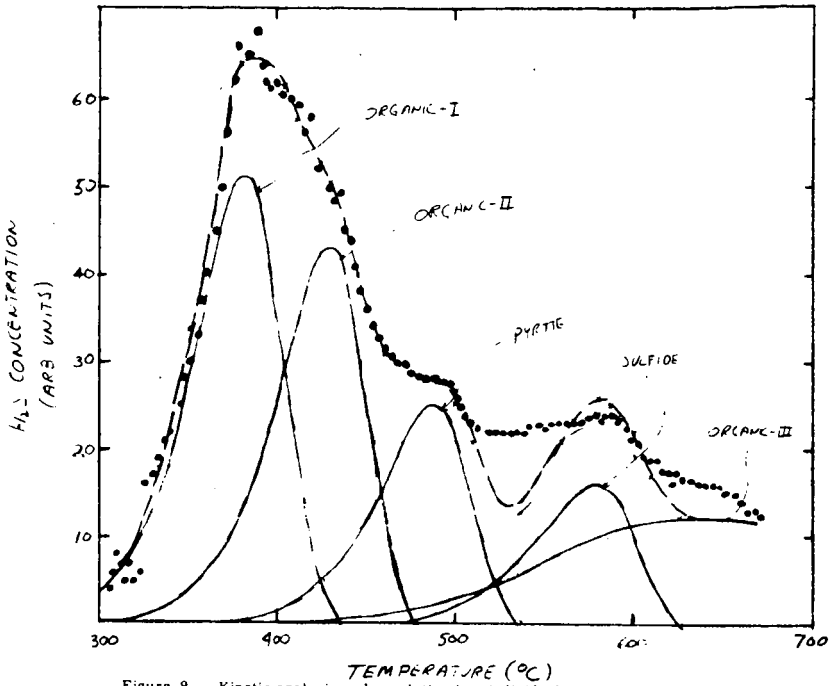


Figure 9. Kinetic analysis and resolution into individual processes of the H_2S evolution in a non-isothermal experiment at one atmosphere of hydrogen on Illinois 5% sulfur coal, SRI No. 4.

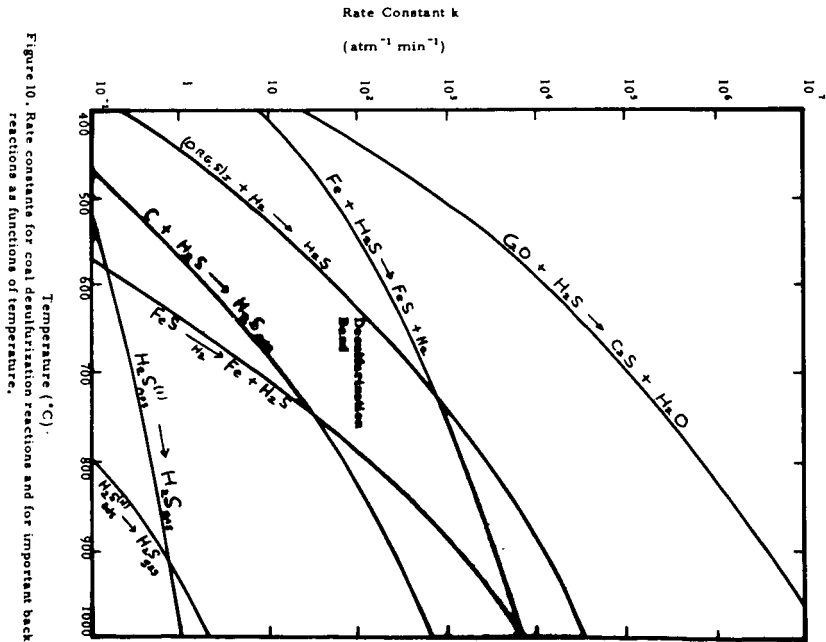


Figure 10. Rate constants for coal desulfurization reactions and for important back reactions as functions of temperature.

MANUFACTURE OF ACTIVATED CARBON AND ITS APPLICATION
TO AIR, WATER, AND NUCLEAR POLLUTION CONTROL

by

W. F. Heneghan
Witco Chemical Corp.

ABSTRACT

Activated Carbon in the United States is mainly made by the steam activation process and important variables in the manufacture and resulting end properties are considered particularly temperature, gas mixtures, and residence time. Economic of granular activated carbon pollution control is primarily dependent on the adsorption properties, both static and dynamic, and the various variables affecting the mass transfer characteristics are illustrated. Practical use of granular activated carbon generally will require on site regeneration and the knowledge of working capacity with various regeneration techniques (furnace, heated solvents, internal, chemical and biological) are required for the most efficient plant design. Size and growth of various end use areas are reviewed.

THERMAL REGENERATION OF ACTIVATED CARBONS

E. Krieger, F. Tepper and A. J. Juhola

MSA Research Corporation
Evans City, Pennsylvania

Introduction

Granular activated carbons are used in tertiary treatment of waste water in several treatment plants, as at Pomona, California, and South Lake Tahoe, California, to name two. Waste water, from the secondary treatment, is passed through carbon beds which then remove the biologically nondegradable impurities and thereby produce water essentially free of organic impurities.

An important phase of the carbon treatment is the regeneration to permit reuse of the carbon over many cycles. The regeneration is accomplished thermally in multiple-hearth furnaces, using flue gas as source of activating gases as well as for heating. Operations of these plants has demonstrated a physical loss of carbon varying from 5% to 10% per regeneration. On each regeneration the carbon also loses some of its adsorptive capacity. Figure 1 presents data, obtained at the Pomona plant, showing these decreases in activity. The iodine number of the virgin carbon is 1090 mg/g and after 10 cycles it has decreased to 608 mg/g. Over the same cycles, the adsorption of water soluble COD impurities decreased from 53% down to about 39% with some leveling off starting at the 5th cycle.

To improve the economics of the carbon treatment, it is necessary to find means for decreasing the physical loss of carbon and loss of adsorptive capacity.

Laboratory Studies to Improve Carbon Regeneration

Mine Safety Appliances Research Corporation has conducted a research program sponsored by the Federal Water Pollution Control Administration to study the regeneration process and determine optimum conditions to reduce carbon losses and adsorptive capacity. The regenerations were done in an indirectly heated rotary tube regenerator shown in Figure 2. Two of the main components are the rotary tube, 3.25 in. inside diameter and 65 in. length, and the three electrically heated furnace sections which can be controlled separately. Each end of the

rotary tube is capped off with a rotary seal, insuring no loss of input and output gases. The gas temperature is measured at five points over the carbon bed. Carbon and gas flows are counter-current.

The regenerating gases are mixtures of N_2 , CO_2 and steam, generally made up in proportions not too greatly different from flue gas. The N_2 and CO_2 are metered from compressed gas cylinders. A calibrated boiler is used for steam generation.

The effluent gas stream can be analyzed for CO , CO_2 and H_2 content.

Carbon input rate is generally 450 cc/hr and gas input rate about 10 ft³/hr (stp).

Carbon residence times are about 1/2 and 1/4 hr.

The recovery of the adsorptive capacity on regeneration is measured by the iodine and molasses numbers and carbon loss by the particle volume decrease. The degree of success is then measured by how closely the iodine and molasses numbers approach the test results of the virgin carbon and by how small the particle volume decrease is.

The carbon used in most of these studies was Filtrasorb 400, once spent at the Pomona, California, plant. Table 1 gives the properties of the spent carbon and also those of the virgin carbon, the latter setting the goals to be attained on the regeneration. For monitoring purposes of the regeneration, the attempt was always made to bring the bulk density down from 0.597 to 0.468 g/cc. This was done by varying the activating gas input rate. By adjustments to other variables, the attempt was then made to also bring the iodine number to 1090 mg/g and molasses number to 250.

TABLE 1 - PROPERTIES OF SPENT AND VIRGIN
FILTRASORB 400

<u>Carbon</u>	<u>Bulk density,</u> <u>g/cc</u>	<u>Pore volume,</u> <u>cc/cc</u>	<u>Iodine number,</u> <u>mg/g</u>	<u>Molasses number</u>
spent	0.583	0.500	630	190
virgin	0.468	0.650	1090	250

Step-wise Nature of Carbon Regeneration

The laboratory regeneration studies and also thermodynamic calculations of the Pomona multiple-hearth furnace indicated that the thermal regeneration of wet spent carbon occurs in three naturally occurring steps. These are (1) drying, (2) carbonization of adsorbate, and (3) activation. Figure 3 shows the temperature profile of the gas and carbon in the Pomona furnace. The gas temperatures were measured and the carbon temperatures calculated from the thermodynamic properties of the system. The carbon temperature profile shows that the carbon is dried on traversing the first three hearths; this requires about 22 min. On the 4th hearth, the adsorbate is carbonized or baked. About 70% of the adsorbate is volatilized and the rest breaks down to free carbon lodged in pores. This step requires about 9 min. On hearths 5 and 6, the free carbon residue is oxidized, constituting the activation step. This step requires 15 min.

In the laboratory studies, the regenerations were then conducted in the three steps. Runs were made in which the drying and baking were conducted in the rotary tube with 1/2 hr carbon residence times. In other runs the drying was done separately in an air-convection oven and the baking then done in the rotary tube with 1/2 hr carbon residence time. It was found that the method of drying and baking produced no difference in the quality of the final product. Because of convenience, drying and baking were subsequently carried out separately.

The activating step was found to be more sensitive to the operating conditions. For instance, CO₂ activation produced regenerated carbons of lower iodine number than pure steam activation. Activation at high temperature of 1650° to 1700°F gave better results than activation at 1600°F and lower, although at about 1500°F, activation rate was too slow to be of any importance in the regenerations.

Optimization of gas input, gas composition and temperature, never produced regenerated carbons quite up to the virgin carbon properties. On cyclic studies, in which virgin carbon was successively spent and regenerated, the iodine number moved downward on each regeneration, not unlike the pattern observed at Pomona. These results are shown in Figure 4. After the second cycle, the iodine number of the regenerated carbon was down to 935 mg/g from the original 1090 mg/g. The regenerations had been done under conditions that were considered optimum with respect to gas input and temperature.

The conclusion is that optimization of gas input and temperature does not lead to complete regeneration.

Effect of Metallic Elements on Regeneration

In the cyclic studies, it was observed that the ash content increased with each successive cycle and that, also, it became easier to activate the carbon. Less activating gas input was required to bring the bulk density to the virgin carbon density. Table 2 gives the percentage ash content and decolorizing test results after each regeneration. The ash content increased from 5.7% to 8.6%. The molasses number increased from 250 to the 300 level, which, as will be explained later, is undesirable.

TABLE 2 - ASH CONTENT AND DECOLORIZING TEST RESULTS ON SUCCESSIVE ACTIVATIONS

Cycle No	Bulk density, g/cc	Ash content, %	Iodine number, mg/g	Molasses number
initial	0.469	5.7	1090	250
1	0.468	7.6	1040	310
2	0.469	8.6	935	290

Table 3 shows the drastic decrease in activating gas input rate required to avoid overactivation.

TABLE 3 - ACTIVATING GAS INPUT REQUIRED ON SUCCESSIVE ACTIVATIONS

Cycle No	Gas input, ft ³ /hr (stp)		
	N ₂	CO ₂	H ₂ O
1	3.6	0.36	1.0
2	1.27	0.17	0.18

The correlation of increased ash content with decrease in iodine number led to an investigation of effects of ash content in the baking and activating steps. Several charges of spent carbon were leached with HCl acid, to remove some of the metallic element content, prior to being regenerated. The ash analysis decreased from about 7.0% to a constant lower limit of 4.7%. Virgin carbon starts with a 5.7% ash analysis. The acid leach also decreased the adsorbate content but no significant difference could be observed in the baked product when

compared to nonacid treated baked product. After activation, however, the acid pretreated carbons consistently had higher iodine numbers. Table 4 shows this comparison. The mean iodine number of the HCl pretreated regenerated carbons is 1034 mg/g compared to 945 mg/g for the nonpretreated.

TABLE 4 - EFFECT OF HCl ACID PRETREATMENT ON IODINE AND MOLASSES NUMBER OF REGENERATED CARBONS

Activation run no	Bulk density, g/cc	Not HCl treated		HCl treated	
		I ₂ no, mg/g	Mol no	I ₂ no, mg/g	Mol no
(virgin)	(0.468)	(1090)	(250)		
30	0.469	960	290		
32	0.467	950	---		
34	0.478			1020	230
36	0.484			1040	230
39	0.461	930	270		
40	0.468	950	250		
41	0.476	950	260		
47	0.468			1050	230
53	0.472			1020	250
77	0.468	930	250		
79	0.480	---	---	1040	230
	means	945	264	1034	234

The mean molasses number of 264 for the nonpretreated is larger than that of the virgin carbon while the mean molasses number of the acid pretreated carbons is smaller. The latter is favorable since activation could be continued to increase the iodine number while raising the molasses number to that of the virgin carbon.

The carbon losses, as measured by particle volume decrease, ranged from 1.6% to 4.0% for the nonpretreated carbons while for the pretreated carbons the range was 2.6% to 5.0%. Some of the advantage of the increased capacity is off-set by increased carbon loss.

The baking and activating conditions were varied for the runs reported in Table 4, but it, nevertheless, became evident that the nonpretreated carbons could be activated to the original bulk density with considerably less activating gas input than the acid pretreated carbons. In Table 5 are operating data on two runs where a valid comparison could be made to show this effect. In the activation Run 79, 30% to 50% more activating gases were required than on Run 30.

TABLE 5 - BAKING AND ACTIVATING CONDITIONS

Run no.	Regenerating step	Temperature, °F			Gas input, ft ³ /hr (stp)		
		1	2	3	N ₂	CO ₂	H ₂ O
29	dry OSF 400 baked	750	1330	1550	7.0	0.90	2.28
30	Run 29 activated	1550	1650	1700	4.0	0.51	1.48
78	dry, HCl treated, baked	800	1350	1550	7.0	0.93	1.96
79	Run 78 activated	1550	1650	1700	6.0	0.50	1.94

TABLE 8 - SURFACE AREA CHANGE AT DIFFERENT PORE DIAMETERS DURING REGENERATION

Carbons compared	Surface area difference, m ² /g							
	>10 Å	>12 Å	>14 Å	>16 Å	>18 Å	>20 Å	>28 Å	>50 Å
F 400 - 79 (HCl)	40	35	30	80	200	150	20	16
F 400 - 67	105	110	105	160	270	215	10	00
F 400 - 68 (CO ₂)	160	160	155	165	370	130	20	00
F 400 - 46	130	115	90	155	170	115	-30	-10
F 400 - 36 (HCl)	30	40	40	70	195	150	30	15

Ash Analyses

Since metallic elements in the carbon were now established as contributing to decreased recovery of the iodine number and over recovery of the molasses number, an investigation was made of the ash content of three carbons. The ash analyses for the three carbons are given in Table 6. Run 67 is a nonpretreated regeneration run and Run 79 an acid pretreated run. The virgin carbon is included, to indicate status of the starting material.

Run 67 shows a considerable increase in the oxides, Fe₂O₃, CaO, MgO, K₂O, Na₂O and Cr₂O₃. As is evident from Run 79, these oxides are considerably reduced by the HCl acid leach, hence one or more of these oxides contribute to lowered recovery of the iodine number and over recovery of the molasses number.

TABL 6 - ASH COMPOSITION OF ACID PRETREATED AND NONPRETREATED REGENERATED CARBONS

Component	Ash composition, %		
	virgin F 400	nonpretreated Run 67	pretreated Run 79
SiO ₂	2.36	2.27	2.24
Al ₂ O ₃	2.51	1.94	1.62
Fe ₂ O ₃	0.42	0.80	0.59
CaO	0.17	1.23	0.05
MgO	0.14	0.34	0.09
K ₂ O	0.06	0.40	0.20
Na ₂ O	0.04	0.15	0.07
TiO ₂	0.03	----	----
Cr ₂ O ₃	0.01	0.12	0.12
Total ash in carbon	5.7	7.2	5.0

Effect of Regeneration on Pore Size Distribution

In pore structure studies performed at Pittsburgh Carbon Company^{1,2}, it was found that the iodine number was proportional to the surface area of pores larger than 10 Å in diameter and the molasses number was proportional to the surface area of pores larger than 28 Å in diameter. Equations 1 and 2 below show these relationships.

$$I_2 \text{ no} = 17 + 1.07 \times (\text{s a of pores } >10 \text{ \AA}) \quad (1)$$

$$\text{Molasses no} = 129 + (\text{s a of pores } >28 \text{ \AA}) \quad (2)$$

With reference to the iodine and molasses numbers given in Table 4, these equations indicate that acid pretreatment minimizes decrease in surface area of the smaller pores and also prevents increase in surface area of pores larger than 28 Å diameter. Ash build up, as occurs on successive regenerations without acid leach, accelerates these changes.

A further study was conducted to determine the manner in which the surface area changes occurred. Pore size distribution curves were determined for selected carbons, using the water adsorption method³ and mercury porosimetry. In preparation for the water isotherm determinations (and also porosimetry), the carbons were HCl acid and pure water leached to remove hydrophilic compounds from the carbon surface. The validity of the water adsorption method depends on the water being adsorbed by capillary condensation, with negligible monolayer adsorption. The adsorption method is applicable to maximum pore diameter of 500 to 1000 Å.

Pores in the larger diameter range are measured by mercury porosimetry⁴. These measurements cover the diameter range 30 to 100,000 Å, hence the two methods overlap in the range 30 to 500 Å. For some of the pore size distributions, the agreement in the overlap range is good while for others, some discrepancy exists. The trend is for the mercury porosimeter to measure a larger pore diameter at a given volume. Figure 5 presents two distribution curves, Run 68 showing the best agreement and F 400 the poorest. A possible explanation for the discrepancy is that the carbons are slightly compressed by the mercury at the higher pressures. Maximum pressure at 30 Å is 60,000 lb/in².

Figures 6 and 7 present the complete pore size distribution curves of the selected samples. The overlap portion as measured by mercury porosimetry was left out in each case.

Those in Figure 6 show the effects of acid leach, steam activation and CO₂ activation. The virgin F 400 is uppermost in pore volume at the 28 Å diameter, and then Runs 79, 67 and 68 in descending order. The iodine numbers were respectively, 1090, 1040, 940 and 840 mg/g, while the molasses numbers were quite close to each other.

Those in Figure 7 also show effect of acid leach; Run 36 being uppermost was pretreated, while Runs 46 and 67 were not. Runs 46 and 67 are presented together because they have iodine numbers close to each other, i.e. 920 and 940 respectively, but have greatly different molasses numbers, 320 and 260, respectively.

The relationship between the decolorizing tests and pore structure is not always apparent by visual inspection of the pore size distribution curve, but comes more discernable when the cumulative surface areas at different pore sizes are compared. The cumulative surface area can be calculated with the equation

$$\Delta A = \frac{4 \Delta V}{D}$$

where ΔA is an increment of surface area associated with increment of pore volume ΔV with mean diameter D . By summing up ΔA over the pore volume the surface area of pores larger or smaller than any specified D can then be calculated. This has been done for the carbons of Figure 6 in Figure 8 and for carbons of Figure 7 in Figure 9.

From Figure 8, the surface areas of pores larger than 10 Å in diameter for the carbons F 400, Runs 79, 67 and 68 are 965, 925, 860 and 805 m²/g, respectively. The surface areas of pores larger than 28 Å are respectively, 120, 100, 110 and 100 m²/g. Likewise from Figure 9, the surface areas of pores larger than 10 Å in diameter for the carbons Runs 36, 67 and 46 are 915, 860 and 840 m²/g, respectively. Surface areas of pores larger than 28 Å in diameter are, respectively, 85, 110 and 150 m²/g. When these surface areas are substituted into equations 1 and 2, the calculated decolorizing numbers agree with test results within ± 5% in the iodine numbers and within 13% in the molasses numbers. These results are given in Table 7.

TABLE 7 - IODINE AND MOLASSES NUMBERS AS DETERMINED BY TEST AND CALCULATED FROM SURFACE AREA

Carbon	Iodine number, mg/g		Molasses number	
	test	calc	test	calc
Filtrisorb 400	1090	1040	250	250
Run 79 (HCl)	1040	1010	230	230
Run 67	940	940	260	240
Run 68 (CO ₂)	840	880	250	230
Run 46	920	920	320	280
Run 36 (HCl)	1040	1000	230	210

Further study of the surface area curves also indicate where the major portion of the adsorption may be occurring. By inspection of the curves in Figure 8, it is observable that most of the change in pore structure occurs in the pores from 14 to 28 Å. Beyond 28 Å, there can be considerable change in pore volume, as is apparent from inspection of curves in Figures 6 and 7. The surface area of these larger pores is, however, too small to be effective. The same is true for Runs 67 and 38, of Figure 9, but Run 46 is an exception. For this carbon considerable change occurs at the 28 Å diameter region.

To show the change in pore structure, the difference in surface area between that of F 400 and each of the other carbons have been calculated for pore diameters from 10 Å to 50 Å. These calculated areas are given in Table 8. Pore structure change for Runs 79, 67 and 68 starts at 14 Å and ends at 28 Å diameter with most occurring at the 19 Å region. For Run 46, the pore structure change varies over the whole range with the largest difference again occurring at the 18 Å diameter. These results indicate a general enlargement of pores larger than 14 Å in diameter. Since the enlargement is greater for the nonpretreated carbons, the results also indicate that the major part of the adsorption occurs in pores of 14 to 28 Å in diameter. From this study it can be concluded, that the metallic oxides catalyze the oxidation of the base carbon structure in this pore diameter range.

Summary

To summarize the results of this experimental program, it was shown that granular carbons spent in tertiary treatment of waste water can be thermally regenerated to properties approaching those of the virgin carbon. Best results are obtained if the spent carbon is HCl leached to remove organometallic compounds of Fe, Ca, Mg, Na and K prior to regeneration, and that the final activation be by steam oxidation. The oxides of these metals catalyze the oxidation of the base carbon structure in the 14 to 28 Å diameter pore size range. The evidence also indicates that these pores are active in the adsorption process.

References

1. A. J. Juhola, W. M. Matz and J. W. Zabor, paper presented at the Am Chem Soc meeting, Div of Sugar Chem, April 1, 1951, "Adsorptive Properties of Activated Carbons."
2. R. J. Grant, "Basic Concept of Adsorption on Activated Carbon", Pittsburgh Activated Carbon Company.
3. E. O. Wiig and A. J. Juhola, JACS 71 2069, 2078 (1949).
4. Measurements made by American Instrument Co, Inc, Silver Springs, Maryland.

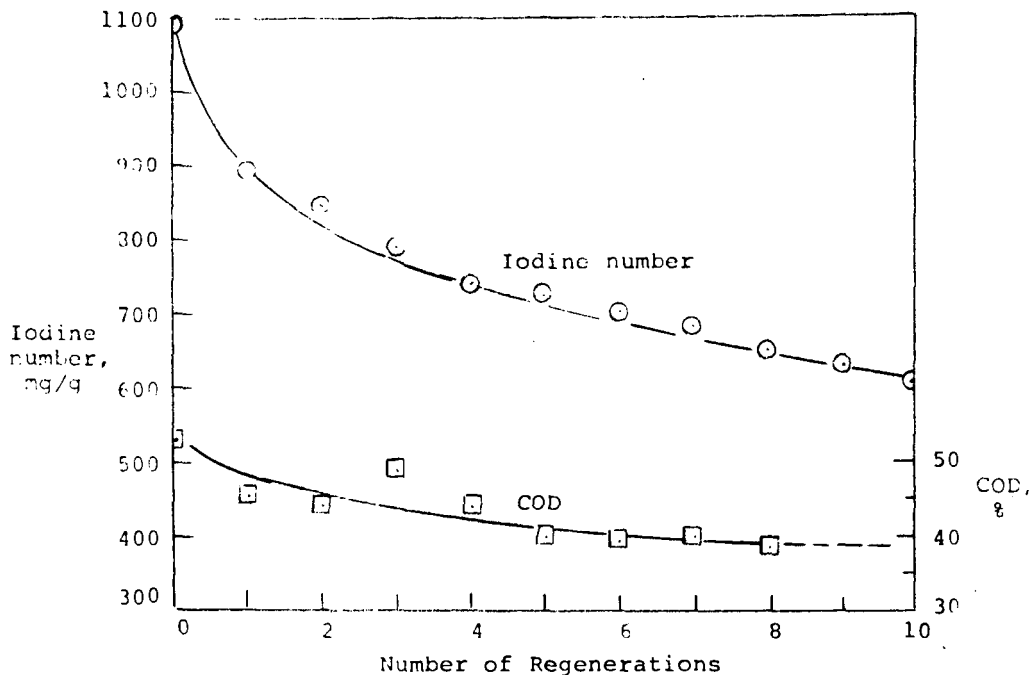


FIGURE 1 - DECREASE IN IODINE NUMBER AND COD ADSORPTIVE CAPACITY WITH SUCCESSIVE REGENERATIONS

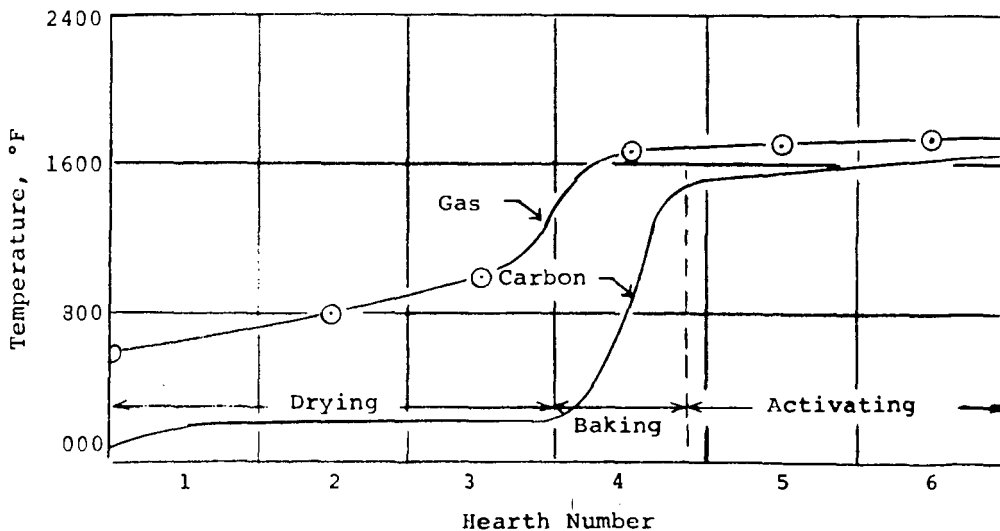


FIGURE 3 - TEMPERATURE PROFILES FOR GAS AND CARBON IN MULTIPLE HEARTH FURNACES, REGENERATION OF WET SPENT CARBON

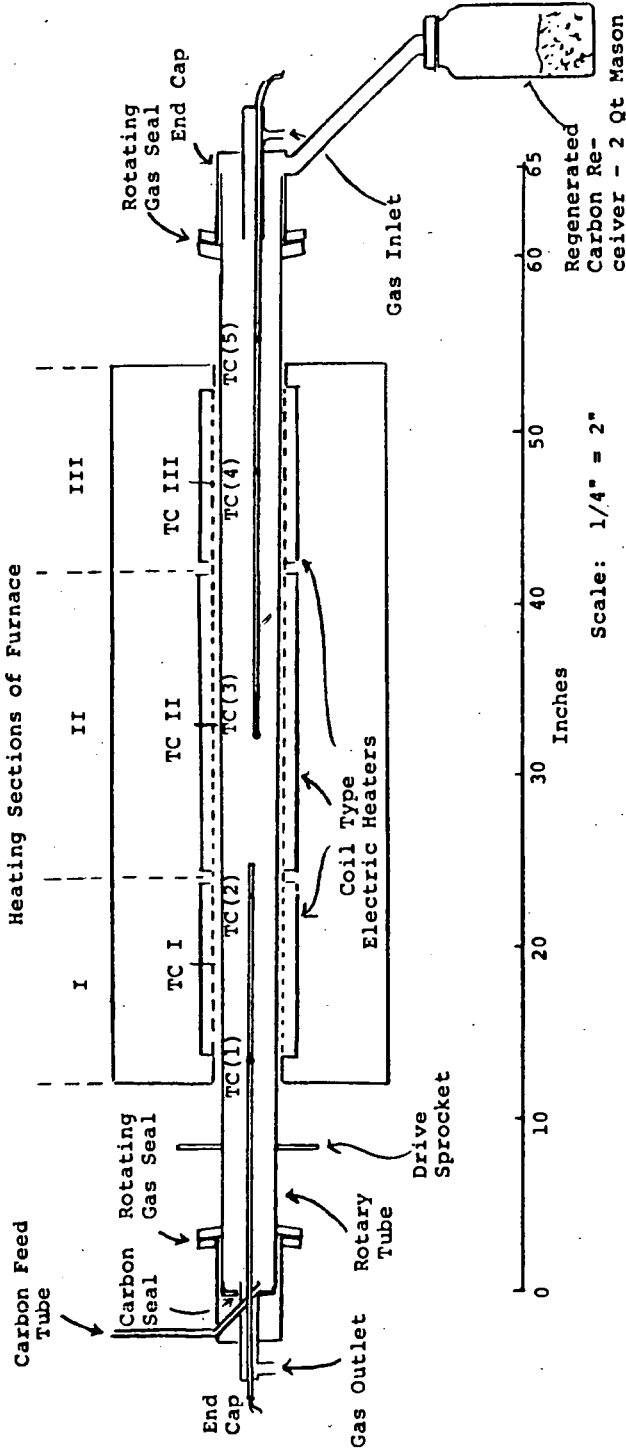


FIGURE 2 - CROSS SECTIONAL VIEW OF ROTATING TUBE, END CAPS AND HEATING FURNACE

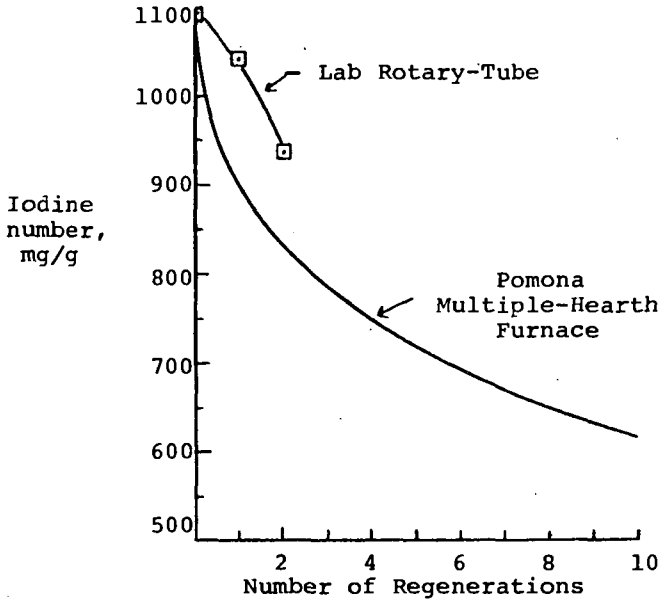


FIGURE 4 - DECREASE OF IODINE NUMBER WITH SUCCESSIVE REGENERATIONS

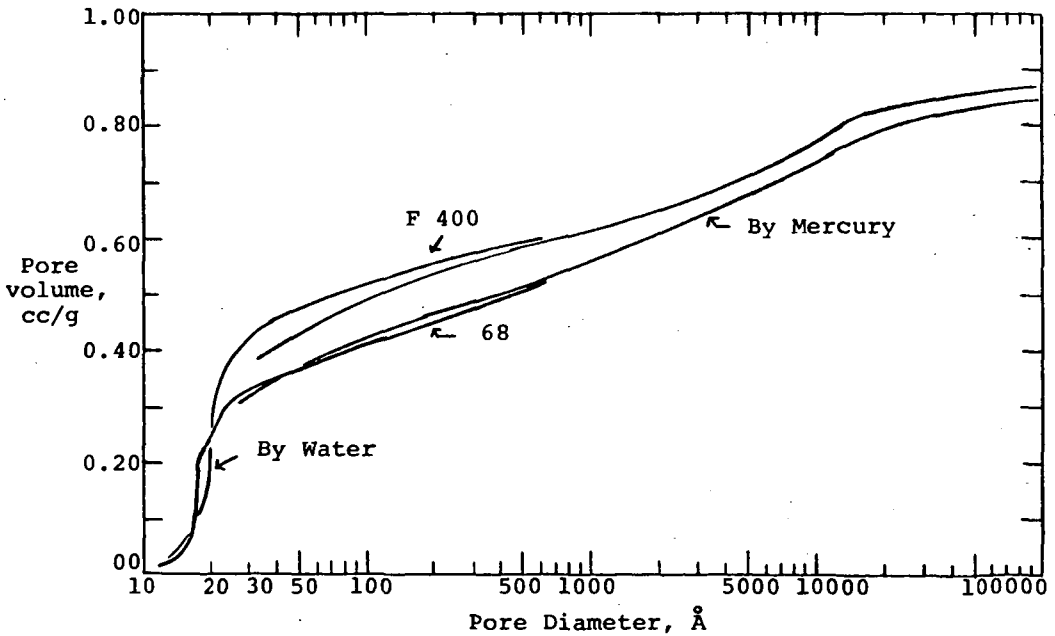


FIGURE 5 - PORE SIZE DISTRIBUTION MEASURED BY WATER ADSORPTION AND BY MERCURY PENETRATION

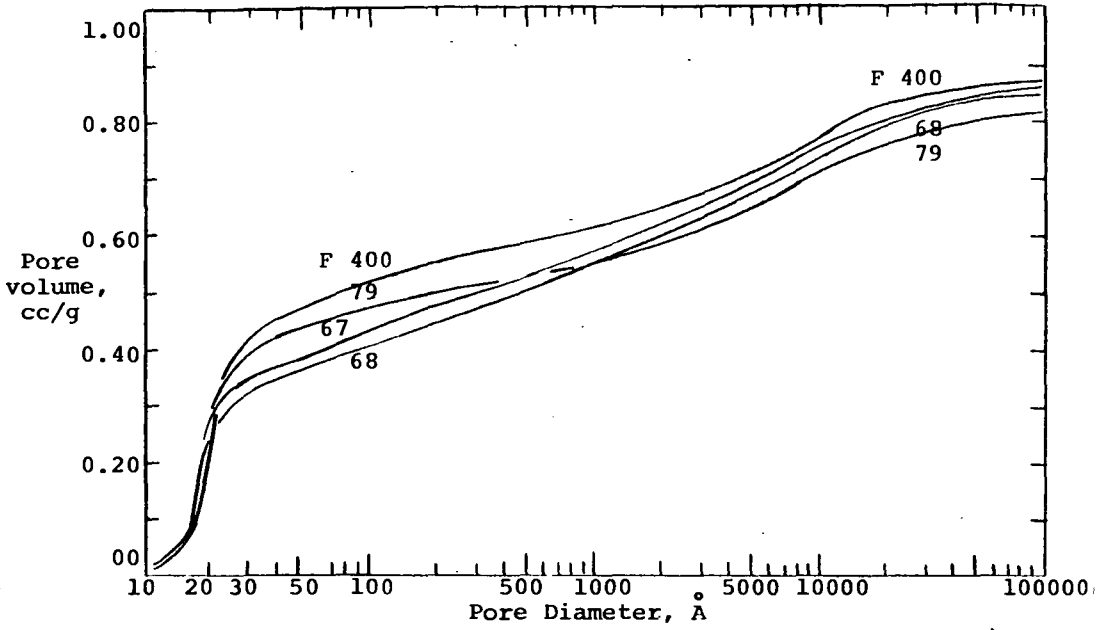


FIGURE 6 - PORE SIZE DISTRIBUTIONS OF REGENERATED CARBONS

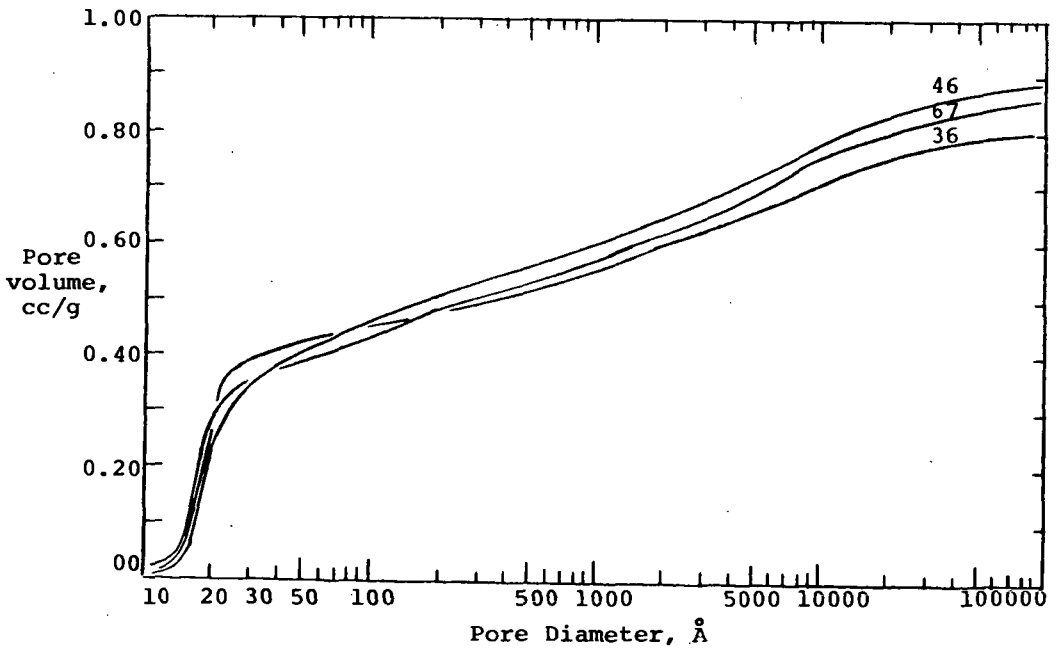


FIGURE 7 - PORE SIZE DISTRIBUTIONS OF REGENERATED CARBONS

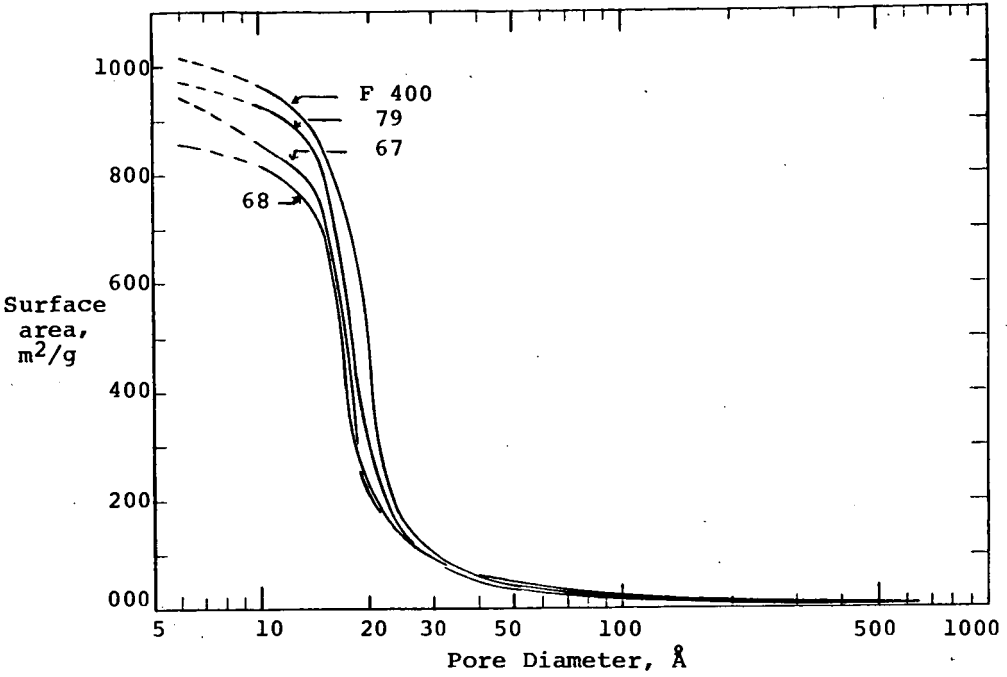


FIGURE 8 - CUMULATIVE SURFACE AREAS OF REGENERATED CARBONS

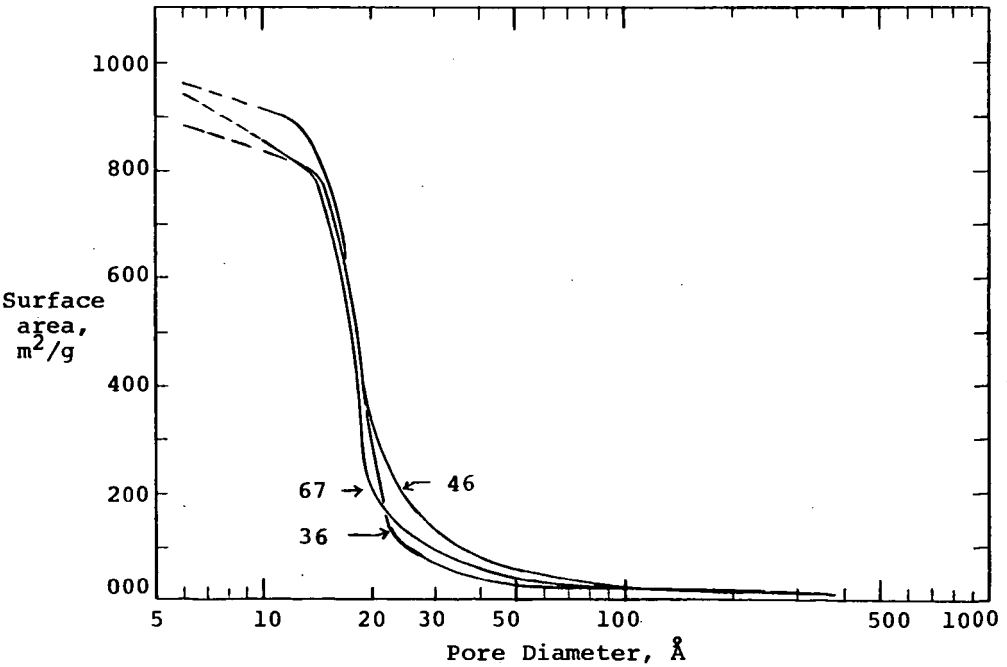


FIGURE 9 - CUMULATIVE SURFACE AREAS OF REGENERATED CARBONS

TREATMENT OF PRIMARY EFFLUENT*
BY LIME CLARIFICATION AND GRANULAR CARBON

R. V. Villiers, E. L. Berg, C. A. Brunner and A. N. Masse**

U. S. Department of the Interior
Federal Water Pollution Control Administration
Advanced Waste Treatment Research Laboratory
Cincinnati, Ohio 45226

Introduction

Conventional systems for treating wastewater are usually composed of two processes: a primary treatment process which removes the bulk of the settleable solids from the wastewater by sedimentation, and a secondary treatment process which removes the bulk of the soluble organic matter by biological oxidation. These processes in combination have shown to be an effective and economical means of improving the discharge quality of wastewater. However, the processes are not without certain disadvantages.

First, the processes require considerable operating control and often generate operating problems of a complex nature. Second, they are easily upset and require time to regain efficient operation. And finally, they produce sludge at such a rate that it poses an ultimate sludge disposal problem of considerable magnitude.

Conceivably, each of these disadvantages could be largely eliminated if wastewater were treated by a system that utilized solely physical and chemical methods. Such a system is shown schematically in Figure 1.

In Figure 1, primary treatment is replaced by lime clarification with the added bonus of phosphate removal and secondary

* To be presented at the May, 1970 meeting of the American Chemical Society in Toronto, Canada.

** R. V. Villiers, E. L. Berg and A. N. Masse are respectively Supervisory Research Sanitary Engineer, Chemical Engineer and Chief, Municipal Treatment Research Program, C. A. Brunner is a Research Chemical Engineer, Contracts and Grants Activities

treatment is replaced by activated carbon adsorption. Recalcination of the spent lime and regeneration of the carbon make the system essentially closed loop. The most intriguing aspect of the system as a whole is that there are no large volumes of waste sludge to contend with.

The results of applying activated carbon adsorption and lime clarification techniques to wastewater renovation have been widely reported in the literature (1) (2) (3) (4) (5). However, virtually all the work has been done on secondary effluent. The number of reported instances in which lime clarification and carbon adsorption have been applied to raw or primary wastewater are few.

Recently, a system utilizing lime clarification followed by biological treatment was applied to raw wastewater (6). Results showed that lime clarification with subsequent recalcination and collateral combustion of the primary sludge solids was economically competitive with conventional methods of removing suspended matter from wastewater by sedimentation and ultimate disposal by incineration. The process had the added benefit of phosphate removal.

In another study, raw wastewater was lime clarified at high pH and then carbon treated (7). The results presented were interpreted as showing that the removal of soluble organic matter by carbon is enhanced by the hydrolytic breakdown at high pH of large molecular weight organic compounds into lower weight ones which are more readily adsorbable. The results also give final effluent COD values that compare favorably with those associated with good secondary effluent.

Thus, to fully assess the feasibility of the system shown in Figure 1, it will be necessary to answer two key questions. First, can activated carbon adsorption compete with biological oxidation as an economical method of removing soluble organics from lime clarified raw wastewater, and second, can a complete physical and chemical system of wastewater treatment produce water of a quality at least equal to that produced by good conventional treatment.

Work addressed to answering these questions is presently underway at the Lebanon, Ohio pilot plant facility of the Federal Water Pollution Control Administration. The purpose of this interim project report is to give the preliminary results of the work.

Methods and Procedures

A flow diagram for the experimental system is shown in Figure 2. Primary effluent from the Lebanon Municipal Treatment Plant is fed to a lime clarification process for removal of suspended matter and phosphates. A schematic of the lime clarification process is given in Figure 3 and its operation is described in detail elsewhere (1). Except for a brief operational period during which the

pH was greater than 11.5, lime clarification was carried out at a pH of 9.5. Following lime clarification and filtration through parallel dual-media filters, the clarified water is pumped through three carbon contactors for removal of soluble organic matter.

Each carbon contactor is 4 ft in diameter and contains 2400 lbs of 8x30 mesh granular activated carbon (a). This quantity of carbon fills the contactor to a depth of 8 ft. The contactors are operated downflow and in series.

Prior to dual-media filtration, the clarified effluent is adjusted to pH 8 with sulfuric acid to minimize calcium carbonate incrustation of the filter media. Following filtration, the clarified effluent is further adjusted to pH 7.5 with sulfuric acid prior to carbon treatment.

The lime clarification process is operated at a steady flow rate of 75 gpm. Part of this flow is stored for use in backwash of the dual-media filters, the remainder goes into a holding tank from which it is pumped at a constant rate of 48 gpm to the carbon contactors. During backwash of the dual-media filters, the water stored in the holding tank serves as feed to the carbon contactors.

At the flow rate of 48 gpm, contactor residence time based on an empty bed is 15 minutes each or 45 minutes total. This and other contactor constants are given in Figure 4.

Operation of the system is continuous over a 24-hour period and over run lengths of roughly one-month duration. During runs, the lime clarification process normally never requires shutdown; however, the carbon contactors require periodic shutdown which normally occurs when the headloss in the lead contactor is such that a flow of 48 gpm cannot be attained. When this occurs, the contactor is shut down, backwashed and then returned to service.

System performance was monitored initially by both grab sampling and composite sampling. Grab samples normally were taken manually every 3 hours at first, and later by automatic samplers every hour. Grab sampling was discontinued midway in the study and only composite sampling done.

Samples of the lime clarification process feed and product were taken for TOC, BOD, COD, turbidity, suspended solids, and phosphate determination. The feed and product of the carbon contactors were sampled for TOC, BOD, COD, and turbidity measurements. In addition, the product from carbon contactor one and two was sampled for TOC, BOD, and COD determinations. Late in the study, nitrogen forms around the system were determined. After establishing

- (a) Filtrasorb 300, Calgon, Inc. Mention of specific proprietary equipment or products throughout this paper is for information purposes only and does not constitute endorsement by the Federal Water Pollution Control Administration and the U. S. Department of the Interior.

a ratio between TOC and BOD, and TOC and COD, only TOC was monitored around the system.

All samples were analyzed by Standard Methods (a).

Results and Discussion

Results will be presented in three parts: first those pertaining to carbon contactor performance; second, those pertaining to lime clarification at high pH; and last, those pertaining to the performance of the system as a whole.

Data on nitrogen and ratio results between TOC and BOD, and TOC and COD are given in the Appendix.

Carbon Contactor Performance

TOC profiles through the carbon contactors for increments of one million gallon throughput are given in Figure 5. The average TOC of the feed was 25 mg/l and the average product TOC was 11 mg/l. The range in feed TOC values was 20 to 33 mg/l. As can be noted, the effect of this variation in feed TOC on product TOC was damped by increased removal of TOC by contactor one. It is apparent that the lead contactor serves the important function of buffering increased TOC loadings.

In Table 1, the percent organic matter removed by the carbon contactors is given as TOC, BOD, and COD. As can be seen, organic removal was about the same regardless of the organic parameter utilized as a quantitative measure.

TABLE 1 - TOTAL PERCENT ORGANICS
REMOVED BY CONTACTORS

TOC (1)	57
BOD (2)	59
COD (2)	60

(1) Based on 5 MG

(2) Based on 3 MG

Organic removal as a function of contactor residence time is shown in Figure 6. The data suggest that the percent of the soluble organic matter removed cannot be substantially improved by increasing contactor residence time.

(a) Standard Methods for the Examination of Water and Wastewater 12th Edition, 1965, American Public Health Association, Inc. 1790 Broadway, New York, N. Y. 10019

Contactor loading data are given in Table 2. The loading in lbs TOC per lb of carbon shown for contactor one is considered very good since the contactor is only partially exhausted. In gallons of primary effluent treated, this loading in gallons treated per pound of carbon is roughly 2000. It appears realistic to project a treatment of 4000 gallons per pound of carbon (250 lb carbon/MG) before the carbon requires changing. This suggests carbon replacement costs of less than \$0.07 per thousand gallons for one-time usage of the carbon and, if carbon regeneration is considered, the costs look economically attractive.

TABLE 2 - CARBON TOC LOADING - 5 MG

<u>Contactor Number</u>	<u>Lbs TOC Removed</u>	<u>Lbs TOC Removed per Lb Carbon</u>
1	367	0.153
2	169	0.070
3	51	0.021

TOC removed per lb of carbon as a function of TOC applied per lb of carbon is shown in Figure 7 for each contactor. These data represent the cumulative TOC applied and removed per million gallon increment of flow through the contactors. As can be seen, the TOC removal rate by contactor one decreased as the carbon became loaded with TOC. However, the TOC removal rate by contactor two increased as the carbon became loaded with TOC. This suggests that as contactor one becomes progressively exhausted it progressively passes an increasing amount of adsorbable organics to contactor two. TOC removal by contactor three was essentially constant at all loading rates. This seems to indicate that contactor two passes a relatively constant amount of adsorbable TOC to the third contactor.

Carbon Contactor Operational Problems

The carbon contactors became anaerobic early in the operational period. This was evident by the odor of hydrogen sulfide gas in the contactor effluent. The amount of hydrogen sulfide present was not measured quantitatively. An attempt was made midway in the study to operate the contactors in an aerobic condition. The first method used was to aerate the holding tank prior to the carbon contactors. Air was used first and then oxygen. Neither method injected enough oxygen into the feed to maintain the lead carbon contactor aerobic. Oxygen was then injected directly into the feed stream at the inlet to the lead contactor. This eliminated the hydrogen sulfide from the contactor effluent after a short operational period which indicated the contactors were operating aerobically. After a period of less than a day running time, however, a large leadloss developed in the lead contactor and maintaining the desired

flow rate through the contactor became impossible. The contactors were shut down, the lead contactor backwashed, and then all contactors put back into operation.

Rapid buildup of headloss across the lead contactor continued despite frequent backwash. The lead contactor was again shut down, partially drained, and its surface layer inspected. The layer was found to be greatly impregnated with calcium carbonate. The holding tank prior to the contactor was then drained and inspected and a heavy deposit of calcium carbonate was found at the bottom. This deposit probably accumulated during the high pH run when large quantities of lime were used to raise the pH above 11.5 in the clarifier. During backwash of one of the dual-media filters, the volume of water entering the holding tank is decreased by a half and the holding tank level drops to half or less. The momentum of the incoming water is probably sufficient enough at low water levels to create a bottom turbulence in the tank and the turbulence puts bottom deposits such as calcium carbonate into the feed to the contactor.

The holding tank was thoroughly flushed out with water, the lead contactor acid rinsed with 40 gallons of pH 2.0 sulfuric acid solution and backwashed, and then the contactor was returned to service. At this point the contactor throughput was approximately 1.5 million gallons. Headloss across the contactor was then normal. It was decided to cease feeding oxygen to the contactors and thereby let them become anaerobic. It was felt that the oxygen was promoting the growth of aerobic slime-producing microorganisms and contributing to leadloss buildup.

Following the acid rinse of the lead contactor and the cessation of oxygenation of the contactors, headloss buildup assumed a reasonable magnitude.

Lime Clarification at pH >11.5

As previously mentioned, it has been reported that lime clarification of raw wastewater at a high pH results in the hydrolytic breakdown of organic matter which subsequently enhances its removal by carbon adsorption (7). In an effort to evaluate this, the lime clarifier was operated at a pH greater than 11.5 over an eleven day operational period. The lime clarifier pH range for the period was 11.10 to 11.75 and the pH averaged 11.59. To achieve this pH level, lime dosages in excess of 1100 mg/l were necessary as compared to 200 to 300 mg/l to achieve pH 9.5. All other operational procedures and methods as previously described were the same. Operational sequence of the high pH run relative to the low pH runs was: 31 days at pH 9.5, 11 days at pH greater than 11.5, and 30 days at pH 9.5.

Removal of organic matter from primary effluent clarified at a pH greater than 11.5 is shown in Table 3. For comparative purposes similar data are given for the pH 9.5 runs. The high pH results were averaged over a throughput of 0.7 million gallons while

the low pH results were averaged over a throughput of 5.0 million gallons. Since a low pH run preceded and followed the high pH run, it is reasonable to assume that prior history of the carbon contactors did not prejudice the results to any significant extent.

As can be seen in Table 3, the pH level did not have a significant effect on product quality as measured by BOD, COD, and TOC, nor did it affect a greater percentage removal of organic matter.

TABLE 3 - CARBON ADSORPTION OF ORGANICS FROM PRIMARY EFFLUENT CLARIFIED AT pH 9.5 and pH >11.5

	<u>TOC</u>	<u>BOD</u>	<u>COD</u>
pH 9.5: % Removed	56.0	58.7	60.4
Product Average, mg/l	11.0	10.0	31.0
Product Range, mg/l	2.9-22	2.0-23	11-70.6
pH >11.5% Removed	53	56.2	59.6
Product Average, mg/l	9.8	14.5	31.0
Product Range, mg/l	6.4-12.2	6.6-19.4	12.0-42.6

Some improvement in the turbidity of the effluent from the lime clarifier was noted at the higher pH. This was probably because of the removal of fine turbidity matter by the magnesium hydroxide floc which forms at a pH above 11.

Overall System Performance

Organic matter removed by the complete system as determined by TOC, BOD, and COD measurements is given in Table 4. As shown, lime clarification removed 76 percent of the organic matter. This suggests that the amount of organic matter present in Lebanon primary effluent that is amenable to removal by clarification and adsorption mechanisms is, on the average, 76 percent suspended and 24 percent soluble in form.

TABLE 4 - TOTAL ORGANIC REMOVAL FROM PRIMARY EFFLUENT BY LIME CLARIFICATION AND CARBON TREATMENT

	<u>TOC</u> (1)	<u>BOD</u> (2)	<u>COD</u> (2)
Total Organic Removal			
mg/l	66	66	165
lbs/MG	550	550	1376
Percent Removed by Lime Clarification	76	76	76
Percent Removed by Carbon Adsorption	24	24	24

(1) Based on 5 MG
(2) Based on 3 MG

The percent removal distribution of the applied organic loading between the processes and that remaining in the product is shown in Table 5. As can be noted, 66 percent of the applied organic matter was removed by clarification, 21 percent by adsorption, and 13 percent was not removed by either process and remained in the product water. Assuming that essentially no soluble organic matter is removed by lime clarification, the data indicates that roughly 34 percent of the applied organic loading was soluble in form and, surprisingly, 13 percent of the soluble organics were not removed by carbon adsorption.

TABLE 5 - THE DISTRIBUTION OF THE APPLIED ORGANIC LOADING

	TOC (1)	BOD (2)	COD (2)
Removed by Lime Clarification, %	66	66	65
Removed by Carbon Adsorption, %	21	21	21
Remaining in Product, %	13	13	14

(1) Based on 5 MG

(2) Based on 3 MG

NOTE: Overall removal by lime clarification and carbon adsorption was 87% TOC, 87% BOD and 86% COD based on primary effluent. If 35% removal of BOD in the primary tanks is assumed, the overall BOD removal by primary treatment, lime clarification and carbon adsorption is 91.5%.

It is anticipated that raw wastewater could be fed directly to the lime clarifier (without primary treatment) without affecting product quality.

Turbidity, suspended solids, and phosphate removal data for the system are given in Figure 8. Removal in each instance was good. As would be expected, the carbon contactors tend to remove suspended matter and thus turbidity, that escapes the dual-media filters. Phosphates are not removed by activated carbon.

Organic concentrations of the feed and product stream as shown in Figure 8 indicate that overall system performance was quite good. The quality of the water obtained solely by lime clarification of primary effluent is probably equal to that discharged by many conventional treatment plants today plus the added benefit of phosphate removal. Final product water quality is equal to that required for direct discharge and for many reuse purposes.

In Table 6, a comparison is made between wastewater quality attainable by good conventional treatment and that attained in the present study by lime clarification and carbon adsorption. The data given for activated sludge treatment was obtained from measurements made on secondary effluent from a pilot plant activated sludge

unit operating at a constant feed rate. This unit utilizes primary effluent from the Municipal Treatment Plant and treats it by conventional activated sludge methods. The secondary effluent from this unit is normally of good quality with an organic carbon content of 20 mg/l or less and a turbidity of 10 or less JTU. As shown in Table 6, the quality of effluent produced by lime clarification and carbon adsorption was slightly better than that of the secondary effluent used as the standard, and probably significantly better in quality than the effluent produced by the majority of treatment plants now in operation that utilize conventional treatment methods.

TABLE 6 - COMPARISON OF CONVENTIONAL TREATMENT AND PHYSICAL AND CHEMICAL TREATMENT

<u>Treatment</u>	<u>BOD</u> ⁽¹⁾	<u>TOC</u> ⁽¹⁾	<u>JTU</u>
Activated Sludge	79-13 (a)	59-12 (b) 72-12	2.4
Lime and Carbon	76-10	76-10	1.1

(1) Based on 1 MG

(a) First group of figures are influent, second group effluent

(b) Results from two separate sampling periods.

General Comments

In assaying the results presented, two factors must be considered. First, the system under study was operated at a steady flow. The effect of diurnal variation in the flow of wastewater on the performance of the system was not determined. However, there is some evidence that several magnitudes of change in flow rate through a carbon contactor do not materially affect product quality (9)(10). The effect of variation in flow on the performance of the lime clarification process is not known.

Second, the primary effluent used as the feed to the system is highly domestic in nature and is weak to moderate in strength. Conceivably the results would be significantly altered if a strong strength wastewater were used as the feed.

The results must also be considered in light of certain deficiencies in the system. For one, the carbon contactors were not designed for efficient backwash. This most likely resulted in the establishment of a microbial population in the contactors, particularly the first one. Undoubtedly, some of the organic matter removed in the contactors was removed through biological metabolic activity. This poses the question as to whether or not the organic matter that survives carbon treatment is qualitatively and quantitatively the same whether or not the contactors are operated anaerobically or aerobically. It probably is not since the metabolic pathways are different and result in different end products. Possibly then, the magnitude of the

organic content in carbon treated effluent could be influenced by operating conditions imposed on the contactors.

Second, operation of the contactors anaerobically is probably not desirable because of the ultimate problem of removing the hydrogen sulfide gas in the effluent. Air stripping would create odor problems. Oxidation to sulfate with chlorine or ozone could be costly. Costs involved, however, could be compared to the costs of oxygenating the contactors.

Summary and Conclusions

The results of the work thus far show that the treatment of primary effluent by lime clarification and activated carbon produces an effluent of good quality suitable for discharge. Averaged over a five million gallon throughput, effluent TOC and BOD were 10 mg/l with an overall range of 2-23 mg/l. Effluent turbidity averaged less than 2 Jackson turbidity units. Phosphate removals were consistently 90 percent or better. These characteristics are consistent with those associated with good quality secondary effluent plus the added bonus of phosphate removal.

Carbon contactor performance to date suggests that the lead contactor will treat 4000 gallons of lime clarified primary effluent per pound of carbon before requiring replacement. This projects a carbon make-up cost of \$0.07/1000 gallons without recovery of carbon, and, possibly, less than \$0.01/1000 gallons if the carbon is regenerated. These costs suggest that carbon treatment may be competitive with biological treatment as a means of removing soluble organics from primary or raw wastewater. However, sufficient information is not presently available to positively conclude this.

The results presented must be considered in the light of certain factors. First, the system was run at steady flow. Second, the feed to the system was a weak to moderate strength domestic wastewater. How the system would respond to a number of magnitudes of change in these factors is presently only speculative.

It is concluded that: (1) wastewater treatment to a quality level comparable to that achieved by good conventional methods is technically feasible using lime clarification and activated carbon treatment, and (2) projected costs based on carbon contactor performance thus far suggest that the removal of soluble organics from raw wastewater by activated carbon will be economically attractive.

References

1. Berg, E. L., and Williams, Robert T., "Single Stage Lime Clarification of Secondary Effluent," FWPCA, AWTRL, July 1968.
2. O'Farrell, Thomas P., et al., "Advanced Waste Treatment at Washington, D. C." FWPCA, AWTRL, May 1969.
3. Bishop, Dolloff F., et al., "Studies on Activated Carbon Treatment," JWPCF, Vol. 39, 188-203 (1967).
4. Culp, Gordon, and Culp, Russell, "Reclamation of Waste Water at Lake Tahoe," Public Works, February 1966.
5. Parkhurst, John D., et al., "Pomona 0.3 MGD Activated Carbon Plant," Presented at the 39th Annual Conference of the WPCF, Kansas City, Mo., September 1966.
6. Schmid, L. A., and McKinney, Ross E., "Phosphate Removal by Lime-Biological Treatment Scheme," JWPCF, July 1969.
7. Zuckerman, M., and Molof, A. H., "Chemical vs. Biological Wastewater Treatment in the Production of High Quality Reuse Water," Presented in part, 2nd National Symposium Sanitary Engineering Research, Development, and Design, ASCE, Ithica, N. Y., July 1969.
8. Van Hall, C. E., et al., "Rapid Combustion Method for the Determination of Organic Substances in Aqueous Solution," Anal. Chem., Vol. 35, 3 (1963).
9. Culp, Gordon, and Slechta, Alfred, "Plant Scale Regeneration of Granular Activated Carbon," Final Progress Report, USPHS Demonstration Grant 84-01, February 1966.
10. Villiers, R. V., "Effect of Diurnal Flow Variation on TOC Removal by Carbon Adsorption," Internal CWRL Report, 1969.

APPENDIX

Nitrogen Data

Some nitrogen data were gathered during the latter part of the study to determine the magnitude of the nitrogen forms present in lime clarified and carbon treated primary effluent. These data are given in Table 7. As can be seen, there was a substantial increase in ammonia nitrogen during carbon treatment. This is probably attributable to the ammonia produced by the hydrolysis of cellular matter present in the suspended organic matter reaching the carbon contactors. This is evidenced by the decrease in organic nitrogen across the carbon contactors. Nitrite and nitrate content of the final product was always less than 0.2 mg/l.

The amount of ammonia nitrogen present is typical of that found in most good quality secondary effluents since few conventional activated sludge treatment plants nitrify. Probably the organic nitrogen is somewhat less than that found in conventional secondary effluent.

TABLE 7 - NITROGEN BALANCES AROUND SYSTEM⁽¹⁾

	<u>NH₃-N</u>	<u>Org-N</u>
Primary Effluent	11.5	4.2
Lime Clarified Primary	13.2	2.1
Lime Clarified-Carbon Treated Primary	16.8	1.0

(1) Based on 2 MG. All data in mg/l.

TABLE 8 - ORGANIC PARAMETER RATIOS

<u>BOD/TOC Ratio</u>		
Lime Clarified Primary	$\frac{25.8}{22.0} = 1.17$	$\frac{26.5}{23.2} = 1.14$
Carbon Contactor No. 1 Product	$\frac{15.5}{15.5} = 1.00$	$\frac{12.7}{11.2} = 1.13$
Carbon Contactor No. 2 Product	$\frac{11.4}{10.9} = 1.05$	$\frac{11.0}{9.6} = 1.15$
Carbon Contactor No. 3 Product	$\frac{11.9}{11.6} = 1.03$	$\frac{9.0}{9.6} = 0.94$

Average of all ratio results = 1.08 = $\frac{\text{BOD}}{\text{TOC}}$

COD/TOC Ratio

Lime Clarified Primary	$\frac{79}{22} = 3.59$	$\frac{72.0}{23.2} = 3.10$
Carbon Contactor No. 1 Product	$\frac{37.3}{15.5} = 2.4$	$\frac{40.2}{11.2} = 3.57$
Carbon Contactor No. 2 Product	$\frac{27.7}{11.6} = 2.39$	$\frac{36.4}{9.6} = 3.79$
Carbon Contactor No. 3 Product	$\frac{27.4}{10.9} = 2.51$	$\frac{35.5}{9.6} = 3.68$

Average of all ratio results = 3.13 = $\frac{\text{COD}}{\text{TOC}}$

TABLE 9 - TOC DATA PER MILLION GALLON INCREMENT OF THROUGHPUT

Gallons Throughput	Feed TOC, mg/l	Contactor Product TOC, mg/l		
		1	2	3
1035000	25.8	13.1	11.3	10.6
2005000	21.3	14.0	11.6	10.8
3040000	18.7	12.9	9.1	8.4
4058000	24.3	19.6	14.8	13.4
5024000	32.9	19.6	11.8	9.6
Average	24.6	15.8	11.7	10.6

TABLE 10 - LBS TOC APPLIED, REMOVED, AND REMAINING PER MILLION GALLON OF THROUGHPUT

LBS TOC APPLIED PER MILLION GALLON INCREMENTS OF THROUGHPUT						
	1	2	3	4	5	Total
Contactore 1	223	173	161	206	265	1028
Contactore 2	113	113	111	166	158	661
Contactore 3	98	94	79	126	95	492

LBS TOC REMOVED PER MILLION GALLON INCREMENTS OF THROUGHPUT						
	1	2	3	4	5	Total
Contactore 1	110	60	50	40	107	367
Contactore 2	15	19	32	40	63	169
Contactore 3	7	7	7	12	18	51

LBS TOC REMAINING PER MILLION GALLON INCREMENTS OF THROUGHPUT						
	1	2	3	4	5	Total
Product	91	87	72	114	77	441

$$\text{TOC Removed, \%} = \frac{\text{Total Removed}}{\text{Total Applied}} = \frac{587}{441 + 587} = 57$$

TABLE 11 - LBS TOC APPLIED AND REMOVED PER LB CARBON
PER MILLION GALLON INCREMENT OF THROUGHPUT

LBS TOC APPLIED PER LB OF CARBON FOR MILLION GALLON INCREMENTS OF THROUGHPUT						
	1	2	3	4	5	Total
Contactora 1	.043	.072	.067	.086	.110	.430
Contactora 2	.047	.047	.046	.069	.066	.275
Contactora 3	.041	.039	.033	.053	.040	.205

LBS TOC REMOVED PER LB OF CARBON FOR MILLION GALLON INCREMENTS OF THROUGHPUT						
	1	2	3	4	5	Total
Contactora 1	.046	.025	.021	.017	.045	.153
Contactora 2	.006	.008	.013	.017	.026	.070
Contactora 3	.0029	.0029	.0029	.005	.008	.021

ADVANCED WASTE TREATMENT OF
SECONDARY EFFLUENT WITH ACTIVATED CARBON

John L. Rose
Chief Sanitary Engineer

Burns and Roe, Inc.
Oradell, New Jersey 07649

Introduction

The past decade has seen a fundamental change in our concepts of waste treatment and pollution control. Originally, the treatment of municipal wastes was primarily concerned with the preservation of public health. Next we became concerned with esthetic concepts such as the elimination of visible signs of pollution and the maintenance of oxygen levels for sustenance of marine life in receiving waters. In the last decade two new concepts have been developed. The first is that in many areas water is becoming scarce so that it may be necessary to use water more than once. The second is that natural waters should be maintained in a condition of purity so that the overall impact of water use on the environment is minimized. Both of these concepts require treatment of wastewaters that is fundamentally different from the treatment that was acceptable at a time when our only concerns were with public health, esthetics, and oxygen depletion. In this context activated carbon adsorption is the key unit process in the treatment of wastewater to produce effluents meeting our present requirement for effluent quality and receiving water preservation.

The use of coal in water treatment goes back to the last century. In 1883, 22 water plants in the United States were reported to be employing charcoal filters. These were later abandoned because of the low adsorptive capacity of the charcoal. The production of activated carbon was started in 1913 by a predecessor of Westvaco. However, its first recorded application to municipal water treatment was not until 1927 when two Chicago meat packing companies used powdered activated carbon to remove tastes from their water supplies. During the 1930's, the use of powdered activated carbon to remove tastes and odors caused by traces of dissolved organics spread rapidly.

In 1960, the U. S. Public Health Service embarked on the Advanced Waste Treatment Research Program with two stated goals - to help abate water pollution problems and, more startling in concept, to renovate water for direct and deliberate reuse. The program focused early on adsorption as the most promising process for achieving its stated goals, and on activated carbon as the most feasible adsorbant. A series of studies were commissioned by the Public Health Service and, since 1966, the Federal Water Pollution Control Administration, to evaluate the feasibility of activated carbon adsorption for wastewater renovation. These studies concentrated on two aspects - the physical configuration for the

most economical use of the adsorptive properties of the carbon and the reactivation of the carbon for reuse.

Based on results of these studies, several demonstration plants were designed to obtain data from commercial equipment. One of these plants is a joint effort of the County Sanitation Districts of Los Angeles County and the Federal Water Pollution Control Administration and is located at Pomona, California. The plant includes five carbon contactors and has a capacity of 400 gpm. A second plant is located at Lake Tahoe, California and is operated by the South Tahoe Public Utility District. The plant has a capacity of 7.5 mgd. A third plant, located on Long Island, New York, is the subject of this paper.

Background

Nassau County occupies 291 sq. mi. of Long Island immediately adjacent to the City of New York. During the last two decades, the County has experienced an explosive growth of population and water consumption. Since the County's only source of water supply is the local ground water, whose safe yield is limited by its rate of recharge, the continuation of this growth presages a crisis in water supply. Over-pumping results in lowering of the ground water levels and intrusion of salt water in the aquifer.

Development of the County has also decreased the rate of recharge of the ground waters. The installation of public sewer system diverts wastewater previously recharged into the ground through septic tanks and cesspools to ocean outfalls. Present projections indicate that, if present trends continue, the net amount of water withdrawn from the aquifers will exceed the rate of recharge by 1977.

One plan to increase the permissible withdrawals is to create a hydraulic barrier in the aquifer. This barrier would prevent a natural outflow in the aquifer, estimated to be of the order of 30 mgd which is now lost to the sea. It would also prevent the intrusion of salt water into the aquifer which is already becoming a problem in some areas of Nassau County. The barrier would be formed by injecting tertiary treated wastewater through a series of recharge wells along the southern perimeter of Nassau County.

Water Quality Requirements

In order to provide water of a quality necessary for injection into public water supply aquifers, the effluent of the existing sewage treatment plant must receive additional treatment to meet the following requirements:

1. U. S. Public Health Service Standards for drinking water.
2. Economical operation of injection system.
3. Chemical compatibility with natural ground water.

The drinking water standard was adopted primarily in order to gain public acceptance of the concept of injecting treated wastewater into an aquifer which is used as a source of public water supply. Present plans provide for maintaining at least one mile separation between injection and water supply wells. This distance will insure that no particulates or bacteria will reach the water supply wells. Nevertheless, it was decided as a policy matter that the water as injected must meet the standards for drinking water.

Advanced Waste Treatment Process

The advanced waste treatment process used to achieve these water quality criteria consists of coagulation with alum, filtration, adsorption on activated carbon and disinfection with chlorine.

Standards of water quality for economical operation of the injection system are being developed as part of the demonstration project. From injection tests conducted thus far, it is apparent that particulates must be maintained at the lowest possible level. Turbidity levels of less than 0.5 J.U. appear to be desirable. Low levels of dissolved gases were considered desirable during the early stages of the project but do not appear to be as critical as they were thought to be. Turbidities in excess of 1.0 Jackson Units result in rapid buildup of pressure required to inject at a given rate of flow.

The principal problems of compatibility involve iron and phosphate concentrations. Iron precipitates in the aquifer, causing irreversible clogging of the formation. The role of phosphates is not yet fully understood. However, changes in phosphate concentration between water injected and injected water recovered have been observed, leading to the conclusion that phosphates interact with the fine clayey sands that comprise the aquifer.

Effluent from the final sedimentation tanks of the Bay Park Sewage Treatment Plant is pumped into a clarifier, where alum and coagulant aids are added. Sludge recirculation is employed to improve coagulation and overcome sudden changes in water quality. Flow then passes by gravity to two mixed media filters operated in parallel, each containing a 36-inch bed of anthracite above a 12-inch layer of sand. Filter backwash is automatic, and includes facilities for air scour, surface wash, and high and low rate backwashing.

Filter effluent is pumped through four granular activated carbon adsorbers operating in series. Adsorber piping is arranged so that the order of the vessels can be rotated to change the sequence of flow and insure the most efficient utilization of carbon. Upon exhaustion, carbon is moved hydraulically to a regeneration system. Here the carbon is restored to its original activity by controlled burning off of the adsorbed organics in a multi-hearth furnace.

The renovated water is disinfected with chlorine prior to being pumped about one half mile to the test injection site. The injection facilities consist of a storage tank, degasifier for removal of residual chlorine and dissolved gases, injection and redevelopment pumps, the injection well

and 12 observation wells. The injection well is 36 inches in diameter by 500 ft. deep, and contains an 18 inch casing which supports a 16 inch screen set between elevations - 420 and 480 ft. The annular space surrounding the screen has been backfilled with graded sand and contains an observation well and geophysical probes. Other observation wells are located up to 200 ft. from the injection well.

Carbon Adsorption System

The design of a carbon adsorption system for the treatment of wastewaters involves consideration of the following parameters:

Type of carbon - granular or powdered
Physical configuration - upflow or downflow, or mixed
number of stages, parallel or series, packed bed or expanded
bed, external regeneration or continuous flow
Carbon capacity - detention time, dosage rate
Method of operation - pure adsorption, filtration, biochemical

For the Nassau County project, granular carbon was selected over powdered carbon primarily because of the state of the art of carbon regeneration. Powdered carbon has some advantages over granular carbon. Its initial cost is lower, 7½ cents per pound against 30 cents for granular carbon. It reacts faster and more completely, and its dosage can be adjusted to meet changes in the composition of the influent to the system. On the other hand, even the cost of powdered carbon is not sufficiently low to permit its discard after a single use. Some experimental work is now in progress on powdered carbon regeneration, but it has not yet reached the stage where a full scale demonstration plant can be designed. Dewatering and incineration are the most feasible methods of disposal of waste powdered carbon.

Granular carbon has been in industrial use for many years and the technology for its regeneration is well established. It has the additional advantage of providing a margin of safety in operation that powdered carbon does not provide. Sudden changes in influent composition are common in wastewater treatment. If the dosage of powdered carbon is not adjusted to meet these changes, the effluent quality will reflect the insufficient dosage. Granular carbon has the capacity to withstand substantial changes in the influent composition with a much reduced effect on the effluent quality. This aspect and the availability of the regeneration technology were the major factors in the selection of granular carbon for the Bay Park project.

Even after the choice has been made between granular and powdered carbon, some further selectivity is required. Activated carbons are manufactured from a variety of raw materials such as coal, wood, nut shells and pulping wastes. A carbon that must undergo multiple regenerations must have the capability of being handled with a minimum of deterioration or abrasion. Since coal derived carbons are harder and denser than other carbons, this type of carbon was specified for the Bay Park project.

As a result of operating experience the additional requirement that the carbon contain less than 0.5% of iron by weight has been added.

The limit on the iron also forced a change in the gradation, so that the specifications for carbon could be met with a commercially available product. The original carbon had a size range of 8 x 30 (passing a standard No. 8 mesh sieve, but retained on a No. 30 sieve). The replacement carbon has a size range of 14 x 40.

A number of physical configurations have been suggested for activated carbon adsorption systems. These include upflow-expanded bed, upflow-compacted bed, downflow-single stage, downflow-multistage, and a quasi-countercurrent system, in which the flow is down in the first unit and up in the second unit, exhausted carbon being continuously removed in the first unit and regenerated or makeup carbon being added continuously in the second.

Upflow systems have the advantages of being less susceptible to plugging and more adaptable to continuous countercurrent operations, which in theory yield the most efficient carbon utilization. Downflow systems require periodic backwashing to prevent the buildup of headloss and multistaging to approach countercurrent operation. The differences in equipment costs are of a second order compared with the costs of regeneration and makeup. Downflow systems are mechanically simpler and have greater flexibility as to rates of flow that can be applied. For the Nassau County project, a four-stage downflow system was selected. The four vessels containing the carbon are piped so that they are in series, with each unit capable of being the lead unit. In normal operation, the flow is applied to the vessel containing carbon closest to exhaustion. As it passes from unit to unit, it encounters successively more active carbon, until in the last unit it passes through the most recently regenerated carbon.

When the organic content of the product water starts to exceed the desired level, the first unit is taken off the line and the carbon in this unit is transferred hydraulically to the dewatering tank of the carbon regeneration system. As soon as the transfer is completed, regenerated and makeup carbon from the storage tank is pumped back into the unit. The unit is then put back on the line, but in the last position in the sequence. In this manner, the countercurrent mode of the operation is maintained.

Laboratory bench and pilot plant studies were relied upon to furnish other design data. Laboratory bench studies were used to derive adsorption isotherms, which give some indications as to carbon dosage. Column tests were then used to determine the required contact time. The hydraulic loading then becomes a matter of convenience for the design of the equipment. For the Nassau County project, the following design parameters were adopted, based on over a year's pilot plant operations:

Total contact time (empty bed volume) 24 min
Hydraulic Loading (approach velocity) 7.5 gpm/sq ft.

The combination of these factors resulted in a vessel diameter of 8 ft and a bed depth of 6 ft in each vessel. Each of the vessels contains 300 cu ft or about 9,000 lb of carbon. The rate of exhaustion has been about 800 gal per pound of carbon or 1.25 lb per 1000 gal treated.

Economics

Unit costs for the advanced waste treatment process are given in the following table. The table is based on a COD reduction 90% from 50 mg/l in the secondary effluent to 5 mg/l in the product water and a phosphate reduction of 90% from 30 mg/l (as PO₄) to 3 mg/l.

Estimated Unit Costs

Cents per 1000 gal	Plant Capacity		
	1 mgd	10 mgd	100 mgd
Process costs, less labor			
Coagulation	4.9	3.5	3.2
Filtration	1.8	1.1	1.0
Carbon adsorption	<u>6.3</u>	<u>4.5</u>	<u>4.0</u>
	13.0	9.1	8.2
Operating labor	<u>28.0</u>	<u>5.6</u>	<u>1.8</u>
	41.0	14.7	10.0

Annual charges have been assumed at 8.5% of the capital costs and include both debt service and an allowance for maintenance, repair and replacement. Unit costs also assume continuous operation at design capacity (100% load factor). The costs are for treatment only and do not include transmission or injection facilities.

Conclusions

The Nassau County project is demonstrating the feasibility of treating secondary effluent with a physiochemical process sequence involving activated carbon to remove organics resistant to biological treatment. The product water meets U.S. Public Health Service Standards for drinking water and has physical properties such as turbidity, color or odor equivalent to those of the domestic water supply. It can be recharged into the ground without causing any deterioration of the aquifer. Based on test operations now in progress, it is believed that the concept of using treated wastewater for hydraulic barriers against seawater intrusion is technically feasible.

The project opens up new potentials for water reuse in areas where fresh water supplies are scarce. Wastewater is always available where there are public water supply and sewerage systems. Newly adopted water quality standards will require many communities to provide more than conventional secondary treatment. With activated carbon treatment, the product water can now be made available for many forms of beneficial reuse requiring high quality water.

USE OF ACTIVATED CARBON FOR MINE WATER TREATMENT

Edward A. Mihok

U.S. Department of the Interior
Bureau of Mines
Pittsburgh Mining Research Center
4800 Forbes Avenue
Pittsburgh, Pennsylvania 15213

ABSTRACT

Extremely rapid oxidation of the ferrous iron in raw acid mine water is possible without the use of costly oxidants and precipitating agents. This was achieved by catalytic oxidation in an activated carbon-air-mine water system. The ferrous iron content of an acid mine water flowing through aspirated, granular, activated carbon was reduced from about 700 to 10 ppm in less than 1 minute. Incorporating a catalytic oxidation step in the treatment of acid mine water containing ferrous iron would facilitate treatment by virtual elimination of aeration equipment and precise stoichiometric control of pH. Limestone would replace expensive alkaline reagents, thus lowering reagent costs. Finally, smaller settling ponds would result through sludge volume reduction. The process would essentially consist of oxidation, neutralization, and settling of solids.

INTRODUCTION

Mine drainage is now classified as an industrial waste. Although mine waters vary widely in chemical composition, the most damaging constituents--acid sulfate and/or iron--are invariably present, and economical removal of these pollutants constitutes the problem of mine water treatment at the present time. From an economic standpoint, one of the most difficult technical aspects of mine water treatment is iron removal. If the iron is in the ferric state (Fe^{+++}), removal would be relatively simple and inexpensive. Iron, aluminum, and acid could be effectively removed from mine water by raising the pH to about 6 with a cheap alkaline agent such as limestone. However, in most mine waters the iron is predominantly in the ferrous form (Fe^{++}). Ferrous iron is more difficult and more expensive to remove, especially when present in appreciable quantity.

Conventional mine-water treatment processes consist of lime neutralization, aeration, and sludge settling. Aeration is utilized primarily to oxidize ferrous iron because less sludge results when iron is in the ferric form, and savings in reagent costs can be realized with the use of lower pH. If aeration were not applied, a high pH (about 9) would be needed to guarantee a low soluble iron content (<7 ppm) in the treated water. Larger sludge volumes would result because of a more flocculent precipitate and thus further complicate the sludge disposal problem.

An inherent disadvantage to this mode of treatment is the difficulty of process control. Neutralization of acidity is not achieved until most of the iron has been converted to the insoluble ferric state. Therefore, regulation of the alkaline reagent feed cannot be established by a set pH limit for efficient operation without continuous monitoring of acidity and ferrous iron load. Some semblance of control is possible if the raw mine water feed is equilibrated in holding ponds and aeration equipment capabilities and performance are firmly established. But sudden changes in the acid and iron load may result in excess alkalinity or acidity in the treated water. Only experience and trial and error, therefore, can provide some degree of control in such a mine water treatment process.

When acid mine water is exposed to the atmosphere the ferrous iron oxidizes to ferric iron. The oxidation rate, however, is exceedingly slow, even with the aid of aeration (1).^{1/} To accommodate large volumes of mine water having appreciable ferrous iron, prohibitively large basins and aeration facilities would be required. Chemical oxidants can be used to accelerate the rate of oxidation, but a brief analysis of the stoichiometric requirements and the unit cost of oxidants show that such oxidation would be too costly. Certain substances (2) enhance the oxidation of ferrous iron, but none are used in practice.

The best approach to acid mine water treatment is to convert the ferrous iron to the ferric form prior to neutralization. Complete iron removal would then readily be achieved by simply increasing the pH above 4.5.

Recent developments (2) in the Bureau of Mines Pittsburgh Mining Research Center laboratory indicate that extremely rapid ferrous iron oxidation in an acid mine water is possible without the use of high-priced chemical oxidants, without expensive precipitating agents, and without extensive aeration equipment. This catalytic oxidation reaction was achieved in an activated carbon-air-mine water system. Activated carbon accelerates the rate of oxidation of ferrous iron in sulfuric solutions (4). Acid mine water effluents are dilute solutions of sulfuric acid and acid salts. Although only an exploratory effort was made with granular activated carbon as a means of catalyzing the air oxidation of ferrous iron in acid mine water, the initial results are promising. The brevity of this study did not allow defining the reaction kinetics or resolving the factors affecting the activated carbon-air-acid mine water system. Therefore, only a general description of the test and the test results can be made.

EXPERIMENTAL WORK

The carbon used throughout the tests was a commercial-type, coal-base, activated carbon sized 12 by 40 mesh. Mine water containing 613 to 945 ppm Fe⁺⁺, 810 to 960 ppm total Fe, 2,100 to 2,400 ppm total acidity, and with a pH ranging from 2.70 to 3.15 was used for the tests. A typical analysis of the mine water is shown in table 1.

TABLE 1. - Typical mine water analysis

pH	3.10
Eh	6.05
Total acidity	ppm 2,370
Fe ⁺⁺	ppm 830
Total Fe	ppm 965
Ca ⁺⁺	ppm 220
Mg ⁺⁺	ppm 66
SO ₄	ppm 4,512
Dissolved solids	ppm 7,080

The experimental apparatus consisted of a glass cylinder with a fritted disk connected to a filtering flask. The disk supported the granular carbon and allowed passage of air and water. A side tube in the filtering flask was connected to an aspirator. The same batch of activated carbon (200 grams, 12 by 40 mesh) was used in all the tests. Two different glass cylinders were used: In one the carbon column was 6.5 cm in diameter and 12.5 cm in depth; in the other (used in later tests) the carbon column was 3.8 cm in diameter and 42 cm in depth. The longer cylinder was used to increase flow through time. A synthetic porous sponge supported the granular carbon in the cylinder and prevented the loss of

^{1/} Underlined numbers in parenthesis refer to items in the list of references at the end of this report.

carbon particles. A sketch of the activated carbon oxidation apparatus is shown in figure 1.

Air was aspirated through the carbon column before the mine water was added and continuously throughout the test until most of the water had passed through the carbon. The mine water volumes flowing through the carbon column ranged from 175 to 1,070 cu cm per batch (test); airflow rates ranged from 0 to 3,500 cu cm per min.

Prior to testing, the batches of raw mine water were analyzed for pH, ferrous iron, and total iron. Identical analyses were made immediately after testing on the effluent from the activated carbon column. All tests were conducted at room temperature. A total of 65 separate runs, consisting of about 25 liters of raw mine water, were made in the same carbon column over a period of about 2 weeks.

TEST RESULTS

The pH of a suspension of the activated carbon in distilled water was about 6.6. With successive additions of the acid mine water (pH 2.70 to 3.15), the pH of the effluent decreased steadily and appeared to level off at a pH of 2.3 to 2.5 when ferrous iron oxidation was virtually complete. The raw mine water was practically colorless, but the effluent from the carbon column was a deep amber color owing to the presence of a hydroxylated ferric sulfate.

The ferrous iron content (635 to 920 ppm) of the raw mine water was reduced to about 10 ppm after flowing through the carbon column for less than 1 minute. By contrast, aeration of an acid mine water (1) in the absence of an oxidizing agent, except for bacteria which may have been present, reduced the ferrous iron concentration from 261 to about 10 ppm in 168 hours. While a direct comparison cannot be made between these results, they do indicate the enormous increase in the ferrous iron oxidation rate that can be achieved with activated carbon.

The test results are summarized in table 2. These preliminary results indicate that activated carbon catalyzed the air oxidation of ferrous iron in a ferruginous acid mine water. The initial tests also show that the activated carbon must be preconditioned to an acidic state for the catalytic reaction to take place. The low ferrous iron content in the effluent, beginning with run 26, was consistently maintained to the end of the experiment. It was likely that the activated carbon was adequately conditioned at this time. For these tests the total iron (practically all in the ferric form) in the effluent represents about 65 percent of the total iron in the feed.

After 25 liters of a ferruginous mine water had passed through the carbon column, there was no appreciable loss in catalytic efficiency and no visible sign of surface fouling or solids deposition on the surface of the carbon particles, although a portion of the iron was adsorbed by the carbon. It is possible that only an insignificant amount of iron would be held by the carbon in a continuous flow operation. If the pH of the system were maintained below 2.5, ferric hydrolysis would be negligible. The air requirements for oxidation of ferrous iron might be minimal. Run 60, conducted without aspirating air through the carbon column, produced equally effective ferrous iron removal.

TABLE 2. - Batch test results of catalytic oxidation of ferrous iron in acid mine water with activated carbon

Date, 1969	Run	pH	Feed			Feed time, min	Volumic collected, cu cm	Total aspi- rating time, min	Flow, through time, min ¹	Air aspi- rating rate, cu cm per min ²	Effluent			
			Fe ⁺⁺ , ppm	Total Fe, ppm	Vol- ume, cu cm						pH	Fe ⁺⁺ , ppm	Total Fe, ppm	
April 15	1	2.80	613	-	260	3.0	250	5	-	-	4.50	417	-	
	2	2.80	613	-	260	4.0	250	5	-	-	4.30	230	-	
	3	2.80	613	-	260	5.0	250	5	-	-	4.10	272	-	
April 16	4	2.80	613	-	260	3.0	250	6	-	-	3.95	175	-	
	5	2.80	613	-	260	3.0	250	7	-	-	3.75	125	-	
	6	2.80	613	-	260	3.0	260	8	-	-	3.60	130	-	
	7	2.80	613	-	260	3.5	235	8	-	-	3.45	105	-	
	8	2.80	613	-	260	3.5	220	8	-	-	3.35	75	-	
	9	2.80	613	-	260	3.0	225	9	-	-	3.50	80	-	
	10	2.80	613	-	260	3.0	230	10	-	-	3.35	85	-	
	Extracted excess water						-	125	9	-	-	3.15	190	-
	11	2.80	613	-	260	3.0	175	10	-	-	3.05	205	-	
	12	2.80	613	-	260	1.5	225	20	-	-	2.90	220	-	
13	2.80	613	-	260	1.5	210	20	-	-	2.70	165	-		
14	2.80	613	-	260	1.0	200	18	-	-	2.60	145	260		
Cleaned fritted disk														
April 17	15	2.75	745	-	260	1.5	260	5	-	-	2.55	245	-	
	16	2.75	745	-	260	2.0	260	5	-	-	2.55	270	-	
	17	2.75	745	-	260	3.5	260	9	-	-	2.50	275	575	
	18	2.75	745	-	260	3.0	260	5	-	-	2.50	90	-	
	19	2.75	745	-	260	3.0	260	6	-	-	2.45	72	-	
	20	3.15	945	-	260	3.0	260	8	-	-	2.45	70	-	
	21	2.85	920	-	260	3.0	260	10	-	-	2.45	10	215	
Cleaned fritted disk														
April 21	22	2.90	920	-	260	1.5	250	4	-	-	2.45	35	420	
	23	2.90	920	-	750	-	750	12	-	-	2.45	85	-	
	24	2.90	920	-	260	-	250	5	-	-	2.40	70	-	
	25	2.90	920	-	260	-	240	4	-	-	2.40	55	-	
	26	2.70	660	-	260	.5	240	8	-	-	2.50	5	-	
	27	2.70	660	-	260	2.0	250	10	-	-	2.45	2	250	
	28	2.70	660	-	260	.8	250	15	-	-	2.35	2	280	
Cleaned fritted disk														
April 23	29	2.70	900	-	260	1.0	260	4	-	-	2.35	5	-	
	30	2.70	900	-	260	1.0	260	6	-	-	2.30	5	550	
	31	2.70	900	-	260	2.0	250	8	-	-	2.40	5	-	
	32	2.90	800	960	260	3.0	250	11	-	-	2.40	<2	365	
	33	2.90	800	960	260	3.0	250	14	-	-	2.45	<2	430	
	Cleaned fritted disk													
	34	2.90	800	960	260	1.0	260	5	-	-	2.40	5	510	
	35	2.90	800	960	260	3.0	260	10	-	-	2.35	5	540	
	36	2.90	800	960	260	3.0	260	13	-	-	2.35	<2	490	
	37	2.90	800	960	260	4.0	260	21	-	-	2.35	<2	535	

See footnotes at end of table.

TABLE 2. - Batch test results of catalytic oxidation of ferrous iron in acid mine water with activated carbon--Continued

Date, 1969	Run	Feed				Feed time, min	Volume collected, cu cm	Total aspirating time, min	Flow through time, min ¹	Air aspirating rate, cu cm per min ²	Effluent		
		pH	Fe ⁺⁺ , ppm	Total Fe, ppm	Volume, cu cm						pH	Fe ⁺⁺ , ppm	Total Fe, ppm
Cleaned fritted disk													
April 23	38	2.90	800	960	260	0.8	260	3	-	-	2.45	15	560
	39	2.90	800	960	260	1.5	260	4	-	-	2.40	12	653
	40	2.90	800	960	260	1.8	260	4	-	-	2.45	10	647
	41	2.90	800	960	260	2.0	250	5	-	-	2.45	<2	410
	42	2.90	800	960	260	2.0	260	6	-	-	2.40	<2	445
April 24	43	2.80	720	865	260	1.3	-	3	-	-	2.50	<2	420
	Installed long cylinder (3.8-cm-diam, 42-cm-long carbon column)												
April 25	44	2.80	720	865	260	2.0	250	5	-	-	2.35	<2	510
	45	2.80	720	865	260	1.8	260	5	-	2,000	2.45	<2	445
	46	2.80	720	865	260	.6	250	2	0.25	3,500	2.40	15	505
	47	2.80	720	865	245	1.3	225	3	.5	2,000	2.40	<2	520
	48	2.80	720	865	260	1.7	240	3	.6	2,000	2.40	<2	585
	49	2.80	720	865	1,000	5.0	990	8	.5	2,000	2.40	7	710
	50	2.80	720	865	720	3.5	710	6	.5	2,000	2.40	15	715
April 28	51	2.80	720	865	260	1.0	250	3	.5	2,000	2.45	15	550
	52	2.75	655	855	260	1.2	240	3	.6	2,000	2.40	<2	560
	53	2.75	655	855	1,050	5.0	1,035	8	.5	2,000	2.30	10	670
	54	2.75	655	855	1,020	5.0	1,000	8	.5	2,000	2.35	32	710
	55	2.75	655	855	1,070	5.5	1,055	8	.5	2,000	2.45	12	620
May 1	56	2.75	655	855	260	1.5	250	4	.5	2,000	2.35	5	635
	57	2.85	635	810	260	1.3	240	3	.6	2,000	2.45	10	315
	58	2.85	635	810	1,040	5.0	1,020	8	.6	2,000	2.40	10	560
May 2	59	2.85	635	810	995	5.0	980	8	.6	2,000	2.40	35	605
	60	2.85	635	810	260	1.8	250	None	.75	None	2.45	<2	320
	61	2.85	635	810	1,090	5.0	1,075	8	.6	2,000	2.40	25	620
	62	2.85	635	810	635	3.0	615	6	.6	500	2.45	7	490
	63	2.85	635	810	510	2.5	495	5	.6	500	2.50	10	470
	64	2.85	635	810	500	2.5	475	4	.6	3,500	2.45	7	490
	65	2.85	635	810	535	2.6	520	5	.6	250	2.45	15	525

¹Not determined for runs 1-45.

²Approximately 2,000 cu cm per min of air drawn through carbon column for runs 1-44.

DISCUSSION

The exploratory tests conducted with activated carbon and a ferruginous acid mine water indicate that ferrous iron oxidation takes place catalytically at an extremely rapid rate. Further investigation is necessary to determine the factors that may limit the effectiveness of the carbon, to determine the efficiency and effective life of the carbon in a continuous flow system, and to determine whether acid regeneration will restore the carbon to its original efficiency when the surfaces become fouled with solids. Cost and performance standards need to be established also.

Rapid oxidation in a carbon-air-acid mine water system to convert ferrous iron to ferric iron prior to neutralization would greatly facilitate the mine water treatment process and reduce costs to a minimum. Catalytic oxidation would provide distinct advantages:

1. Limestone, the least costly alkaline agent, would supplant the more expensive alkaline agents in common use for neutralization.
2. Stoichiometric relations could be precisely controlled at a pH level which would ensure optimum use of alkaline agent.
3. Aeration after neutralization would be eliminated.
4. The dense, small volume of sludge produced at near neutral pH conditions would significantly reduce the cost of sludge separation and sludge handling.

Other potential advantages include production of practically pure iron oxide by fractional precipitation; maintenance of optimum ferrous-ferric ratios, by means of controlled oxidation, to form dense, low-volume sludges; and the use of more reactive alkaline agents, which can be justified if significant reductions in sludge volume can be attained.

REFERENCES

1. Kim, A. G. An Experimental Study of Ferrous Iron Oxidation in Acid Mine Water. Proc. 2d Symp. Coal Mine Drainage Res., Mellon Inst., Pittsburgh, Pa., May 16-17, 1968, pp. 40-45. Available from Bituminous Coal Research, Inc., Monroeville, Pa.
2. Mihok, Edward A. Mine Water Research: Catalytic Oxidation of Ferrous Iron in Acid Mine Water by Activated Carbon. BuMines Rept. of Inv. 7337, 1969, 7 pp.
3. Singer, Philip C., and Werner Stumm. Kinetics of the Oxidation of Iron. Proc. 2d Symp. Coal Mine Drainage Res., Mellon Inst., Pittsburgh, Pa., May 16-17, 1968, pp. 12-34. Available from Bituminous Coal Research, Inc., Monroeville, Pa.
4. Thomas, G., and T. R. Ingraham. Kinetics of Carbon Catalyzed Air Oxidation of Ferrous Iron in Sulphuric Acid Solutions. Proc. Unit Processes of Hydro-metallurgy, Conf., SME-AIME, Dallas, Tex., Feb. 25-28, 1963, v. 24, 1963, pp. 69-79.

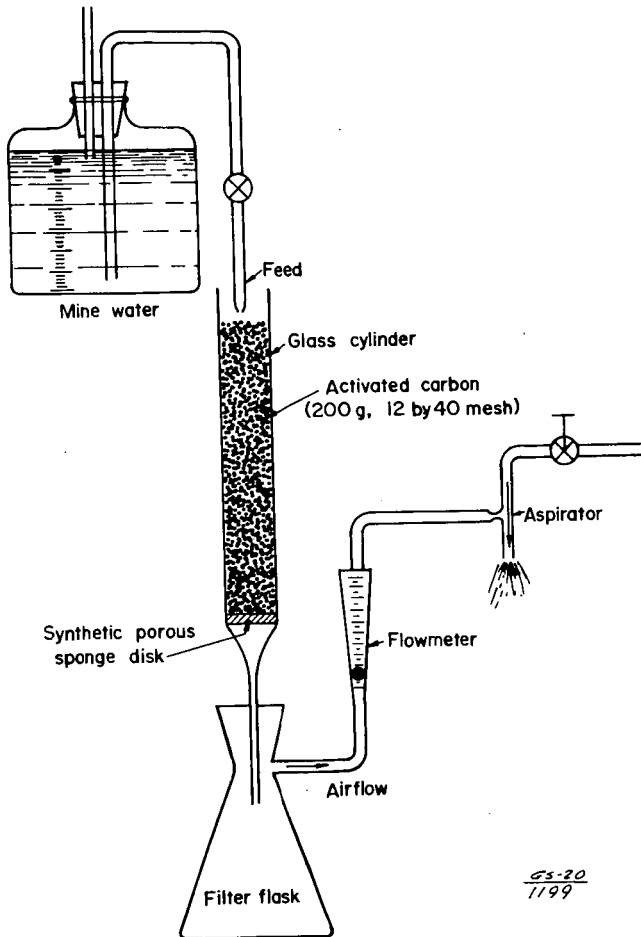


FIGURE 1. - Activated Carbon Oxidation Apparatus.

TREATMENT OF PULPING WASTES BY PERCOLATION
THROUGH GRANULAR BITUMINOUS COAL

by

P. L. Silveston
University of Waterloo

ABSTRACT

A group of experiments on the removal of suspended solids, lignins and their derivatives, and other soluble components causing chemical oxygen demand (C.O.D.) from industrial pulping wastes are summarised. An HVCB coal from Nova Scotia was used for most work. Percolation of a ground wood white water waste (total solids - 1850 ppm) through 28/48 mesh ground coal gave about 80% reduction of suspended solids and 20% removal of the soluble components exerting a C.O.D. Percolation of a sulphite residual cooking liquor (total solids 106,000 ppm) containing mainly lignin derivatives show substantial adsorption of lignins. Reduction of the C.O.D. of a Kraft bleachery effluent was also found. Batch adsorption measurements show Nova Scotia coal capable of adsorping lignins up to 4% of its weight. Coal based treatment may be feasible when suspended solids are the important pollutant, but when lignin content or the soluble C.O.D. is to be lowered this treatment is probably feasible only when coal is used as a pulp mill fuel.

On the Sorption of Water Vapour by Coal and its Spontaneous Heating

Kamal K. Bhattacharyya *

Department of Mining Engineering, University of Nottingham, England

1. Introduction

The effect of humidity on the rate of heat release due to oxidation of coal has been reported in an earlier communication(1). The results therein do not suggest that spontaneous heating in coal can occur due to oxidation reaction alone under normal ventilation practice. In the literature, however, frequent reference has been made by many investigators to the particularly humid conditions during heating incidents. Observations over a long period by Migdalski(2) and Wolowczyk(3) have revealed that in the Zwickau-Oelsnitz Coalfield in Germany the occurrence of spontaneous heatings coincided with the presence of high humidity in the mine atmosphere. According to Ashworth(4), humid air is "essential" for the starting of gob-fires. Mine fires have been reported starting at places where water issues in considerable quantity from the roof of the coal seam(3). The incipience of heating in stored coal especially after rainy weather is well known. According to Hoskin(5), fires in coal piles occur generally at the junction of wet and dry coals. Development of heating in the storage of coal-washery tailings has also been reported by Cabolet(6).

Earlier Winmill(7) and more recently Hodges and Hinsley(8) have reported that some dry coals catch fire when saturated oxygen is passed through them at 30°C, but the temperatures of the same coals rise only a little when dry oxygen is used. Subsequently, Hodges and Acherjee(9) have found that at a temperature of 30°C the heat release due to oxidation is very small in comparison with that due to sorption of water by the coal. Berkowitz and Schein(10) have commented that "the heat of wetting (or for that matter heat of condensation) may act as an important 'trigger'" in accelerating the oxidation of coal.

Although the above observations are useful in understanding the role of water vapour in the spontaneous heating of coal, the experimental conditions used in the tests fall far short of those generally found in practice. Extreme conditions of dryness and wetness of both coal and air (or oxygen) have been used in most cases. In practice, neither would the ventilation air in mines and the atmosphere in the vicinity of a coal pile necessarily remain saturated with water vapour, nor would the coal in question be dry all the time. Due to its hygroscopicity coal tends to remain in equilibrium with the surrounding atmosphere. If the humidity of the atmosphere increases, then the coal will take up some more moisture to achieve a new equilibrium. During the process of attaining equilibrium the coal undergoes certain chemical, physical and thermal changes. The present investigation is concerned with the estimation of thermal changes in various coals under such conditions. The coals equilibrated at a particular humidity have been subjected to air equilibrated at a higher humidity, and the heat release in coals has been estimated calorimetrically. Apart from the influence of humidity, the effects of some other variables on the process have also been studied.

* Present address: Faculty of Engineering Science, University of Western Ontario, London, Ontario, Canada.

2. Experimental

The arrangement and operational procedure of the apparatus used in this investigation were similar to those described in an earlier paper(1). The additional feature was that after the whole system had attained stable thermal and hygrometric conditions, the flow of nitrogen was substituted by air of humidity higher than that with which the coal sample in the calorimeter had been brought to equilibrium. The experiments were carried out in an isothermal condition at 30°c, except on one occasion when the test was done at 35°c. The humidities at which these tests were performed were also the same as in the previous investigation. The data on the analysis of each of the eight coals used are given in Table 1. Generally, the coals were tested with samples of -72 mesh (B.S.S.), but to study the effect of particle size on the heating rate due to sorption of water vapour, four sized fractions of -25+36, -36+52, -52+72 and -72+200 mesh (B.S.S.) were prepared from the Coal F. Normal precautions using nitrogen were taken to avoid oxidation of the samples during their preparation and drying. In order to investigate the influence of weathering of coal on the process a few oxidised samples were prepared from the Coal H. A bulk sample of -72 mesh (B.S.S.) of this coal was oxidised at room temperature in dry condition by pure oxygen, and the sub-samples were subsequently withdrawn after 30, 50 and 70 days.

3. Results and Discussion

The progress of the experiments was registered by recording the output of the calorimeter, and the results were subsequently calculated from the thermograms. All the thermal data reported here are expressed on a dry coal basis, and the term "saturated" is used to state the equilibrium conditions of both coal and air at the particular relative humidity concerned. The Coals B, D, G and H were tested under several humid conditions using dry as well as moist samples. The rest of the experiments were done in one particular condition by passing air saturated with water vapour through dry coal at 30°c.

Tests with glass wool under extreme conditions showed that the rate of heat release due to sorption of water vapour by the small amount of glass wool, mixed with the coal samples during experiments, had a negligible effect on the results obtained with the coals.

The variation of the rate of heat release with time for each of the coals studied at different humid conditions is shown in Figures 1 to 3. A few tests were carried out to isolate the heating effect of oxidation from that of water sorption. In some of these experiments nitrogen was used throughout as the moisture carrier, and in others the flow of moist air was changed to moist nitrogen or vice versa in the course of a particular experiment. It appears from the results that at temperatures of 30° and 35°c the rate of heat release due to oxidation is very small in comparison to that due to the sorption of water vapour by the coal. The absence of any recognisable effect of oxidation under such conditions has also been reported by other investigators(9 & 10). It is known that coal sorbs a comparatively larger amount of water than oxygen, and that the heat of oxidation is much less than the latent heat of condensation of water vapour. According to Sevenster(11), coal sorbs water vapour at a much faster rate than it consumes oxygen. Therefore, it is expected that in above conditions the heat release due to sorption of water vapour becomes the rate-determining factor.

Tests with Dry Coals

The results of this series of tests are shown in Figures 1 and 2. It is seen that excepting the curve for the anthracite (Coal A in Fig.1) all other rate curves have the common feature of a peak at the early stage of experiment. With the introduction of moist air (or nitrogen) into the dry coal there occurs

a sharp rise in the rate of heat generation in the coal. After a short while it decreases for some time before rising again. It appears from Fig.2 that the height and shape of the initial peak are dependent on both the humidity of the moisture carrier and the type of coal. An attempt is made in a later section to explain the occurrence of this peak in the rate curves.

Scanning of the results reveals that the nature of the rate curve after the initial peak is related to the type of coal sorbing the water vapour. With the anthracite (Coal A in Fig.1) and high rank coal B (Fig.2) the rate of heat generation approaches the maximum value rapidly. However, it starts decreasing soon after at a faster rate, followed by a progressively slower rate. In the case of the medium and low rank coals (Coals C,D,E,F,G and H) not only does the rate reach the maximum gradually, but it also continues in that range for some time before decreasing slowly. This difference in the nature of the heating rate in various coals can be attributed to the difference in their hygroscopicity. From Fig.2 it is evident that with a particular coal the rate of heat generation increases with the increase in the saturation humidity of the atmosphere. This is discussed in detail in a later section.

Tests with Moist Coals

In this series the coals containing different amounts of moisture were subjected to moist air (or nitrogen) under conditions in which sorption of water vapour by the coals was ensured. The results, as plotted in Fig.3, show that the rate of heat release vs time curves do not have any initial peak as obtained in the previous series of tests. The curves for the tests with a particular coal, however, follow the general characteristics of those obtained after the initial peak during experiments with the same coal in dry condition. It is also evident that for each coal the rate of heat generation increases with the increase in the difference in the initial equilibrium humidities of the moisture carrier and the coal.

Influence of Various Factors on the Rate of Heat Release

The effects of several factors on the heating rate of coal due to the process under investigation have been studied on a common basis of comparison. The basis used is $Q_{t=20}$ cal/g of dry coal, the total heat produced in twenty hours of testing, and is termed the characteristic rate of heat release. In a few cases where the experiments have been terminated before twenty hours the $Q_{t=20}$ values are taken from the extrapolation of the respective graphs.

Influence of the Deficiency in the Equilibrium Humidity of Coal

The characteristic rates of heat release during various tests with each of the coals B, D, G and H are plotted against different values of e , representing the difference between the equilibrium humidities of the atmosphere and the coal, in Figure 4. In Fig.4(i) the results of the tests with dry coals are shown, and the $Q_{t=20}$ value at zero e for a particular coal is the characteristic rate of heat release during its dry oxidation(1). The results of the experiments with moist coals are illustrated in Fig.4(ii); and the corresponding $Q_{t=20}$ value at zero e for each coal is represented by the average of the $Q_{t=20}$ values obtained during oxidation of the coal in several moist conditions reported earlier(1).

It is seen in Fig.4 that the characteristic rate of heat release for each coal increases with the increase in the equilibrium deficiency of the coal; the relationship, however, is not directly proportional. This is as expected because of the fact that the coal-water sorption isotherms, obtained from the equilibrium moisture values at various relative pressures of water vapour, are

of sigmoid type. A comparison between the Figs.4(i) and 4(ii) show that in each case the rate of increase in $Q_{t=20}$ with e during the tests with dry coal is more than that obtained when the experiments were done with moist coal. To confirm this feature, however, it would be necessary to estimate the heat of sorption of water vapour by the coal during the process. The present experimental set-up precluded any such attempt.

Influence of the Rank of Coal

The general relationship between the characteristic rate of heat release due to sorption of water vapour and the rank of coal is illustrated in Figure 5. The $Q_{t=20}$ value for each coal in the above figure is taken from the result of the test with dry coal and air (or nitrogen) saturated at 100% R.H. at 30°C. The variations of the characteristic rate value with carbon and volatile matter contents of the coals are similar to those usually observed between the hygroscopic properties of coals and the parameters of coal rank. It appears, therefore, that the heat release due to sorption of water vapour in a coal is in general dependent on its hygroscopicity.

Influence of Coal Particle Size

Each of the four sized fractions of the coal F was tested under similar conditions. Dry samples of these fractions were subjected to air saturated at 100% R.H. at 30°C. The changes in the rate of heat release with time of sorption of water vapour by the sized fractions are shown in Figure 6. The curves are of similar nature, and there is a tendency for the rate to increase with the fineness of the coal particles. This feature is more prominent in Figure 7 where the characteristic rates are plotted against the average particle diameters. It is seen that while a decrease in particle diameter below about 358 microns has little effect on the characteristic rate, a significant decrease in the rate of heat release occurs when the particle sizes are increased from 358 to 511 microns.

The observed difference in heat release in various sized fractions of the same coal is due to the difference in the exposed external surface area of the samples. The common shape of the rate curves indicates that the mechanisms of the sorption of water vapour remain similar. The results also suggest that there may be a critical diameter of the coal particles below which any further sub-division has little effect on the rate of heat release. However, since only four tests were carried out it was not possible to find the point at which such distinct change takes place.

Influence of Weathering of Coal

For the purpose of investigating the effect of weathering on the heat generation in coal during sorption of water vapour, three oxidised samples of the coal H were tested under similar conditions. The rates of heat release in dry samples were measured when air saturated at 100% R.H. at 30°C was passed through them. The results are shown in Figure 8 together with those obtained during a similar test with the fresh sample of coal H. It is noticeable from the general feature of the curves that the mechanisms of heat release remain unaffected after weathering of the coal, although the rate of heat generation generally increases with the extent of weathering.

The equilibrium moisture contents of the above samples at the saturation vapour pressure at 30°C are shown in Table 2, together with the characteristic rates of heat release. Both the characteristic rate of heat release and the equilibrium moisture content increase with the period of weathering of the coal. The increased moisture retaining capacity of weathered samples is an established fact, and it is expected that there would be a corresponding increase in the total heat release at the end of the sorption process. The present data,

however, show that with the extent of weathering there occurs an increase in the rate of heat release in the coal too, and this is of particular significance to the problem of spontaneous heating.

The Initial Peak in the Rate of Heat Release vs Time Curves for the Tests with Dry Coals

In absence of any quantitative data on the amount of water sorbed by the coals, it is only possible to put forward some qualitative explanations, on the basis of the present results and the existing knowledge on coal structure, for the appearance of the initial peak in the rate curves obtained from the tests with dry coals.

From the past work(2) it is apparent that this peak is not directly related to the rate of sorption of water in the early period of the process. The absence of any peak in the rate curve for the test with the anthracite (Coal A in Fig.1) seems to confirm this. A broad comparison of the heat release in the initial stage, until the rate curve starts rising again, in various coals tested under similar conditions, shows that this amount generally decreases with the maturity of the coal. It is also noticed that this quantity increases with decrease in the average particle diameter of the coal (Fig.6). The occurrence of similar peaks during the tests with moist nitrogen and also with the oxidised samples rules out the effect of oxidation. The close similarity in shape between the rate curves after the initial peak for the tests with dry coals and those obtained from the experiments with the respective moist coals indicates that the dry coal surface is probably responsible for the appearance of the initial peak.

Young and Crowell(12) and Brunauer(13) have referred to the occurrence of similar initial peaks during sorption studies of some porous solids. They have explained it as the result of the heterogeneity of the sorbent surface which plays an important role, particularly at low sorbate pressures. Considering the heterogeneous nature of coal it seems reasonable that the above theory may also be applicable in general to the present observations. This theory, however, fails to explain not only the case of the anthracite, but also the observed initial peaks with the finer coal particles.

From the studies of coal constitution, it is known that the number of polar groups, such as -OH and =CO groups, in coal decreases with the maturity of the coal, and that these groups are almost absent in the anthracite(14). Evidence has also been put forward by a few investigators(15 & 16) suggesting that a part of the water in coal is held by forces other than physical. On the basis of these facts the present observations can be explained in the following manner.

During sorption of polar substances such as water there occurs immediate interaction between the water molecules and the active groups in coal, and thus more heat is liberated than that due to physical adsorption. As this preferential sorption proceeds and the most active sites become occupied, so the less active sites come into play resulting in lesser heat generation. With the progress of the process the rate of heat release starts increasing again as the phase changing of the water vapour takes place. Thus the observed difference in heat release during this early period of sorption of water in various types of coal is understandable. With the finer particles the active sites on the coal surface are more easily accessible to the water molecules and so an increased amount of heat release at the first stage is expected. More elaborate study is necessary for a complete picture of the phenomena involved.

4. Conclusions

It has been shown that under conditions where a coal is likely to sorb

water vapour, the chance of heating is more. In a humid atmosphere when simultaneous sorption of water vapour and oxygen takes place, the rate of heat generation in coal due to the sorption of water vapour becomes the rate-determining factor. For a given coal, this rate of heating has been found to reach the maximum within a few hours of the start of the process, and to increase with the increase in the equilibrium deficiency of the coal.

The variations of the characteristic rate of heat release during sorption of water vapour with factors such as rank, particle size and weathering of coal are observed to be related to the hygroscopicity of coal. This indicates that the causes of self-heating in coal are in part associated with its fundamental nature; it also explains the greater susceptibility of low rank coals towards spontaneous heating. The method used in this work is found suitable for this kind of work, and the results obtained can serve as a basis for further work.

Acknowledgements

The author wishes to express his gratitude to Dr.D.J.Hodges and Professor F.B.Hinsley, Emeritus Professor of the Department of Mining Engineering, University of Nottingham for their continuous interest in this work. Thanks are also due to Professor H.J.King, Head of the department for his help, and to the National Coal Board, U.K. for supplying the coal samples and mostly for the financial aid to the project.

References

1. Bhattacharyya, K.K., Hodges, D.J. and Hinsley, F.B.
The Mining Engineer, Feb. 1969, p 274
2. Migdalski, H.
Bergbau-Technik, 7, 1957, 1, p 3
3. Wolowczyk, P.
Bergakademie, 12, 1960, p 4
4. Ashworth, J.
Disc. on Trans. Inst. Min. Engrs., London, 51, 1915-16, p 545
5. Hoskin, A.J.
Purdue Univ. Exot. Sta. Bull., 30, 1928, p 61
6. Cabolet, P.
Gluckauf, 75, 1939, p 953
7. Winmill, T.F.
Trans. Inst. Min. Engrs., London, 48, 1914-15, p 535
8. Hodges, D.J. and Hinsley, F.B.
Trans. Inst. Min. Engrs., London, 123, 1963-64, p 211
9. Hodges, D.J. and Acherjee, B.
Trans. Inst. Min. Engrs., London, 126, 1966-67, p 121
10. Berkowitz, N. and Schein, H.G.
Fuel, 30, 1951, p 94
11. Sevenster, P.G.
Fuel, 38, 1959, p 405
12. Young, D.M. and Crowell, A.D.
Physical Adsorption of Gases, Butterworths, London, 1962, Ch. 7
13. Brunauer, S.
The Adsorption of Gases and Vapours, Vol.1, Oxford Univ. Press, 1945, Ch. 10
14. Lahiri, A. and Iyengar, M.S.
Jl. Sci. & Ind. Res., 17A, No.2, 1958, p 60
15. Mukherjee, P.N. and Lahiri, A.
Fuel, 36, 1957, p 176
16. Mukherjee, P.N., Nandi, S.P. and Lahiri, A.
Jl. Sci. & Ind. Res., 15B, No.11, 1956, p 638

TABLE 1

ANALYSIS OF COALS USED

(As supplied by the N.C.B. Coal Survey Laboratories)

SAMPLE DETAILS		ANALYSIS, PER CENT									
Index	Colliery	Seam	Moisture	Ash	Air-dried			Total S	V.M.	C.	H.
					V.M.	F.C.	dmmf *				
A	Cynhaudre	Pumpquart	1.6	1.3	4.8	92.3	1.2	4.8	94.2	2.8	
B	+		1.9	5.0	29.7	63.4	0.7	30.6	88.5	5.2	
C	Easington	High Main	1.6	5.1	32.1	61.2	1.6	33.9	86.6	5.4	
D	Thoresby	Top Hard	7.5	4.9	30.2	57.4	0.8	33.5	83.7	4.9	
E	Bentinck	Yard	5.8	7.4	31.6	55.2	1.4	35.4	83.9	5.6	
F	Whitewell	High Hazles	8.4	2.7	33.3	55.6	1.3	36.9	82.8	5.4	
G	Denby Drury Lowe	Belpar-Lawn	4.6	7.5	34.2	53.7	1.9	39.9	81.5	5.8	
H	Measham	Stockings	5.3	6.0	36.7	52.0	1.6	42.1	80.7	5.2	

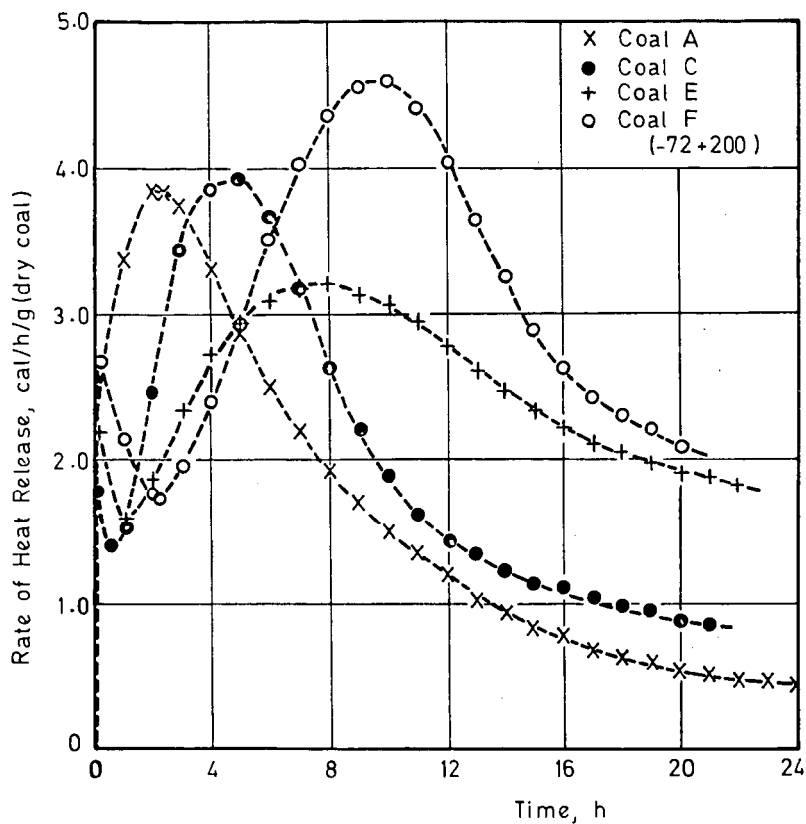
* Dry, mineral-matter free

+ Supplied by Cardiff Coal Survey Laboratory, Sample No. CSL 2708

Table 2

Effect of weathering of coal on the equilibrium moisture content and the characteristic rate of heat release due to sorption of water vapour

Days of oxidation	0	30	50	70
Equilibrium moisture, % (w/w)	19.22	20.83	21.80	23.44
$Q_{t=20}$, cal/g (dry coal)	56.70	62.28	63.07	69.12



Dry coal and air saturated at 100% R.H. at 30°C

Figure 1. Variation in the rate of heat release with time during oxidation and sorption of water vapour by dry coals.

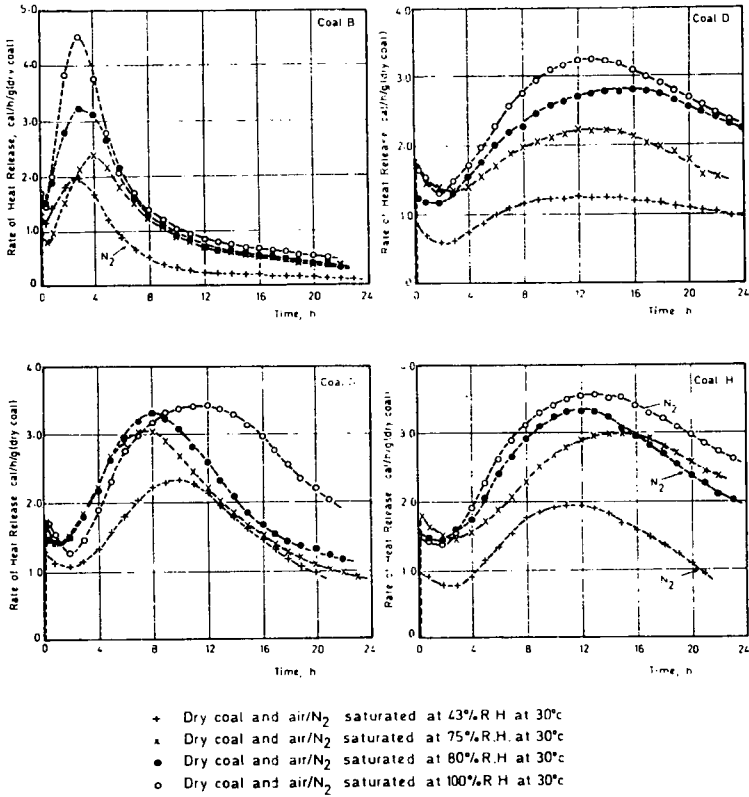


Figure 2. Variation in the rate of heat release with time during oxidation and/or sorption of water vapour by dry coals.

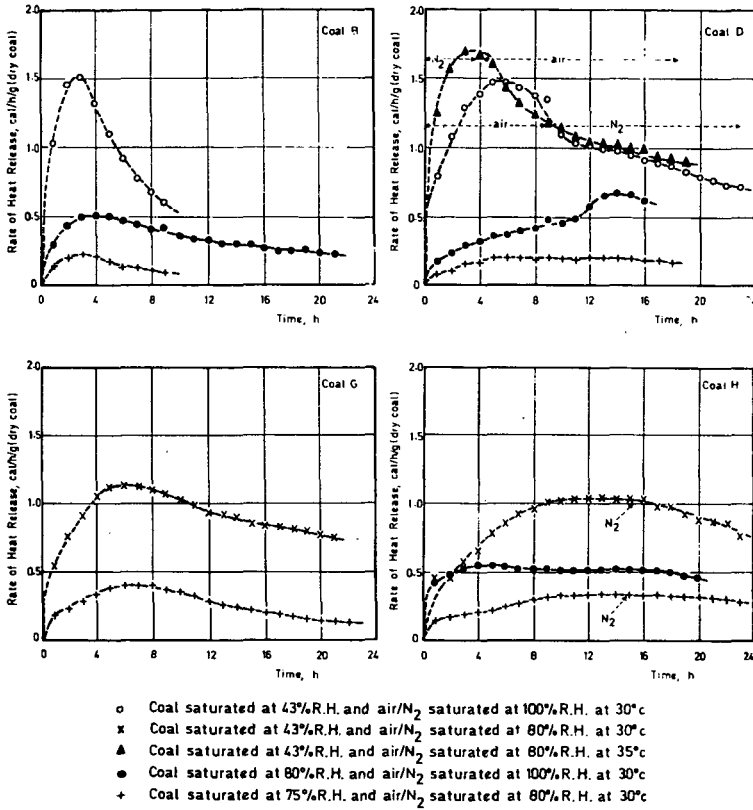
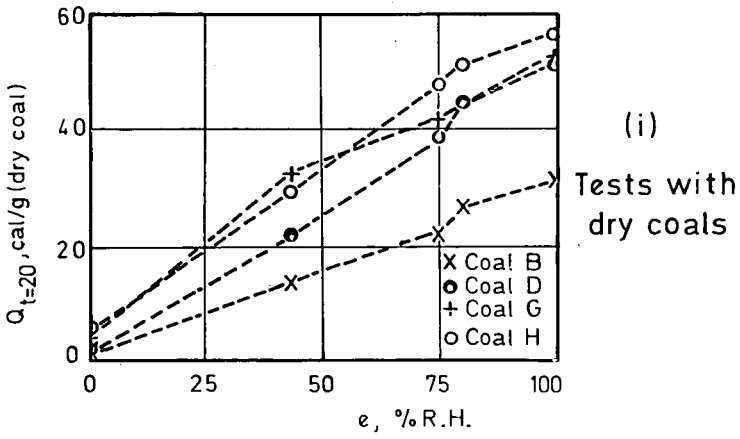


Figure 3. Variation in the rate of heat release with time during oxidation and/or sorption of water vapour by moist coals.



(ii)

Tests with moist coals

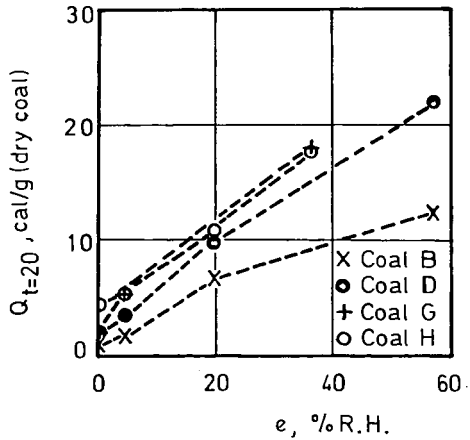


Figure 4. Variation in the characteristic rate of heat release with the equilibrium deficiency of the coals.

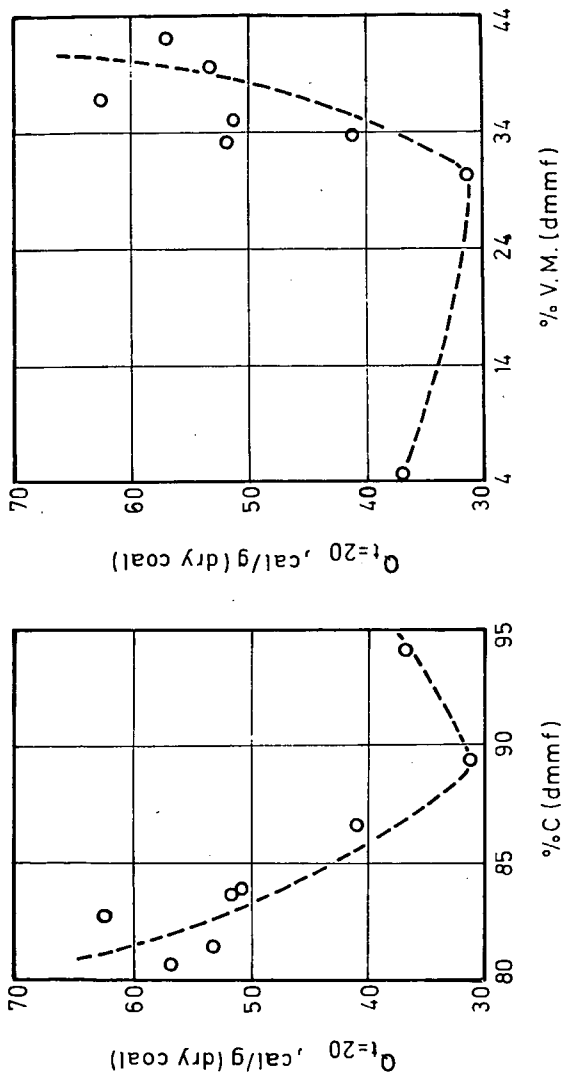
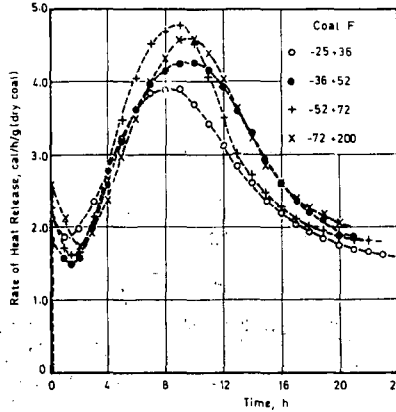


Figure 5. Variation in the characteristic rate of heat release with the rank of coal.



Dry coal and air saturated at 100% R.H. at 30°C

Figure 6. Effect of coal particle size on the variation in the rate of heat release with time during oxidation and sorption of water vapour by dry coal.

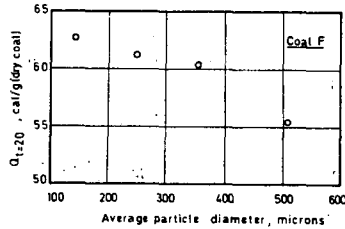
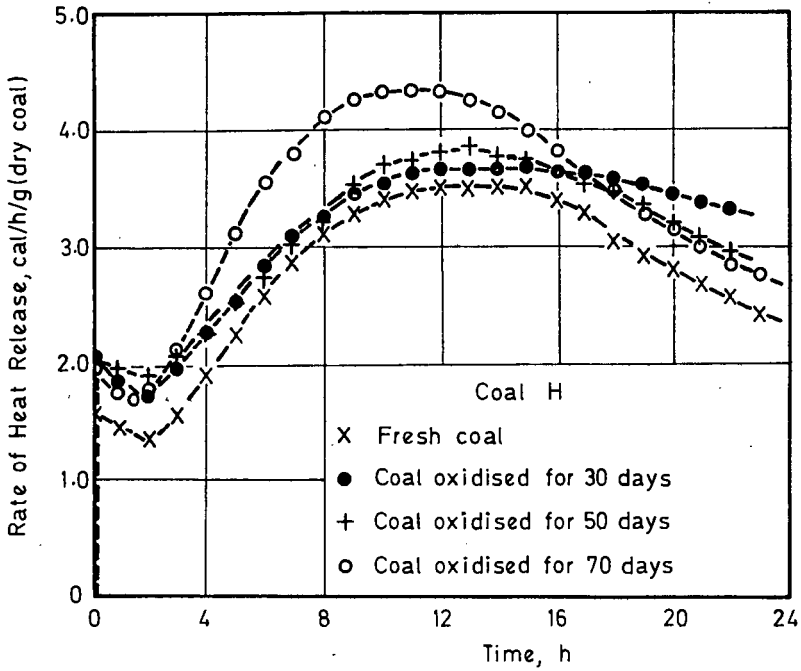


Figure 7. Effect of average coal particle diameter on the characteristic rate of heat release.



Dry coal and air saturated at 100% R.H. at 30°C

Figure 8. Effect of weathering on the variation in the rate of heat release with time during oxidation and sorption of water vapour by dry coal.

REFLECTANCE OF LOW-RANK COALS

D. M. Mason

Institute of Gas Technology, Chicago, Illinois 60616

INTRODUCTION

The reflectance of the vitrinite in bituminous coals is very useful as an indicator of their rank and behavior in coking. Determination of reflectance might serve a similar purpose in the characterization of coal for hydrogasification; however, the relation of reflectance to rank of low-rank coal is not so straightforward. Moisture content has been reported to affect the determination of reflectance of Illinois coals, especially those having high surface areas.¹ Furthermore, in the study of the coals tested in our hydrogasification program, we have found that the reflectance does not always fall in line with the rank of the low-rank coals; thus, contrary to expectation, the reflectance of a Colorado subbituminous coal (0.52%) was higher than the reflectance of an Illinois high-volatile C bituminous coal (0.45%). This paper constitutes a progress report on our efforts to elucidate the parameters, including moisture content, that influence the reflectance of low-rank coal.

THEORY

The normal reflectance of the surface of a light-absorbing material such as coal is governed by Beer's relation:

$$R_o = \frac{(n_c - n_o)^2 + k^2}{(n_c + n_o)^2 + k^2}$$

where

- R_o = reflectance in oil
- n_c = refractive index of the material, here a coal constituent
- n_o = refractive index of the immersion medium, here immersion oil
- k = extinction coefficient of the coal constituent

Scattered light from beneath the surface has also been considered as a possible source of difference in reflectance between moist and dry vitrinite. Scattering increases with increasing difference in refractive index between the pore and the matrix, as when water in the pore is replaced with air. However, the extinction coefficients of these vitrinites are high enough that the beam of light can penetrate no more than a few microns, and the pores in question are so small that they are very inefficient scatterers. For these reasons it appears that back-scattering cannot contribute significantly to the reflectance.

McCartney and Ergun have determined refractive indices and extinction coefficients on vitrinites of a series of coals.³ Among low-rank coals the extinction coefficient is low enough that it has only a small effect on the reflectance. Thus, its contribution to the reflectance of a Wyoming subbituminous coal is 0.026% out of 0.54% and to that of a high-volatile A bituminous coal is 0.24% out of 0.88%. Presumably the only significant source of any effect is the change in refractive index with change in the pore content of the submicroscopic pores.

The effect of density and pore content on the refractive index can be handled by the Lorenz-Lorentz relation in the form:

$$\frac{(n_c^2 - 1)}{(n_c^2 + 2) d} = r = w_1 r_1 + w_2 r_2 + \dots w_n r_n$$

where

r = specific refraction

$w_1, w_2,$ and w_n = weight fractions of components in the coal just beneath the surface

$r_1, r_2,$ and r_n = specific refractions of components

d = apparent density with submicroscopic pores (but not larger ones) included in the volume

The relationships between reflectance and refractive index and between reflectance and refraction $[(n^2 - 1)/(n^2 + 2)]$ are shown graphically in Figure 1. These curves were obtained by setting the extinction coefficient in the Beer relation equal to zero, which gives us the well-known Fresnel relation. The actual reflectance of a coal of a given refractive index will be slightly higher than the calculated value from the graph.

To elucidate the effect of moisture and pore filling on reflectance, we need to know the fine porosity properties of the coal. These include true and particle densities, and the extent to which the immersion medium enters the pores.

EXPERIMENTAL

Pore Structure

Samples of high-surface-area Illinois coal were obtained from the Illinois State Geological Survey. Pieces of high vitrinitic content were picked from a sample from No. 2 seam, identified as IGS-IGT No. 1, by observation under a low-power microscope. These were crushed and screened to obtain a 40 to 80-mesh USS sieve fraction. This particle size was chosen to be small enough to make a 5-gram sample representative and large enough to minimize error in the density determination, where the penetration of the interstices between fine particles by mercury is a problem. One portion of the sample was dried over a desiccant; another was treated with boiling water to fill its pores. The latter was then dried in a desiccator over potassium sulfate, the saturated solution of which gives an equilibrium atmosphere of about 96% relative humidity.

After the two samples had come to constant weight, particle density was determined on each sample by mercury displacement with a 6-ml Aminco penetrometer cell. The moist sample was cooled to about 0°C before evacuation to prevent appreciable loss of moisture. Volume readings and densities at 100 and 400 psig pressure were obtained; at 400 psig pores of the dry coal should be filled down to a diameter of 0.35 μ . Moisture was also determined on these two samples; moisture, ash, carbon, hydrogen, and pyrite were determined on a separate sample ground to pass a 60-mesh sieve. True density was also determined on this sample by means of a Beckman air pycnometer with helium. Results are shown in Table 1, together with results of the calculation of densities and pore volumes to a mineral-matter-free basis.

Table 1. PORE VOLUME OF VITRINITE FROM AN ILLINOIS COAL

Sample	Moist 40-80 USS mesh	Dried 40-80 USS mesh	Ground <60 USS mesh
True Density, g/cu cm	--	--	1.291
Particle Density, g/cu cm			
Hg at 100 psig	1.252	1.109	
Hg at 400 psig	1.254	1.113	
Moisture, %	15.12	1.14	2.54
Composition (dry basis), wt %			
C			78.8
H			5.54
FeS ₂			0.93
Ash			1.78
Moisture Content (mmf*), wt %	15.47	1.17	2.61
Particle Density (mmf), g/cu cm	1.236	1.094	--
Moisture (mmf), vol %	19.13	1.28	--
Porosity† (mmf), vol %	19.13	15.55	--
Pore Volume† (mmf), cu cm/g dry coal	0.183	0.144	--
Particle Volume (mmf), cu cm/g dry coal	0.957	0.925	--
True Density (dry and mmf), g/cu cm	--	--	1.280

*Mineral-matter-free.

†Including water volume. Normal density of water assumed.

According to the particle specific volumes (pore space included), it appears that the coal shrinks about 3% in volume when it dries. The "true" specific volume (pore space excluded) calculated from the particle density and moisture content of the moist sample agreed within 1% with the "true" specific volume of the dried sample determined with helium in the Beckman air pycnometer.

Reflectance

Moist and dry samples of the coal described above were prepared for reflectance determination by the method described by Harrison¹. Cargille Type-B immersion oil was used. Other details of our apparatus for the determination are described elsewhere².

The results indicate no difference in reflectance between moist and dry samples. The reason for our failure to obtain Harrison's effect has not been discovered as yet.

DISCUSSION

Harrison¹ found differences in reflectance between moist and dry samples of about 0.1% on high-volatile C bituminous coals having high surface area; the dry samples gave the higher reflectances. With this in mind, it is instructive to calculate the change in reflectance to be expected if water in the pores is replaced with either air or immersion oil. From the measured reflectance of the moist sample we calculate its specific refraction and subtract the contribution of the water, assuming the specific refraction of the moisture in the coal to be equal to the specific refraction of bulk water. From the specific refraction on the coal itself thus obtained, we back-calculate the reflectance of the dry sample if oil does not enter the pores. Similarly, using the density and specific refraction of the oil as determined on a bulk sample, we can calculate the specific refraction and reflectance if the oil does enter the pores. We have done this for the sample on which the pore property and reflectance data above was obtained, with results as follows:

Observed Reflectance of Moist Sample, %	0.45
Calculated Reflectance, %	
Dried Sample, No Oil in Pores	0.22
Dried Sample, Oil in Pores	0.58

Thus, the difference in reflectance between the moist sample and the oil-filled sample is of the right amount and algebraic sign to agree with Harrison's results. However, further work is required to clarify conflicting results on the effect of moisture and to determine to what extent immersion oil enters the pores of low-rank coal.

ACKNOWLEDGMENT

This study was supported by IGT as a part of its in-house basic research program.

REFERENCES CITED

1. Harrison, J. A. and Thomas, J., Jr., "Relation Between Moisture Content, Reflectance Values and Internal Surface Area of Coal," Fuel 45, 501-03 (1966).

2. Mason, D. M. and Schora, F. C., Jr., "Coal and Char Transformation in Hydrogasification," Fuel Gasification; A Symposium, Advan. Chem. Ser. No. 69. Washington, D.C., 1967.
3. McCartney, J. T. and Ergun, S., "Optical Properties of Coals and Graphite," Bur. Mines Bull. No. 641. Washington, D.C.: U. S. Department of the Interior, 1967.

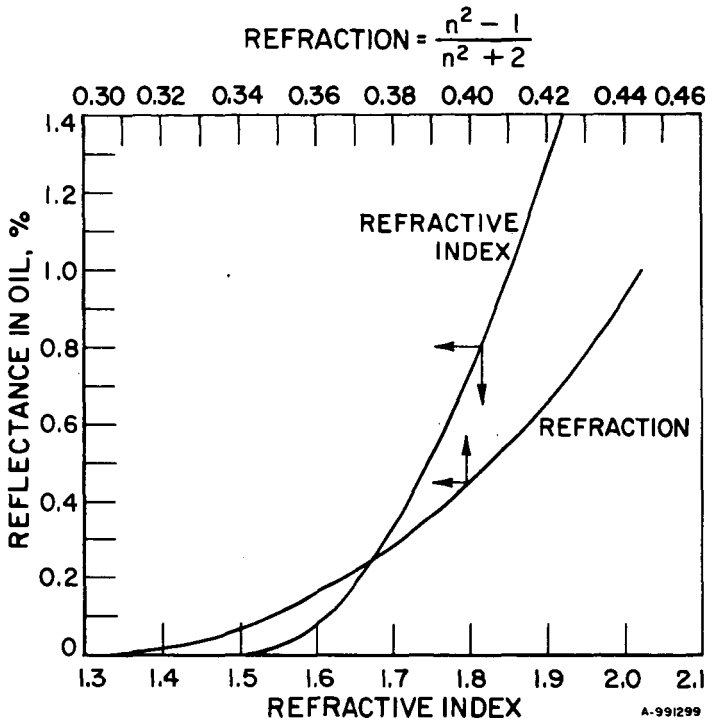


Figure 1. OPTICAL RELATIONSHIPS

THE STUDY OF COAL BY A SCANNING ELECTRON MICROSCOPE AND ELECTRON PROBE

B. N. Nandi and D. S. Montgomery

Department of Energy, Mines and Resources, Mines Branch, Fuels Research Centre
Ottawa, Canada

and

E. Martin

Application Laboratory, Philips Electronic Instruments
Mount Vernon, New York

- - - - -

The object of this study of selected coal samples using a Scanning Electron Microscope (SEM) and Electron Probe (EP) was to ascertain whether coal macerals, normally observed by reflected light in an optical microscope, could be identified in the emission images of backscattered secondary electrons. As it was difficult to characterize finely disseminated mineral matter in coal macerals using an optical microscope, it was also important to explore the possibility of evaluating the distribution and chemical character of the mineral matter in the maceral types using the x-ray electron probe capability of the Philips SEM.

To compare the optical and SEM microscopes it was essential to select coal samples containing a wide variety of maceral types and to polish the surface to be examined as flat as possible. This was essential to prevent surface relief from contributing artifacts to the secondary electron emission. Everhart (1) has shown that changing the surface inclination to the beam by only a few degrees produces an appreciable change in the number of secondary electrons produced.

Kimoto and Russ (2) point out that the resolution of an image with a SEM is limited to the size of the area emitting photons or electrons at any moment. When the electron probe hits the specimen, scattering causes the probe to spread so that the final volume of electron capture is roughly teardrop-shaped as shown in Figure 1. Secondary electrons, with energies up to about 50 eV, are produced throughout this volume; however they are reabsorbed after travelling only about 100\AA , so it is only the volume within 100\AA or less of the surface that emits secondary electrons that can be detected. This volume is only a few tens of angstroms larger than the diameter of the incident probe which has not had much chance to spread. Hence the secondary electron image provides the highest resolution.

Backscattered electrons come from a greater depth, and hence from a point where the probe has spread further, so that the resolution of the back-scattered image is poorer than the secondary electron image. Elements with high atomic numbers backscatter a greater fraction of incident electrons than ones with low atomic numbers.

The photons of x-rays or visible light come from essentially the entire teardrop volume and hence give the poorest resolution.

EXPERIMENTAL

A sample of Moss #3 coal was polished flat and examined with a Leitz Pan Pol Phot Microscope at a magnification of 450 using an air objective. Figure 2 shows a location selected for examination which contained vitrinite, semifusinite, and a large extremely dark wedge-like structure of what appears to be spore material, which could be readily identified by its wedge shape in the various other modes of examination in the scanning electron microscope. A comparison of Figure 2 with Figure 3, which was taken of the same location in the secondary emission mode, showed that dark bands of exinite (E) at the top of Figure 2 may be associated with similar dark bands at the top of Figure 3. The broad band of semifusinite (SF) in Figure 2 corresponds with a lighter region in Figure 3. The dark wedge-like structure of what appears to be spore material in Figure 2 seems to have an outer rim of high electron emission, as shown in Figure 3, with a characteristic dark thread-like structure midway between the two walls of the bright zone. Possibly this structure has a very high electrical resistance due to the high hydrogen content and thus builds up a negative charge that might reflect the electrons from the probe. The significance of this thread-like structure is not clear at present. The dark apparent voids in the semifusinite in Figure 2 do not correspond in shape with sufficient accuracy to be positively matched with the bright areas in the semifusinite in Figure 3.

Figure 4 shows the same location in the backscattered mode. The white areas in Figure 4 in the semifusinite correspond with the white areas in the secondary electron mode in Figure 3. The converse of this statement is not true. The definition is sufficiently sharp to permit the shapes of the white areas in Figures 4 to be accurately matched with those in Figure 3. The areas of high electron emission in the backscattered electron mode are thought to be due to mineral matter. The high electron emission of these particular areas is attributed to the much higher atomic number of the mineral matter as compared with that of the coal substance. It is noted that bright areas in Figure 3 do not necessarily correspond to bright areas in Figure 4. A striking example of this is the particle marked X.

This preliminary assessment was done using a Cambridge Scanning Electron Microscope which at the moment has no facilities for microprobe analysis. In

view of the importance of characterizing the mineral matter in coal, this preliminary investigation was extended using a Philips Model 4500 Electron Probe Analyzer with beam scanner.

A sample of coal from the Tantalus Butte Mine, N.W.T., Canada, was selected for examination for its relatively high concentration of semifusinite-containing mineral matter. This sample was polished flat and a location was selected that was approximately half vitrinite, and half semifusinite. This was done using a Leitz Microscope at a magnification of 300 with a water-immersion lens, Figure 5.

This same location was then examined in the backscattered electron mode and the resulting image, shown in Figure 6, reveals numerous light areas corresponding to the presence of the mineral matter in the semifusinite. On examining this same area with the microprobe analyzer using the first-order Si $K\alpha$ line, the bright areas as shown in Figure 7 indicate the location of the silica. These areas of high silicon concentration are located in the region occupied by the vitrinite. With the Fe $K\alpha$ first-order line, the bright areas correspond to areas of high iron concentration as shown in Figure 8. The area, in which the iron occurs, appears to be largely concentrated in the semifusinite regions of the field. Using the Ca $K\alpha$ line from a mica crystal the distribution of calcium is shown to be concentrated in the semifusinite as may be seen from the location of the bright areas in Figure 9. Similarly, the carbon content was shown to be higher in the semifusinite region than in the vitrinite portion of the field, as may be seen in Figure 10. In this case, the $CK\alpha$ first-order line from a lead stearate crystal was used.

CONCLUSION

1. The macerals (vitrinite, exinite, fusinite, and semifusinite) are visible in the secondary electron image. The indications are that the optical interpretation can be considerably extended by taking into account the differences observed between the secondary electron image and that obtained from back-scattered electrons.
2. The backscattered emission image generally indicates the presence of mineral matter in and between the maceral types.
3. The X-ray electron probe analyzer shows the iron and calcium to be concentrated in the semifusinite and fusinite portion of the field while the silica is concentrated in the vitrinite in the particular coal being studied. This tends to confirm the data recently obtained from washability studies that the high ash content is associated with higher concentrations of fusinite and semifusinite.(3)
4. The carbon content appears to be higher in the fusinite and semifusinite portion of the

portion of the field than in the vitrinite. This would be expected from the existing information on the chemical character of these macerals.

ACKNOWLEDGEMENT

The authors extended their special thanks to the following persons: Dr. E. Smith, Research Scientist and Dr. K.M. Pickwick, Research Scientist, Metal Physics Section of Physical Metallurgical Laboratories, Mines Branch, for taking photographs of Cambridge Scanning Electron Microscopy and for constructive suggestions and discussions; Mr. S.E. Nixon, technician, Fuels Research Centre, for his help in preparing sample.

REFERENCES

1. Everhart, T.E., Wells, O.C., Oatley, C.W. "Factors Affecting Contrast and Resolution in the Scanning Electron Microscope" *Journal of Electronics Control*, Vol.7, 1959, pp 97-11.
2. Kimoto, S. and Russ, J.C. "The Characteristics and Applications of the Scanning Microscope", *Materials Research & Standards*, Vol.9, 1969, pp 8-16.
3. Nandi, B.N., Montgomery, D.S. and Tibbetts, T.E. "Reconnaissance Studies of Coal from Livingstone Range, B.C. from the Canadian Pacific Oil & Gas Limited, Divisional Report of the Fuels Research Centre, 1970, in progress.

BNN:DSM:KMB:gdb

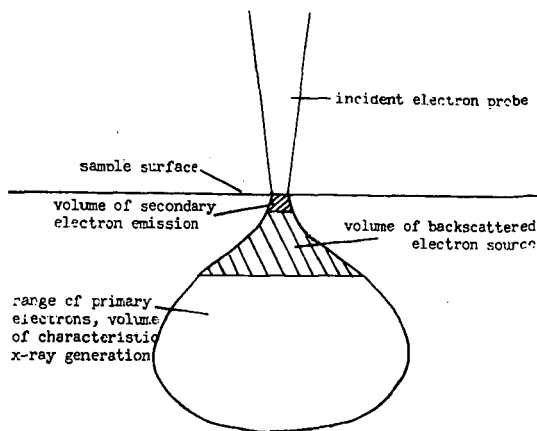


FIG. 1 Penetration of incident electron probe into sample.



FIG. 2 Optical micrographs of the macerals air objective reflected light X450.



FIG. 3 Scanning micrograph of the macerals of the same location as in Fig. 2 X400 approximately.



FIG. 4 Back-scattered electron micrograph of the same location as in Fig. 2 approximately X400.



FIG. 5 Optical micrograph of the macerals of coal from Tantalus Butte Mine; water immersion reflected light X300.

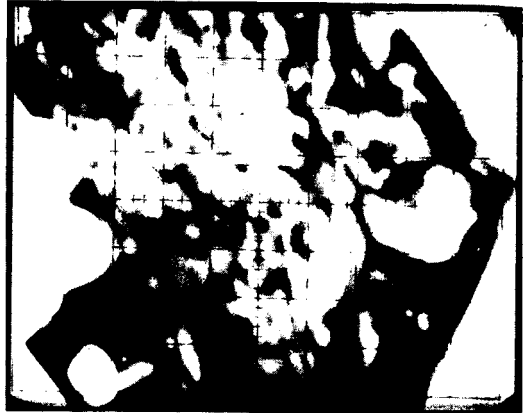


FIG. 6 Back-scattered electron micrograph of the same location as in Fig. 5, approximately X500.

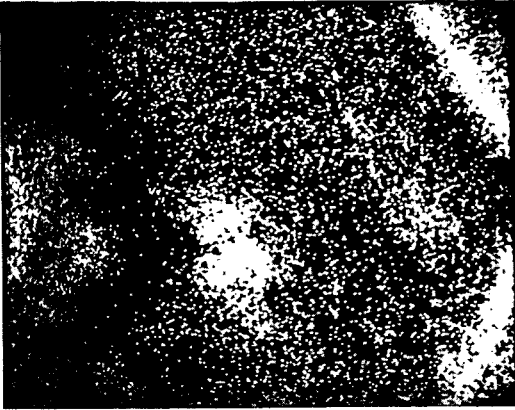


FIG. 7 Microprobe photograph of the silica
X500

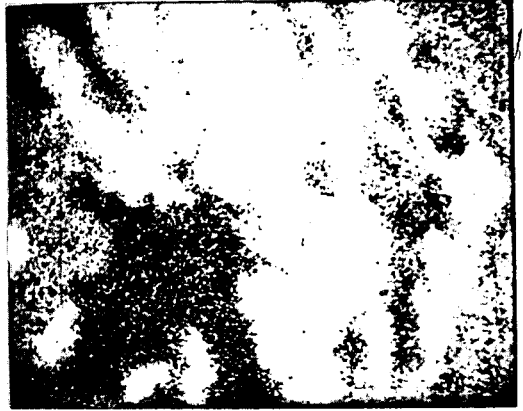


FIG. 8 Microprobe photograph of the iron
X500



FIG. 9 Microprobe photograph of the calcium
X500

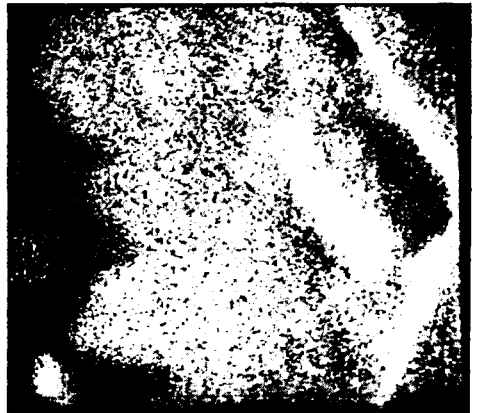


FIG. 10 Microprobe photograph of the
carbon X500

ON THE SOLUBILIZATION OF COAL VIA REDUCTIVE ALKYLATION

Heinz W. Sternberg, Charles L. Delle Donne, and Peter Pantages

Pittsburgh Coal Research Center, U. S. Bureau of Mines,
4800 Forbes Avenue, Pittsburgh, Pa. 15213

INTRODUCTION

We have recently shown (1) that treatment of Pocahontas (lvb) coal with alkali metal in hexamethylphosphoramide produced a "coal anion." The latter reacts readily with methyl iodide to give a methylated coal soluble in benzene at room temperature. We now present further work on the formation and alkylation of the coal anion.

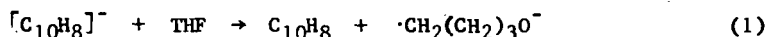
EXPERIMENTAL DATA AND RESULTS

Reagents. Metallic potassium, naphthalene, alkyl halides, and tetrahydrofuran (THF) were of the highest purity available commercially. Potassium, naphthalene, and the alkyl halides were used as received. Tetrahydrofuran was purified by refluxing over potassium metal for 72 hr. followed by distillation under a protective cover of helium.

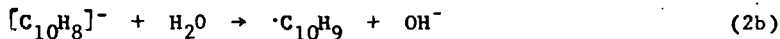
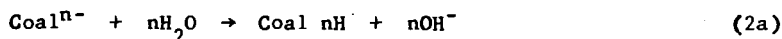
Coal. In all experiments, a hand-picked Pocahontas (lvb) vitrain sample, ground to pass 325 mesh, was used.

Petroleum Asphaltenes. The asphaltene sample was the pentane insoluble, benzene soluble (21%) fraction of a straight run residual asphalt of a California crude (85/100 penetration).

Formation and Titration of the "Coal Anion". Three anion species are produced when coal is treated with alkali metal in THF in the presence of naphthalene: naphthalene anion ($[C_{10}H_8]^-$), coal anion ($coal^{n-}$), and solvent anion ($\cdot CH_2(CH_2)_3O^-$). The latter is formed (2) by electron transfer from naphthalene anion to THF,



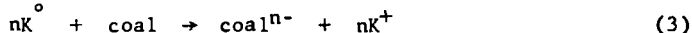
Each anion, on treatment with water, liberates an equivalent amount of hydroxyl ion:



The amount of hydroxyl ions formed can be readily determined by potentiometric titration with acid. By subtracting the equivalents of hydroxyl ions formed according to equations 2b and 2c from the total equivalents of hydroxyl ions, one obtains the equivalents of hydroxyl ions formed by the coal anion according to equation 2a. Knowing the amount and carbon content of the coal and the equivalents of hydroxyl ions formed according to (2a), one can calculate the number of negative charges associated with the coal anion in terms of negative charges per 100 carbon atoms.

In a typical experiment, under a protective cover of helium, a 250-ml Erlenmeyer flask provided with a glass enclosed stirring bar and suitable ground joint connections was charged with 120 ml of tetrahydrofuran (THF), 112 millimoles (4.4 grams) of potassium and 2.4 millimoles (0.304 gram) of naphthalene. The contents of the flask were stirred for 24 hr. A 1-ml sample of the dark green solution was withdrawn, placed in a 50-ml volumetric flask and diluted with water.

The aqueous solution was titrated with n/100 hydrochloric acid. To the dark green THF solution was added 6.17 grams of the vitrinite and stirring was continued for 72 hr. Every 24 hr. a 1-ml sample was withdrawn from the stirred reaction mixture and diluted with water to 50 ml. On addition of water, the coal anion suspension coagulates into a voluminous, brownish precipitate entirely different in appearance from the original coal. The aqueous mixture was allowed to stand for 48 hr. with occasional agitation to insure complete hydrolysis prior to titration. The results are summarized in Figure 1. Figure 1 shows that a sharp increase in the number of equivalents (43) takes place during the 24 hr. following the addition of coal. This increase is due mainly to the formation of coal anion,



The increase of 9 equivalents occurring during the final 48 hr. of stirring is caused by the formation of anions produced by electron transfer from naphthalene anion to solvent (THF) molecules according to equation (1). The value of 43 equivalents obtained for the neutralization of the coal anion, in conjunction with the amounts of coal used (6.17 grams) and the carbon content of the coal (88.3%), leads to the conclusion that the coal anion derived from Pocahontas coal contains 9.5 negative charges per 100 carbon atoms. The value of charges per 100 carbon atoms obtained in six separate titrations of freshly prepared coal anion suspensions varied from 9.5 to 12.1. The average value of these six titrations was 10.7 negative charges per 100 carbon atoms.

Alkylation of the Coal Anion. Under a protective cover of helium, the coal anion suspension described above was removed from unreacted potassium and was placed in an Erlenmeyer flask provided with a glass enclosed stirring bar. The flask was cooled in an ice bath. A solution of 10 ml of C-14 labelled ethyl iodide in 30 ml THF was added dropwise to the stirred dark red, almost black coal anion suspension in the course of 30 min. The mixture was allowed to warm to room temperature as stirring was continued for 2 hr. During this period the mixture became dark brown. The contents of the flask were poured into 600 ml of ethanol and the alkylated coal was separated by centrifugation. The supernatant ethanol solution was decanted and the residue treated with fresh ethanol. Treatment with ethanol and centrifugation was repeated until a sample of the ethanol washing was free of iodide ion. The precipitate was then repeatedly treated with water and centrifuged to remove any water soluble material. Finally, the precipitate was dried in vacuo at 100° to constant weight. The dried, treated coal weighed 6.03 grams. Taking into account the amount of coal withdrawn for titration (0.23 gram) and the amount of ethyl groups (8.8) added per 100 carbon atoms (see below), this corresponds to a recovery of 86%. The C-14 activity of the ethylated coal expressed in dpm/mg (disintegrations per minute per milligram) was 3.09×10^3 and that of the ethyl iodide (in dpm/ml) was 7.05×10^6 . The C-14 activity of the coal was determined by combustion analysis and that of the ethyl iodide by direct liquid scintillation analysis using an internal standard. On the basis of these data, the ethylated coal contained 8.8 ethyl groups per 100 carbon atoms. In similar experiments, coal was alkylated with C-14 methyl iodide and also with unlabelled normal butyl iodide. Radioactivity and combustion analysis of the methylated coal showed that the latter contained 8.1 methyl groups per 100 carbon atoms. Analyses of the original coal and alkylated coals as well as those of the benzene soluble and benzene insoluble fraction of the methylated coal are shown in Table 1. Hexane and benzene solubilities at room temperature (Table 2) were determined by tumbling 0.1 gram of alkylated coal and 15 ml of solvent in a sealed test tube for 1 hr. and centrifugation of the undissolved coal. This process was repeated two more times and then the residue was dried in vacuo at 100° to constant weight. The benzene soluble fraction of the methylated coal was practically free of ash (0.03%) while the original coal

contained 1.97% ash. In contrast to ethylated and butylated coal which were 95 and 93% soluble in benzene, methylated coal was only 48% soluble in benzene. Based on C-14 analysis and carbon content of the benzene soluble and benzene insoluble portion, the benzene soluble portion contained 8.4 methyl groups and the benzene insoluble portion 7.4 methyl groups per 100 carbon atoms. Infrared spectra (KBr pellet) of the alkylated coals showed strong bands at 3.4 μ and 7.25 μ attributable to the methyl group and the associated stretching vibration. The intensities of these bands in the original coal were only about one tenth of those found in the alkylated coal.

TABLE 1. Ultimate analyses of alkylated coal

	C	H	N	S	O ^{1/}	I	Ash
Original coal	88.25	4.55	1.19	0.57	3.47	.00	1.97
Methylated coal	87.22	6.03	1.14	.13	3.34	.00	1.54
a. Benzene soluble fraction	89.40	6.34	1.15	.06	3.02	.00	.03
b. Benzene insoluble fraction	85.71	5.43	1.09	.30	4.33	.00	3.14
Ethylated coal	87.81	6.33	.94	.37	2.52	.02	2.02
Butylated coal	87.24	7.23	.90	.31	2.17	.08	2.08

1/ By difference.

TABLE 2. Solubility of the alkylated coal

	Percent soluble	
	Hexane	Benzene
Original coal	nil	0.5
Methylated coal	3	48
Ethylated coal	11	95
Butylated coal	17	93

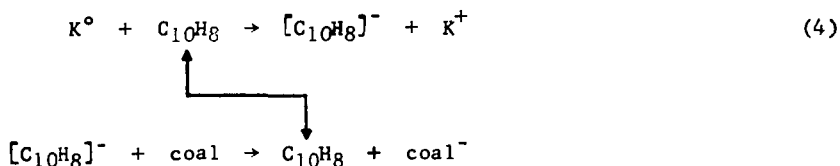
Molecular Weight Determinations. Number average molecular weights of the benzene soluble portions of alkylated coals and, for comparison, of one sample of petroleum asphaltens, were obtained by vapor pressure osmometry. Four samples, ranging in concentration from 5 to 35 grams per 1000 ml of benzene were used in each determination and the molecular weight at infinite dilution was obtained by the method of least squares. A typical plot of molecular weight vs. concentration is shown in Figure 2. The results are summarized in Table 3 along with the molecular weights calculated on an alkyl-free basis. In calculating the molecular weight of butylated coal on a butyl-free basis, it was assumed that the butylated coal contained the same number (8.8) of alkyl groups per 100 carbon atoms as the ethylated coal.

TABLE 3. Number-average molecular weights of alkylated Pocahontas vitrain and petroleum asphaltens

	Number-average molecular weight	
	Found	Calculated for alkyl-free coal
Ethylated coal	3300	2800
Butylated coal	4100	3000
Petroleum asphaltens	4200	

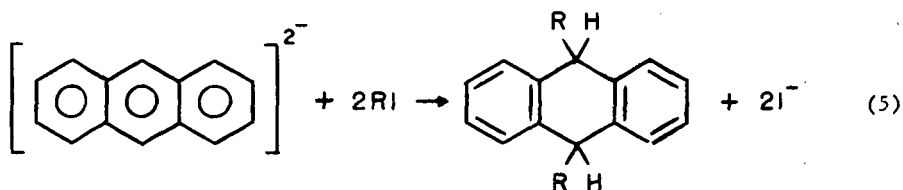
DISCUSSION

Formation of the "Coal Anion." Pocahontas vitrinite, when treated with potassium in tetrahydrofuran in the presence of a small amount of naphthalene, is converted to a coal anion. An electron transfer agent such as naphthalene is required because neither potassium nor coal are soluble in THF. Naphthalene, being soluble in THF, readily reacts with K^0 to form the anion $[C_{10}H_8]^-$. The latter is a strong electron donor and transfers its charge to the polycyclic aromatic hydrocarbons in coal as illustrated in equation (4)



By this method, a large amount of coal can be converted to coal anion in the presence of a small amount of naphthalene. The number of charges associated with the coal anion was found to be 9.5 charges per 100 carbon atoms. When hexamethylphosphoramide (HMPA) is used as a solvent, an electron transfer agent is not required since alkali metals are soluble in HMPA and can react directly with coal (1).

Alkylation of the Coal Anion and the Effect of Alkyl Groups on the Solubility of the Alkylated Coal. Alkylation of the coal anion by alkyl halide is analogous to that of anthracene anion (equation 5)



and may be formulated according to equation (6)



where n, the number of negative charges associated with the coal anion expressed in charges per 100 carbon atoms, is about 11. These are the negative centers that are theoretically available for alkylation. The number of alkyl groups actually introduced was 8.1 and 8.8 per 100 carbon atoms in the case of methyl and ethyl, respectively.

A large portion (52%) of the methylated coal is insoluble in benzene in spite of the fact that the number of methyl groups per 100 carbon atoms is almost as high (7.4) in the benzene insoluble as in the benzene soluble portion (8.4).

Table 2 illustrates the effect of alkyl groups on solubility. Ethyl and butyl groups are about twice as effective as the methyl groups in imparting benzene

solubility to the alkylated coal. The ethyl group is almost four times as effective as the methyl group and the butyl group almost twice as effective as the ethyl group in solubilizing coal in hexane.

Molecular Weights and Structure of Alkylated Coal and Petroleum Asphaltenes. The fact that introduction of alkyl groups into lvb coal produces a benzene-soluble material points to a relationship between this type of lvb coal and petroleum asphaltenes. The latter are soluble in benzene in spite of the fact that they contain a larger number of rings (3,4) (8 to 9) per cluster than coal (4) (3 to 4 rings per cluster). However, petroleum asphaltenes, in contrast to coal, contain a considerable number of alkyl groups attached to the aromatic clusters (3). It is these alkyl groups which impart benzene solubility to the petroleum asphaltenes by preventing stacking of the aromatic clusters. The conversion of a lvb coal into a benzene-soluble product by introduction of alkyl groups indicates that the difference between this coal and petroleum asphaltenes is not one of molecular size but one of molecular structure. This view is supported by the fact that the molecular weights of alkylated coal and petroleum asphaltenes are in the same range as may be seen in Table 3. The higher molecular weight of the butylated as compared to the ethylated coal is merely a reflection of the higher molecular weight of the butyl group. On an alkyl-free basis, the difference between the molecular weights is only 7%, i.e., within the limit of experimental error. Hodek (5), who converted coal by acylation into a benzene-soluble product, reported a molecular weight (on acyl-free basis) of about 2000. The molecular weight of 4200 obtained for the petroleum asphaltenes is in good agreement with values reported in the literature (6). Petroleum asphaltenes resemble lvb coal not only with regard to molecular weight but also with regard to chemical reactivity. A petroleum "asphaltene anion," prepared in the same manner as the coal anion, contained 8 negative charges per 100 carbon atoms, i.e., about as much as the corresponding coal anion. Methylation of the asphaltene anion with C-14 labelled methyl iodide yielded a methylated asphaltene containing 5 methyl groups per 100 carbon atoms, i.e., about half as many alkyl groups as were incorporated into the coal molecule. This difference may be due to steric hindrance caused by the presence of alkyl groups in the aromatic clusters of the petroleum asphaltenes.

SUMMARY

Pocahontas (lvb) coal, when treated with alkali metal in tetrahydrofuran in the presence of a small amount of naphthalene, is converted to a "coal anion." The coal anion is formed by transfer of negative charges from the alkali metal to the aromatic clusters in coal with naphthalene acting as an electron transfer agent. The coal anion, containing about 11 charges per 100 carbon atoms is readily alkylated by alkyl halides. The alkylated coals contain about 8.5 alkyl groups per 100 carbon atoms and are soluble in benzene at room temperature. The molecular weight of the alkylated coals is in the same range as that of petroleum asphaltenes. The solubility in benzene of alkylated coal and of petroleum asphaltenes is believed to be due to the presence of alkyl groups which prevent stacking of the aromatic clusters.

REFERENCES

1. Sternberg, H. W. and Delle Donne, C. L. American Chemical Society, Division of Fuel Chemistry, Preprints, Vol. 12, No. 4, p. 13, September 1968.
2. Henrici-Olivé, G. and Olivé, S. Z. physik. Chem. Neue Folge, 1964, 43, 334.

3. Winniford, R. S. and Bersohn, M. American Chemical Society, Division of Fuel Chemistry, Preprints, September 1962, 21-32; C.A., 1964, 61, 509.
4. Friedel, R. A. and Retcofsky, H. L. Proceedings of the Fifth Carbon Conference, Vol. II, pp. 149-165, Pergamon Press, New York, 1963.
5. Hodek, W. Paper presented at the 7th International Conference on Coal Science, Prague, 1968.
6. Altgelt, K. H. American Chemical Society, Division of Petroleum Chemistry, Vol. 13, No. 3, 37, September 1968.

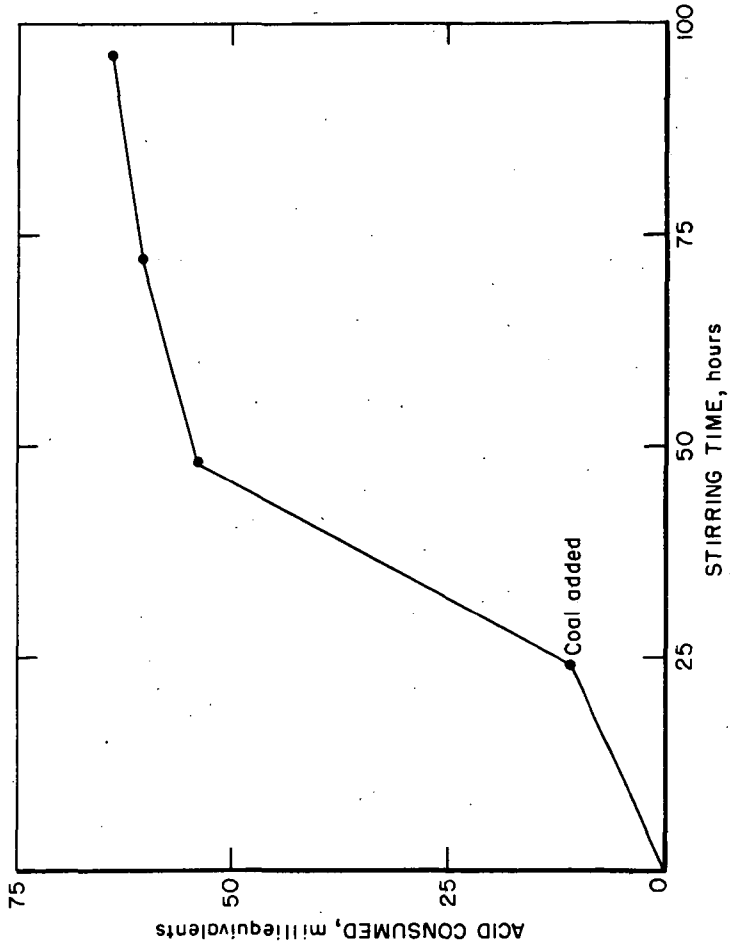


Figure 1 - Titration of the coal anion

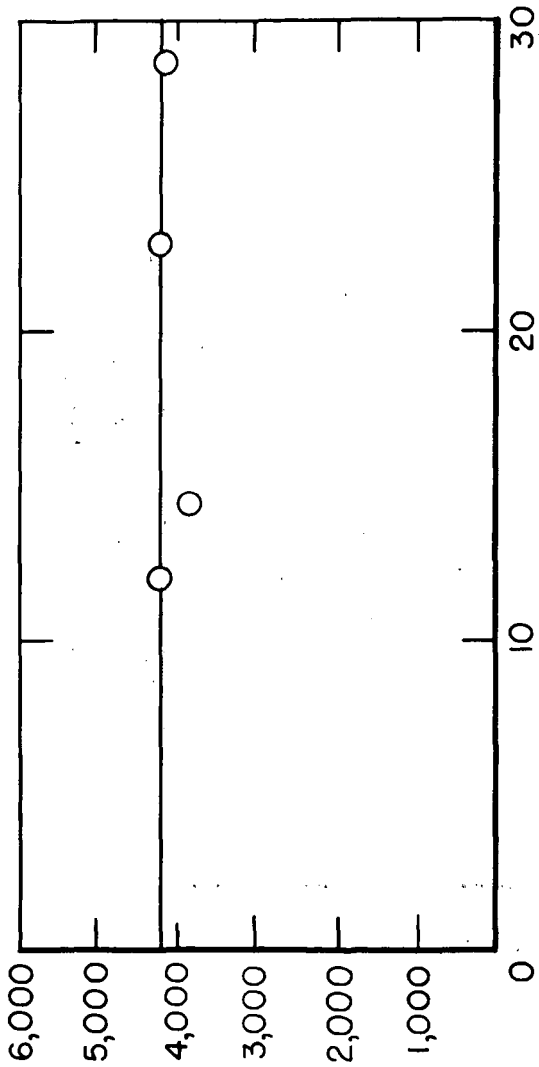


Figure 2 - Concentration dependence of apparent molecular weight by VPO of butylated coal.

L-11493

OXIDATION STUDIES ON COKING COAL RELATED TO WEATHERING

Part II: The Distribution of Absorbed Oxygen in the Products Resulting from the Pyrolysis of Slightly Oxidized Coking Coal

by

B. S. Ignasiak*, D. M. Clugston** and D. S. Montgomery***

INTRODUCTION

In the previous paper (1) of this series, the reduction of the dilatation of coking coal caused by oxidation in air (2) was studied in connection with the development of a more sensitive and a more generally applicable method of detecting trace oxidation of coal. It was found inter alia, that for Moss 3⁺ coal, the decrease in dilatation was a very sensitive indicator of the degree of oxidation. The total oxygen content, measured by neutron activation, was 8.55%. A relatively insignificant increase in the oxygen content of this coal by an additional 0.2% to 0.4% caused a decrease of the dilatation from 15% to 25%. The exposure of a minus 20-mesh, fresh sample of this coal for three days in the laboratory, at room temperature caused a marked decrease (5% to 10%) in the dilatation. An increase of the oxygen content in this coal by approximately 1.3%, bringing the total to 9.85%, caused the complete disappearance of both coking and dilatation properties. This level of oxygen content was reached after air oxidation of this coal in an oven at 100°C for 72 hours.

There are some differences of opinion on the subject of the mechanism of the low-temperature oxidation of coal. However, on the basis of a number of papers (3, 4, 5, 6), the conclusions are that low-temperature oxidation from a chemical point of view leads only to:

1. An increase in the reactive oxygen groups (-OH, -COOH, C=O).
2. A small decrease in the aliphatic and alicyclic carbon and hydrogen content of coal.

+ ASTM Classification, high-volatile A bituminous coal, International Classification of Hard Coals 535.

* Postdoctorate Fellow, National Research Council of Canada; permanent address: Department of Coal Chemistry, University of Adam Mickiewicz, Poznan, Poland.

** Research Scientist, and

*** Head, Fuels Research Centre, Mines Branch, Department of Energy, Mines and Resources, Ottawa, Canada.

It was therefore of considerable interest to examine in greater detail the manner in which small changes in the reactive-oxygen groups affect certain physicochemical properties of coking coal, for instance, dilatation. It seemed to us that any light that could be shed on this problem would be of great significance from the point of view of understanding the role of oxygen in the chemistry of the coking process. This investigation was therefore aimed at clarifying certain aspects of this problem.

EXPERIMENTAL

The investigations were conducted mainly on Moss 3 coal, though Itmann coal^{††} was occasionally used.

Samples of the fresh coals, which were delivered directly from the mines, were ground in an argon atmosphere to pass the 200-mesh (Tyler) screen. Each was oxidized in the two following ways:

- by using atmospheric air, and
- by using labelled oxygen (O_2^{18}).

The oxidation by atmospheric oxygen was performed either in an oven (100° for seventy-two hours), or by use of an IR lamp (250W) under the conditions described in a previous paper (1).

Oxidation by labelled oxygen was carried out, as follows:

A 10.5-g portion of Moss 3 coal was placed in a 250-ml Erlenmayer flask. A gas-tight one-way capillary stopcock was then sealed to the top of the flask. The sample was evacuated for three hours at room temperature. Then the temperature was raised to 70°C and the evacuation continued until the inside pressure dropped to 0.2 mm of Hg. At that time, 100 ml of labelled oxygen (99.85% by volume of O_2^{18}) was introduced, followed by an equal volume of argon. The capillary stopcock was closed and the flask was sealed below the stopcock to completely exclude the introduction of atmospheric oxygen. The sealed flask was subsequently placed in an oven at 100°C for seventy-two hours. The concentration of O^{18} in such oxidized coal was 0.66% by weight. The product after oxidizing the coal with O_2^{18} is referred to as oxy- O^{18} coal.

The coal samples, which were oxidized by use of atmospheric oxygen or an IR lamp, were pyrolyzed under vacuum in the manner previously described (1), except that the total time of pyrolysis was increased from ten minutes to fifteen minutes. The pyrolysis experiments were conducted by heating successive samples of coal to successively higher temperatures, at intervals of approximately 50°C, over the range of temperature 350°C to 800°C. The

^{††}ASTM Classification, low-volatile bituminous coal, International Classification of Hard Coals 333.

content of carbon dioxide and carbon monoxide was analyzed in the pyrolysis gas evolved up to a given temperature using a Fisher Partitioner with a double-column hexamethylphosphoramide on Chromosorb P, followed by Linde molecular sieve 13X. Helium, with a thermal conductivity detector, was used as the carrier gas at a flow rate of 40 ml/min.

Identical experiments were conducted on samples of fresh unoxidized Moss 3 coal. The results are presented in Figure 1, which shows the difference between fresh and oxidized coal with respect to the oxygen evolved, in the form of CO and CO₂ per gram of coal, as a function of the final temperature of pyrolysis. The pyrolysis of Moss 3 coal, oxidized with O₂¹⁸, was conducted in a manner that excluded oxidation by atmospheric oxygen. After oxidation, the coal samples were transferred to the vacuum-pyrolysis apparatus described previously (1), and pyrolyzed in the temperature range 450° to 950°C. The concentrations of CO¹⁶, CO₂¹⁶, CO¹⁸, CO₂¹⁶¹⁸ and CO₂¹⁸ in the pyrolysis gases were determined by a CEC 21-104 Mass Spectrometer.

The cokes obtained from the pyrolysis of oxy-O¹⁸ coal under a vacuum at temperatures from 100° to 950° were subjected once more to a pyrolysis process at a temperature of 1050°C. All oxygen-containing gaseous products of pyrolysis were then converted to carbon monoxide by use of a lampblack-nickel catalyst. The pyrolysis and conversion were conducted using the method described previously (7), with the exception that the composition of converted gas was analyzed by mass spectrometer. To obtain the necessary level of accuracy in determining the concentration of CO¹⁸ and CO¹⁶, it was necessary to analyze the content of C₂H₆ and C₂H₄ in the gas samples from the direct pyrolysis of oxy-O¹⁸ coal. The contents of ethane and ethylene were determined using a chromatograph (Aerograph 1500 equipped with a flame-ionization detector and a copper column, 0.25-inch ID by 30 feet length and one-quarter inch diameter, packed with silicone DC 200 on Chromosorb P). The flow rate of nitrogen used was 33 ml/min.

RESULTS AND DISCUSSION

Interesting information can be derived from Figure 1, concerning the influences of the two methods of oxidizing coal (IR lamp or oven at 100°C) on the differences in yield of oxygen, in the form of CO₂ and CO, in the resulting gaseous products from the pyrolysis of the oxidized coal (oxycoal). The conditions were selected so that the amount of oxygen absorbed by each coal during oxidation was the same for both methods of oxidation. At a given temperature of pyrolysis, more oxygen in the form of CO₂ and CO was evolved per gram of coal when samples were subjected to photo-oxidation under the IR lamp than if they were oxidized in the oven. For the samples photo-oxidized by IR lamp, the temperatures of pyrolysis for which $O_2 = O_2^{oxid} (CO_2 + CO) - O_2^{fresh} (CO_2 + CO)$ = a constant are relatively clear, and can be determined as 650°C for Itmann coal and 752°C for Moss coal. A similar plateau cannot be

found in the case of the oxidation of the coals in air in an oven at 100°C. It will also be observed that the amount of oxygen evolved in the form of CO₂ and CO during pyrolysis of the samples, oxidized at 100°C, was much lower than that when oxidation was conducted by use of an IR lamp. A possible explanation of this is that a considerable amount of oxygen absorbed by coal oxidized during the process of oxidation at 100°C, was later evolved in the form of water or linked with the tar during the subsequent pyrolysis of this oxycoal. The shapes of the appropriate curves in Figure 1 suggests this possibility.

The investigations to follow were limited to Moss 3 coal which was selected for the ease with which this coal oxidizes and for its fluid character. Labeled oxygen, O₂¹⁸, was used for the oxidation of this coal at 100°C, as previously described. It was assumed that the mechanism of the oxidation of Moss 3 coal at 100°C would resemble a somewhat accelerated weathering process. The advantages of this method of oxidation were that even though the coal was but slightly oxidized, similar to weathered coal, it was still possible to identify and determine, with precision, the low concentrations of products, such as, CO¹⁸, CO₂¹⁸, CO¹⁸O¹⁶ and H₂O¹⁸. The results obtained directly from pyrolysis of oxy-O¹⁸ coal are presented in Table I. These data are presented graphically in Figure 2 to show the different manner in which the gases are evolved. The amount of O¹⁸ in the form of CO₂¹⁸ and CO¹⁸O¹⁶ in gas from pyrolysis reaches the highest value at 450°C and remains on the same level during successive pyrolysis experiments at higher temperatures, right up to 950°C. The manner in which the CO₂¹⁸ and CO¹⁸O¹⁶ are evolved during pyrolysis of oxy-O¹⁸ coal seems to be strong evidence that some oxygen groups, created during oxidation of this coal, decompose completely to CO₂¹⁸ or CO¹⁸O¹⁶ below 450°C.

The continuous increase of O¹⁸ evolved in the form of CO¹⁸ may be observed in Figure 2, during the increase of the temperature of pyrolysis. The shape of the curve of evolution of O¹⁸ in the form of CO¹⁸ is similar to the analogous curve for CO¹⁶. However, even here, especially at lower temperatures of pyrolysis, the relative amount of evolved CO¹⁸ is much higher than for CO¹⁶.

The relatively high concentration of combined O¹⁸ in the gaseous products of low-temperature pyrolysis agrees with the independently measured rapid decrease of O¹⁸ in the resulting coke, as shown in Figure 3. About 60% by weight of O¹⁸ present in oxy-O¹⁸ coal is removed during pyrolysis of this coal at 400°C. Only about 14% of O¹⁶ is removed from the same coal during pyrolysis at 400°C. It will also be observed in Figure 3 that when the pyrolysis temperature reached 430°C, which is the temperature of maximum contraction of Moss 3 coal, a rapid decrease in the concentration of O¹⁸ and O¹⁶ in semi-coke occurred.

The evidence from the pyrolysis of oxy-O¹⁸ coal, presented in Figure 4, showed that the main part of O¹⁸ occurs in the pyrolysis product we may call

"tar + water". The data presented in this figure were obtained from a material balance derived from the results previously presented in Tables 1 and 2. This material balance was based on the quantity of coke and gas produced per gram of coal, the experimental concentrations of O^{18} in the coke and gas, and the measured initial amount of O^{18} in oxy- O^{18} coal before pyrolysis. The determination of O^{18} in the coke and gas requires some additional comment. For the determination of O^{18} in coke, the method described in the earlier paper (8) was applied, with the exception that the concentration of CO^{18} in converted gas was determined by mass spectrometry on the basis of the peak at m/e 30. The concentration of C_2H_6 in the converted gas, was found by gas chromatography to be less than $10^{-3}\%$ by volume. So, the interference by this constituent at m/e 30 should not be a serious matter. When the concentrations of CO^{18} and CO^{16} in gas from direct pyrolysis of oxy- O^{18} coal were determined, the concentrations of C_2H_6 were measured in the gas samples from each pyrolysis experiment by gas chromatography.

The results obtained were taken into account to find the proper concentrations of CO^{18} from mass spectrum. From the precautions taken and the level of reproducibility, it was considered that the concentrations of O^{18} found in coke and gas, as shown in Figure 4, were characterized by a relatively high level of accuracy. Therefore, the calculated concentration of O^{18} in tar + water owing to its relative magnitude, should likewise have comparable accuracy. It is necessary to stress the importance of this accuracy, due to the significance attached to the oxygen present in the tar in determining the coking properties of coal, and due to the surprisingly high concentration of O^{18} in tar + water obtained from pyrolysis at $450^\circ C$. This amounts to a concentration of O^{18} in the tar + water of about 3.8% to 4.0% by weight. In spite of the fact that the tar + water consisted only of about 10% by weight of oxy- O^{18} coal, it contained approximately 60% of all O^{18} absorbed by this coal during oxidation. On the other hand, the concentration of O^{18} in the semicoke from pyrolysis at $450^\circ C$ is relatively small, that is, 15% of the labelled oxygen existing in oxy- O^{18} coal, which is approximately 0.08% to 0.1% by weight of coke.

The observation that the highest concentration of O^{18} was found in the part of the organic matter of coal, which cracks to produce tar + water during low-temperature pyrolysis, appears to be consistent with the view that this part of the organic matter of coal can be roughly identified with the most extractable part of coal. This fraction, in the opinion of many authors, is responsible for coking properties (8,9).

Removacek (9) has found that the oxidation of coking coal can cause the change of the chemical character of its chloroform extract, which becomes similar to the chloroform extract from non-coking coals. In this paper, by quite a different route, it has been found that relatively slight oxidation of coal causes the largest changes, measured by increase of oxygen, in the part of the coking coal, which can most easily be cracked during heating to form tar.

It seems highly unlikely that the mild conditions of oxidation applied in this research could basically change the structure of the tar portion of this coal other than that a number of reactive-oxygen groups were introduced. Berkowitz (8) suggests that the oxygen in the form of COOH or OH groups cannot cause the change of coking properties of coal. Though a slight increase of these groups, during oxidation of coal, can probably not bring about - by itself - so marked a change in the physico-chemical properties of coal; nevertheless, there appears to be a strong possibility that the thermal decomposition of the OH groups, created during oxidation, results in the formation of ether-type crosslinks of very considerable thermal stability. A very small number of such bonds can stiffen the whole structure, and decrease the plastic properties of coal, especially the dilatation. The tar fraction is of special significance as a potential source of ether bonds, because of the high content of oxygen shown to be introduced into this fraction. Creation of crosslink ether bonds should be accompanied by the evolution of water, in our case, H_2O^{18} . It was found by mass spectrometry that the ratio H_2O^{18}/H_2O^{16} possessed the highest value when the pyrolysis experiments were conducted at the lowest temperatures, Table 3. Mass spectrometry also revealed that approximately 0.5 ml of H_2O^{18} (in gaseous state; 760 mm of Hg; 20°C) was evolved during pyrolysis of oxy- O^{18} coal. Since there exists the same probability of evolution of H_2O^{18} as H_2O^{16} as the result of the condensation of such groups as $R_1 - O^{16}H$ and $HO^{18} - R_2$, this means that the volume of gaseous water at 760 mm of Hg and 20°C evolved from condensation reactions leading to the disappearance of dilatation properties will be approximately one ml. It can be concluded from this observation that only about 12% of the total labelled oxygen absorbed during oxidation is responsible for the loss of dilatation resulting from the ether bonds. It should be mentioned that the proportionate increase of non-reactive oxygen groups (ether groups) in cokes, that occurs on low-temperature pyrolysis has been noted by other scientists (10,11). This seems to be substantial, though not sufficient confirmation of our hypothesis that it is not the OH groups per se that cause the loss of swelling properties but the fact that these groups undergo condensation reactions as the temperature is elevated to yield ether type cross links. The search for additional support for this hypothesis will be the purpose of the next paper of this series.

REFERENCES

1. IGNASIAK, B.S., NANDI, B.N. and MONTGOMERY, D.S., FUEL, London, in press.
2. BOYER, A.F. 'Controlled Oxidation of Coal', in Proc. Internat. Conf. on Chemical Engineering in the Coal Industry, Stoke Orchard, 1956, Pergamon Press: London, 1957.
3. MAZUMDAR, B., CHAKRABARTY, S. and LAHIRI, A. Journal of Scientific and Industrial Research 1962, 21, 84.
4. MAZUMDAR, B., ANAND, K., ROY, S. and LAHIRI, A. Brennstoff Chem. 1957, 38, 305.

5. ANDRZEJAK, A., IGNASIAK, B. Freiburger, F-hefte 1968, Heft 429,7.
6. ANDRZEJAK, A., IGNASIAK, B. Zeszyty Naukowe UAM.
7. IGNASIAK, B.S., NANDI, B.N. and MONTGOMERY, D.S., Anal. Chem., in press.
8. BERKOWITZ, N.
9. REMOVACEK, J., SIMANEK, J. Sb. Vysoke Skoly Chem. Technol. Prase, Technol. Paliv 1963, 6, 171.
10. KUCZYNSKI, W. personal information.
11. HILL, G.R. personal information.

Table 1. Per cent by volume of CO₁₆, CO₁₈, CO₂, CO₁₆, CO₁₆O₁₈, and CO₂ in gas from the direct pyrolysis, at different temperatures, of Moss 3 coal oxygenated with O₂¹⁸.

Temperature of Pyrolysis (°C)	% By Volume					Total Gas ml/R
	CO ₁₆	CO ₁₈	CO ₂	CO ₁₆ O ₁₈	CO ₂ ¹⁸	
450	4.7	1.71	5.6	3.45	1.72	23.2
500	3.9	1.04	4.1	1.62	0.81	49.2
550	5.4	0.92	3.0	1.08	0.54	74.0
600	5.1	0.73	2.4	0.76	0.38	105.0
650	5.0	0.64	2.1	0.61	0.30	132.0
700	6.5	0.51	1.8	0.48	0.24	168.0
750	6.4	0.47	1.6	0.40	0.20	201.0
800	6.9	0.52	1.4	0.35	0.17	229.0
850	7.2	0.44	1.2	0.29	0.14	280.0
900	9.1	0.55	1.1	0.24	0.12	329.0
950	9.4	0.50	1.1	0.23	0.11	354.0

Table 2. The composition of gas from pyrolysis and conversion process (1050°C) of cokes obtained from Moss 3 coal oxygenated with O₂¹⁸ and pyrolyzed at indicated temperatures.

Temperature of Pyrolysis (°C)	% By Volume							Total Gas ml/g
	CO ₁₆	CO ₁₈	CO ₂ ¹⁶	H ₂	CH ₄	H ₂ S		
70	17.4	1.16	0.01	81.0	0.14	0.00	712.0	
350	17.3	0.68	0.03	81.4	0.19	0.00	661.6	
400	16.5	0.51	0.10	82.7	0.15	0.00	640.7	
450	14.5	0.27	0.00	84.9	0.15	0.21	478.2	
500	15.1	0.18	0.00	84.5	0.15	0.02	413.1	
550	15.9	0.13	0.12	82.6	1.10	0.10	382.1	
600	17.7	0.11	0.10	81.3	0.50	0.25	332.9	
650	18.2	0.11	0.12	81.3	0.14	0.10	283.1	
700	19.7	0.08	0.00	81.3	0.11	0.11	224.7	
750	24.1	0.08	0.10	75.1	0.05	0.11	171.7	
800	21.5	0.05	0.16	78.0	0.00	0.09	137.8	
850	25.3	0.07	0.10	74.5	0.00	0.07	104.4	
900	27.4	0.06	0.09	71.8	0.00	0.00	70.9	
950	31.4	0.04	0.01	68.2	0.03	0.00	46.5	

Table 3. The percentage of H_2O^{18} in totally evolved water.

Temperature of Pyrolysis ($^{\circ}C$)	% By Volume H_2O^{18}
450	12.4
500	11.2
550	8.3
600	6.0
650	6.4
700	6.0
750	5.9
800	5.4
850	4.9
900	4.9
950	3.6

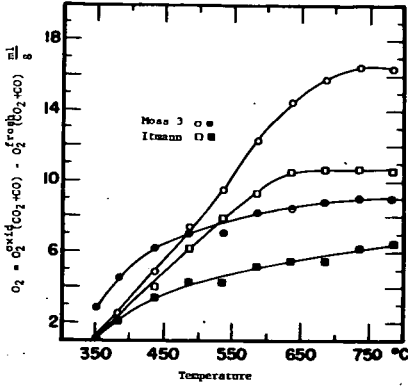


FIG. 1 The difference in the evolution of CO_2 and CO expressed as O_2 from fresh and oxidized coal as a function of the temperature of pyrolysis.

○ 15 min. IR and air
 □ 75 min. IR and air

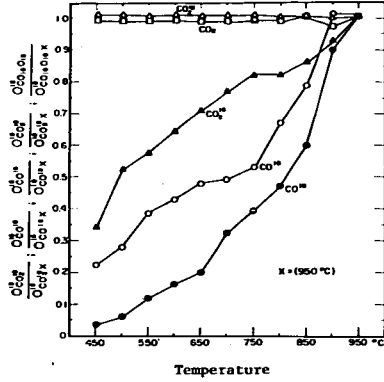


FIG. 2 The evolution of O^{18} and O^{16} in form of gaseous products of pyrolysis compared to amount of these products evolved at temperature 950°C .

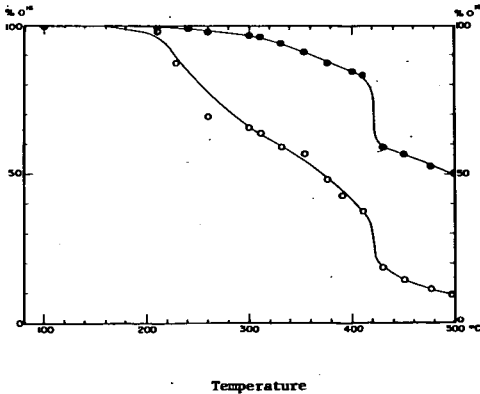


FIG. 3 Decline of the content of O^{18} and O^{16} in semicokes obtained during heating at indicated temperatures Moss 3 coal oxidized with labeled oxygen.

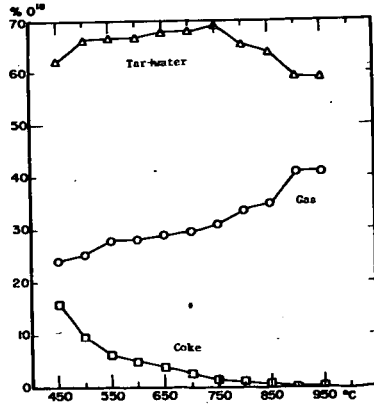


FIG. 4 Distribution of O^{18} in pyrolysis products of Moss 3 coal oxidized with labeled oxygen.

SOLVATION OF SOME BITUMINOUS COALS IN QUINOLINE BY
ULTRASONIC IRRADIATION

T. Kessler, R. A. Friedel, and A. G. Sharkey, Jr.

Pittsburgh Coal Research Center, Bureau of Mines
U.S. Department of the Interior, Pittsburgh, Pa.

INTRODUCTION

The first application of ultrasonic irradiation to disperse the α fraction of coal in pyridine was reported by Berkowitz.^{1/} Kirkby, Lakey, and Sarjant have investigated the ultrasonic solvation of coals of different ranks in pyridine.^{2/} In addition to an infrared study of the coal extracts, these authors have described the effects of irradiation time, coal rank, particle size, and charring temperature on the amount of coal solubilized. Littlewood, who also used pyridine as a solvent, studied the solubilization of coal as a function of the distance of the extraction vessel to the ultrasonic transducer, generator output power, and coal rank.^{3/} We have described the ultrasonic solvation of hvab coal at ambient temperature using quinoline, pyridine, formamide, N-N-dimethylformamide, and 1,2,3,4-tetrahydronaphthalene as solvents.^{4/} In our investigation the highest yield of extract was obtained with quinoline; after 4 hours of ultrasonic irradiation approximately half of the coal was solubilized, two and one-half times the yield with pyridine.

EXPERIMENTAL

The identification of the coals used in this investigation are given in table 1.

Table 1.- Identification of coals

<u>Coal</u>	<u>Identification</u>
1	Vitrain, high-volatile A bituminous Pittsburgh seam, Bruceton, Allegheny County, Pennsylvania
2	High-volatile A bituminous, Pittsburgh seam, Valley Camp No. 3, Ohio County, West Virginia
3	High-volatile A bituminous, bottom bench, Noon Mine, Ohio
4	High-volatile A bituminous, Kentucky No. 11 bed, Vogue Mine, Muhlenberg County, Kentucky
5	High-volatile B bituminous, Illinois No. 5 (c) Red Ember No. 2, Fulton County, Illinois

A commercial ultrasonic generator operating at a frequency of 80 Khz with a total power output of 80 watts was used. Samples of coal in 5 ml of solvent were ultrasonically irradiated at ambient temperature in an air atmosphere. The irradiation time used is given in each experiment. The coal-quinoline slurries were irradiated in flat bottomed glass vials (80 mm x 20 mm diameter). The vials were immersed in the ultrasonic generator tank (containing H₂O) to the position at which maximum agitation of the sample was observed. After irradiation, the solvent-extract mixture was removed from the coal residue by centrifugation. The

coal residue was then washed with two 5-ml portions of quinoline and two 5-ml portions of benzene. The residue was then air dried at 100° C to constant weight and used as the basis for determining the amount of solvation according to the method of Curran and co-workers;^{5/} the yields of extract determined by this method are on a maf basis.

RESULTS AND DISCUSSION OF RESULTS

Parameter Investigation

Carbon Content

One-half gram samples of various coals (-325 mesh) and 5 ml of quinoline were ultrasonically irradiated for 4 hours at ambient temperature. The results are given in table 2.

Table 2.- Amount of coal solvated versus carbon content

<u>Sample</u>	<u>Rank</u>	<u>Weight percent solvated</u>	<u>Carbon content of starting coal, percent (maf)</u>
Coal 1*	hvab	49.2	82.9
2	hvab	23.2	81.7
4	hvab	17.8	78.8
5	hvbb	17.6	76.9

* See table 1 for complete identification of samples

These data show that a correlation exists between carbon content and the amount of coal extracted with quinoline. Of the coals investigated, the amount of material solubilized decreased as the carbon content of the starting coal decreased. Kirkby and co-workers reported a definite relationship between carbon content and the amount of coal solubilized by pyridine.^{2/}

Irradiation Time--Coal

One-half gram samples of Pittsburgh seam hvab vitrain (-325 mesh) and 5.0 ml of quinoline were ultrasonically irradiated for periods ranging from 15 minutes to 24 hours at ambient temperature. A control was obtained by adding coal to the quinoline and then immediately removing the solvent using the standard procedure described earlier. The results are shown in figure 1. The amount of coal solvated varied from 16 percent for 15 minutes of irradiation to 77 percent for 24 hours. The largest increase in solubilized material occurred during the first 2 hours of irradiation. Littlewood has reported that the highest extraction rate for Brockwell 301 coal in pyridine occurred during the first hour of irradiation.^{3/}

Coal Chars

The chars used in these experiments were prepared by the following procedure: Pittsburgh seam hvab coal was heated to the desired temperature for 1 hour in a nitrogen atmosphere, air cooled, and then crushed to size. Chars were produced at temperatures of 275° C, 375° C, and 475° C. One-half gram samples of the starting coal (30 x 80 mesh) or char (30 x 80 mesh) were added to 5 ml of quinoline and ultrasonically irradiated for 4 hours. The results are shown in table 3.

Table 3.- Solvation as a function of charring temperature

<u>Char</u>	<u>Weight percent solvated</u>
Starting coal	18
275° C	6
375° C	37
475° C	17

Solvation of similar chars has been described by Walters and co-workers using Soxhlet extraction with chloroform as the solvent.^{6/} Chloroform solubilities of 0.6, 4.8, and 1.1 percent were reported for 300° C, 400° C, and 500° C chars, respectively. In both the ultrasonic and Soxhlet extractions, yields followed the same pattern. Walters has also concluded that maximum extraction occurs for chars prepared at the temperature of maximum fluidity. In contrast to this, Kirkby and co-workers reported that, for a vitrain-pyridine mixture, greatest ultrasonic solvation occurred with the original coal.^{2/}

Particle Size

A portion of the 375° C char (30 x 80 mesh) used in the experiments described previously was crushed to -325 mesh. One-half gram samples of the 30 x 80 mesh or -325 mesh chars and 5 ml of quinoline were ultrasonically irradiated for 4 and 24 hours. The results are shown in table 4.

Table 4.- Solvation versus particle size

<u>Irradiation time (hours)</u>	<u>Mesh size</u>	<u>Weight percent solvated</u>
4	-325	65
4	30 x 80	37
24	-325	82
24	30 x 80	77

For the shorter irradiation time, these data show that the particle size of the starting coal is an important factor for the ultrasonic solubilization of chars in quinoline. After extensive irradiation (24 hours) both sizes of char produced approximately the same amount of solvate. Littlewood, using coal-pyridine systems, has also reported that the amount of ultrasonic solubilization is dependent upon the particle size of the starting material.^{3/}

Irradiation Time--Char

Figure 1 also shows the percent solvation in quinoline versus irradiation time for a 375° C char (-325 mesh) produced from Pittsburgh seam coal. The amount of char solvated ranged from 46 percent for 2 hours to 82 percent for 24 hours. The solvation rate for the char is similar to that of the vitrain, the highest extraction rate occurring during the first 2 hours of irradiation for both materials.

Temperature

Ten percent slurries of Pittsburgh seam hvab coal (-325 mesh) in quinoline were ultrasonically irradiated for 4 hours at ambient temperature and 80° C. The results of these experiments are given in table 5.

Table 5.- Coal solvation as a function of temperature

<u>Temperature</u>	<u>Weight percent solvated</u>
Ambient (36° C)*	22
80° C	25

*Ultrasonic action increased the temperature of the water bath to 36° C

Littlewood found that extraction at 90° C did not increase the yield of solubilized coal in pyridine.^{3/} Littlewood also stated that this was contrary to the findings of Mertins, who reported that a temperature of 80° C gave a three-fold increase in solvation yield.^{7/} Our data appear to substantiate the findings of Littlewood; namely, a two-fold increase in temperature relative to ambient temperature has little effect on ultrasonic solubilization.

Sulfur Removal

One-half gram samples of various bituminous coals (-325 mesh) in quinoline were ultrasonically irradiated for 4 hours at ambient temperature. Total sulfur analyses were obtained for the extracts. The results of these analyses and the analyses of the starting coals are shown in table 6.

Table 6.- Sulfur analyses

<u>Sample</u>	<u>Rank</u>	<u>Weight percent sulfur</u>		<u>Percent removed</u>
		<u>Extract</u>	<u>Starting coal</u>	
Coal 1*	hvab	0.6	1.0	40
2	hvab	1.9	3.5	46
3	hvab	4.1	7.5	46
5	hvbb	2.1	3.9	45
375° C char, Pittsburgh seam coal		0.7	1.2	42

* See table 1 for complete identification of samples.

In these five samples the sulfur is 40 to 46 percent lower in the extracts than in the starting coal.

To determine the type of sulfur removed by ultrasonic solubilization of coal, sulfur forms analyses were obtained from a quinoline extract of a Kentucky No. 11 raw head coal sample. See Coal 4, Table 1, for complete identification of sample. The results of the extract together with data for the starting coal are given in table 7.

Table 7.- Sulfur forms analyses

	<u>Total S</u>	<u>Weight percent</u>		
		<u>Pyrite S</u>	<u>Organic S</u>	<u>Sulfate S</u>
Starting coal	5.5	3.7	1.8	0.12
Extract	1.9	0.03	1.8	0.04

These data show that removal of the pyritic sulfur accounts for the decrease in sulfur content of the extract.

Ash Removal

Ash determinations were made on the extracts prepared as described above. The results, together with the analyses of the starting coals, are given in table 8.

Table 8.- Ash analyses

<u>Sample</u>	<u>Rank</u>	<u>Weight percent</u>		<u>Percent removed</u>
		<u>Extract</u>	<u>Starting coal</u>	
Coal 1*	hvab	1.3	1.7	24
2	hvab	1.0	6.7	85
3	hvab	3.4	15.4	78
4	hvab	3.3	12.4	87
375° C char, Pittsburgh seam hvab		1.0	7.5	73

* See table 1 for sample identification

The lower ash values in the quinoline extracts can be attributed to ultrasonic grinding which causes submicron size particles to be formed; the ash particles are removed from the extracts by a washing procedure during the extract preparation described earlier. Evidence for this phenomenon was observed in the following experiment. The wash water from one of the extract preparations was saved and evaporated to dryness. The fluffy light-brown residue that remained was analyzed by emission spectroscopy and found to contain 20-30 percent Si, 10-20 percent Al, and 1-5 percent Fe. The concentrations of Si, Al, and Fe are similar to those found in coal ash.

Reuse of Quinoline

It has been observed in an investigation utilizing a high-boiling coal-tar fraction as a solvent that the solvating power of the recycle material decreased by several percent with each pass.^{8/} In order to determine if high molecular weight compounds produced by the sonolysis of quinoline or extracted during the

ultrasonic irradiation of coal-quinoline mixtures affect the efficiency of recycled quinoline, the following experiments were performed.

The fresh quinoline used in this investigation has a boiling range of 235°-237° C and contains approximately 0.1 percent methyl quinolines as determined by mass spectrometry. The distillate of the solvent from ultrasonically irradiated quinoline-coal extract mixtures contains a fraction boiling from 235°-239° C (primarily quinoline), Fraction 1, and a fraction boiling higher than 239° C, Fraction 2. Fraction 1 constitutes 98 percent of the distillable solvent and Fraction 2 constitutes the other 2 percent. The doped solvent used in this experiment consisted of 90 percent of Fraction 1 (b.p. 235°-239° C) and 10 percent of Fraction 2; the concentration of higher boiling material was, therefore, 5 times more than that found in ultrasonically irradiated quinoline-coal mixtures.

One-half gram samples of Pittsburgh seam hvab coal (-325 mesh) and 5 ml of doped quinoline or Fraction 1 (see above) were ultrasonically irradiated for 4 hours at ambient temperature. The results of these experiments, and of an extraction with "fresh" quinoline, are shown in table 9.

Table 9.- Solvation of coal in used quinoline

<u>Solvent</u>	<u>Weight percent of coal solvated</u>
Doped-reclaimed quinoline (10 percent boiling > 239° C)*	28
Fraction 1 (b.p. 235°-239° C)*	29
"Fresh" quinoline (b.p. 235°-237° C)	27

* See text for description

In another series of experiments, slurries consisting of 0.5 gm Pittsburgh seam hvab coal (-325 mesh) and 5.0 ml of solvent were ultrasonically irradiated for 4 hours at ambient temperature. After the coal residue was removed following each extraction, the quinoline and extracted material were used as the "solvent" for the next extraction of "fresh" coal. The results of these experiments are shown in table 10.

Table 10.- Recycled quinoline extract and fresh coal

<u>Experiment</u>	<u>Solvent</u>	<u>Cumulative extract, weight percent</u>	<u>Weight percent solvated in 4 hours</u>
I*	Fresh quinoline	26	26
II	Quinoline + extract from I**	52	26
III	Quinoline + extract from II**	88	28
IV	Quinoline + extract from III**	-	Not obtained, see text

* 0.5 gm Pittsburgh seam hvab coal (-325 mesh) used for all 4 experiments.

** Solvent (quinoline + extract) obtained from preceding experiment by removal of coal residue by centrifugation.

The mixture at the end of Experiment IV was so viscous that it could not be separated by centrifugation. Consequently, the percent of coal solvated could not be determined.

From these data it appears that high-boiling compounds extracted (or produced by the sonolysis of the solvent) during the ultrasonic irradiation of coal-quinoline slurries have little or no effect on the amount of coal solubilized by reused quinoline.

Crude Quinoline-Base Mixture

A 0.5 gm sample of Pittsburgh seam hvab vitrain (-325 mesh) and 5 ml of crude quinoline bases were ultrasonically irradiated for 4 hours at ambient temperature. The crude quinoline bases (obtained from a commercial high-temperature coking operation) had a boiling range of 99° C to 238° C and contained 50 percent quinoline. Only one percent of the coal was solubilized.

The crude quinoline-base fraction was found to contain 9 percent H₂O. To determine if H₂O inhibits ultrasonic extraction, 0.5 gm of the Pittsburgh seam vitrain (325 mesh) used above and 5.0 ml of a mixture containing 80 percent pure quinoline and 20 percent H₂O was irradiated for 4 hours. This experiment produced only 9.5 percent extract, compared with 49 percent using pure quinoline.

Water was distilled from the crude quinoline-base fraction, and the experiment was repeated. The water-free fraction (boiling range 220°-238° C) solvated 38 percent of the coal. These data indicate that the presence of water reduces the solvation power of the quinoline. Mertins also reported that the presence of water in pyridine reduced the extraction efficiency of the solvent.¹¹

SUMMARY

This investigation of the ultrasonic irradiation of bituminous coal-quinoline mixtures has shown:

1. There is an apparent correlation between the carbon content of the bituminous coals investigated and the amount of material solubilized; that is, the amount of material solubilized decreased as the carbon content of the starting coal decreased.
2. The solvation rate for vitrain in quinoline is greatest during the first 2 hours of irradiation
3. A greater yield of extract can be obtained by first charring the coal at the temperature producing maximum fluidity
4. For shorter irradiation times the particle size of the starting coal is an important factor for increased solubilization
5. Increasing the temperature from 36° C to 80° C does not affect the yield of extract
6. The presence of water in quinoline reduces the extraction efficiency of the solvent
7. The solvates produced show marked decreases in sulfur content compared to the starting coal. The decrease in sulfur in the extracts is caused by removal of pyritic sulfur
8. There is a decrease in the ash content of the extracts.

9. Quinoline can be reused as a solvent with no impairment of solubilizing efficiency.

ACKNOWLEDGMENTS

The authors gratefully acknowledge the contributions of the following: J. G. Walters for preparation of the coal chars used in this investigation, M. Jacobson for particle size determinations, J. A. Queiser for obtaining the infrared spectra, and Joseph Malli, Jr., for determining the mass spectra.

REFERENCES

1. Berkowitz, N., Nature, 1949, 163, 804.
2. Kirkby, W. A., J. A. Lakey, and R. J. Sarjant, Fuel, Lond., 1954, 33, 480.
3. Littlewood, K., Sheffield Univ., Fuel Sci. Jour., 1960, 11, 27.
4. Kessler, T., R. A. Friedel, and A. G. Sharkey, Jr., in press.
5. Curran, G. P., R. T. Struck, and E. Gorin, Preprints of Papers, Div. Fuel Chem., Am. Chem. Soc., 151st Nat'l Meeting, 1966, C130-148.
6. Walters, J. G., J. L. Shultz, and T. A. Glaenger, Bureau of Mines Rept. of Inves. 6973, 1967, 28 pp.
7. Mertins, A. G., see Reference 3 above.
8. Ladner, W. L., private communication.

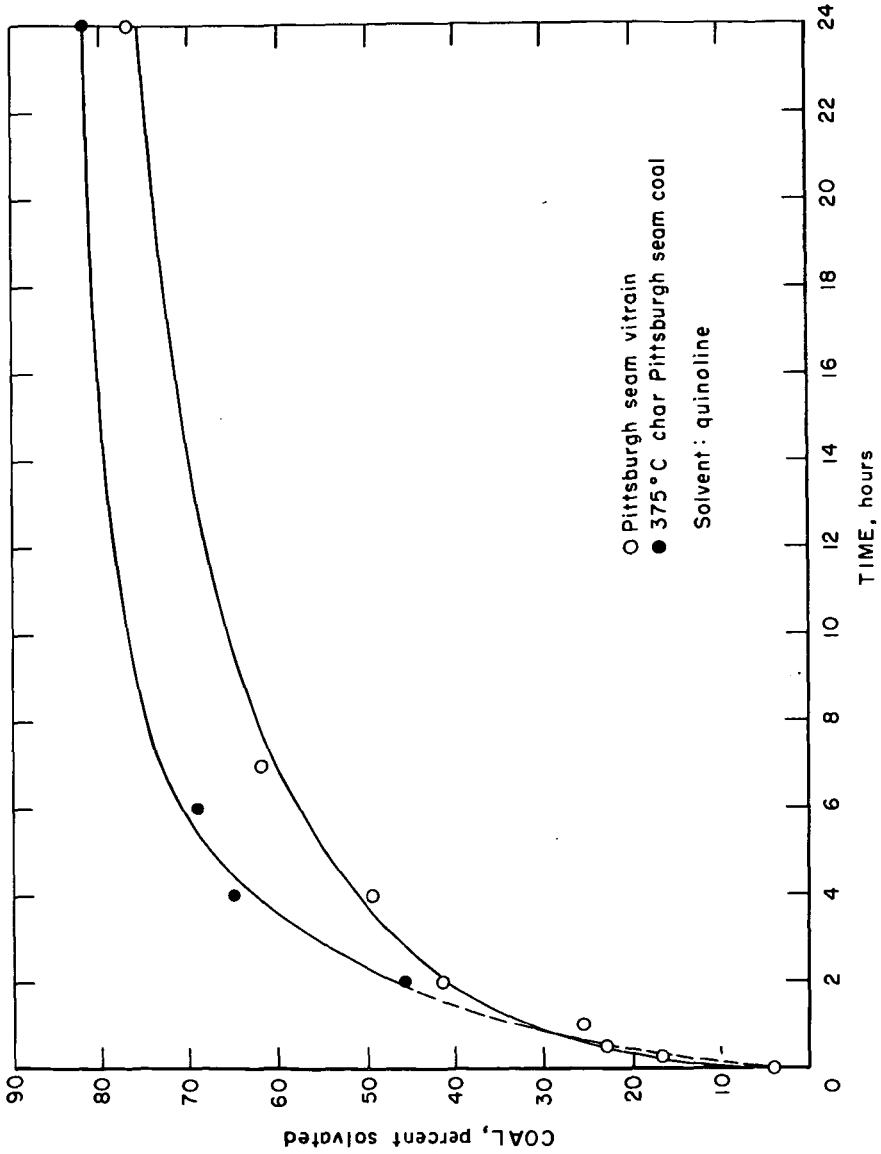


Figure 1.- Percent hvab vitrain and char solvated versus ultrasonic irradiation time.

ULTRASONIC ENERGY EFFECTS ON COAL EXTRACTION BY A HYDROGEN DONOR SOLVENT

by

Larry L. Anderson, M. Yacob Shifai and George R. Hill
University of Utah

ABSTRACT

The kinetics of a high volatile bituminous coal extracted with 1,2,3,4-tetrahydronaphthalene (tetralin) under the influence of ultrasonic energy has been studied.

The extraction of coal has been carried out at five different temperatures: 47°, 57°, 67°, 77°, and 87°C. Effects of intensity of ultrasonic energy, particle size, and hydrogen content of the coal were also obtained.

Analysis of the data showed that a second order rate reaction followed by a first order rate reaction describes the kinetics of the extraction process.

The enthalpies of the second-order and first-order regions were 8.70 K cal/mole and 2.5 K cal/mole, respectively, which suggests that the extraction process is under essentially physical control. Auxiliary experiments and the kinetic data obtained suggest a model for the extraction process. The mechanism of the overall reaction is undoubtedly complex but the data indicate that weak van der Waals and hydrogen bonding forces are most affected by the ultrasonic energy.

INTRODUCTION

The dissolving of coal in solvents has been studied from many aspects. Since the first systematic experiments by De Marsily in 1860¹ many investigators have extracted coal with a variety of organic liquids.

The work carried out before 1950 has been ably reviewed by Dryden². The first experiments using ultrasonic energy were conducted by Berkowitz³ with some later similar experiments by Littlewood⁴. The influence of solvent properties, experimental conditions and coal types on the yield of extractable material from coal has also been reviewed by Dryden⁵. Very little data have been reported on the kinetics of the extraction process⁶. The influence of ultrasonic energy on the kinetics has also received little attention. Undoubtedly the overall extraction is the result of several types of simultaneous and consecutive reactions due to the complexity of the coal structure involved. However, the results of this study are extremely interesting and, perhaps, can help one to understand the particular effects of ultrasonic waves on the extraction process.

From previous work on coal extraction in the presence of ultrasonic energy the following general conclusions can be drawn:

The amount of material extracted can be significantly increased by the use of ultrasonic energy^{3,7,8}.

The total amount extracted is dependent upon the temperature of the extraction⁶.

The rate of extraction was highest with coal of the smallest particle size⁷.

In this study these conclusions were verified for the coal-tetralin system and some further results were obtained leading to other conclusions regarding the mechanism of the reactions taking place.

MATERIALS AND PROCEDURE

The coal used for this study was from the Spring Canyon Coal Mine, Carbon County, Utah. An analysis is given in Table I. The tetralin used was reagent grade.

TABLE I
ANALYSIS OF SPRING CANYON COAL
(Commercial Testing and Engineering Company)

<u>Dry Ultimate</u>	<u>Weight %</u>	<u>Dry Proximate</u>	<u>Weight %</u>
Carbon	72.88	Ash	8.4
Hydrogen	5.58		
Nitrogen	1.51	Volatile Matter	45.70
Oxygen	10.82	Fixed Carbon	45.90
Sulfur	0.62		
Chlorine	0.119		

Dry Heating Value - 13,240 Btu/lb.

The following procedure was followed in the extraction of Spring Canyon Coal:

The coal was ground and sized to -200+270 Tyler mesh. A portion of the ground coal was removed from stock bottle and put in a beaker. The sample was then dried in a vacuum oven at 110°C for a period of four hours, removed from oven, and then placed in a desicator.

The extraction apparatus used for the experiments was a commercial ultrasonic cleaner which generated waves with a frequency of 25 kc/second. The maximum power output was 300 watts. The ultrasonic energy was directed to a stainless steel tank with a surface area of 80 square inches. Figure 1 is a schematic drawing of the extraction apparatus. A measured

volume of solvent was introduced inside the stainless steel tank and heated. When the selected operating temperature was reached, a weighed amount of coal (solvent to coal ratio = 50 ml/1 gram for tetralin and coal and 60/1 for ethylene diamine and coal) was introduced into the tank and mixed with the solvent; then mechanical stirring started. Stirring assured the uniformity of coal-solvent mixture and eliminated the precipitation of coal. Reaction time = zero for each experiment was taken as the time when the coal was added to the heated solvent. Samples were drawn into glass flasks after 5, 10, 20, 30, 40, 50, 60, 90 . . . 540 minutes. The samples were cooled to room temperature and weighed.

Each sample was then placed in a weighed, double thickness Soxhlet extraction thimble. The thimble containing the sample was placed in the Soxhlet extraction tube and was washed with acetone for 24 hours. The thimble containing the coal residue was dried in a vacuum oven at 110°C for 4 hours. The paper thimble and coal residue was then weighed. The weight of the coal residue or that which was not extracted was found by subtraction.

PRELIMINARY EXPERIMENTS

In order to determine some specific effects of operating conditions several preliminary experiments were conducted. These included the following with the results as indicated.

Decomposition of tetralin: Since it has been shown that ultrasonic energy can cause molecular fragmentation of organic liquids^{9,10} and also degradation of mixtures and organic solvents in the presence of water¹⁰ some experiments were carried out to determine the effects upon tetralin under the extraction conditions to be used for coal.

Tetralin was analyzed by gas chromatography to determine the quantities of other species present (Figure 2). Next tetralin was irradiated for 24 hours in the tank to be used for extraction with ultrasonic waves (3.75 watts/in^2) at 87°C . Samples of the tetralin were taken during the experiment and analyzed. No detectable decomposition was observed for the first 15 hours; the total decomposition after 24 hours was less than 1.0 per cent. Figure 3 is a chromatogram of the irradiated tetralin.

Coal-Solvent Ratio: In order to be sure that neither the rate nor the extent of extraction would be limited by the amount of solvent present for the coal sample some experiments were conducted to determine the amount extracted by various coal/solvent ratio. Figure 4 shows that for a coal/solvent ratio of 1 gram coal/30 ml of solvent or lower the per cent extracted is essentially constant. For subsequent experiments a ratio of 1 gram coal/50 ml solvent was used.

Particle Size: The effect of particle size on the per cent extracted at a particular temperature was found to be negligible. However, as shown in Figure 5 the initial rate of extraction was higher for the coal with a smaller particle size.

Intensity of Ultrasonic Energy: The ultrasonic generator and power control unit was equipped with facility for controlling the mechanical energy to the tank where the experiments were conducted. As shown in Figure 6 the amount extracted was a function of the ultrasonic energy supplied to the system. For all of the experiments conducted after these preliminary tests 100% of the energy available (3.75 watts/in^2) was used.

Some of the coal used in the experiments was reduced with Lithium-ethylenediamine. Calculations indicated an addition of 12.6 hydrogen

atoms per 100 carbon atoms in the coal. Both raw coal and the reduced coal was extracted with tetralin in the presence of ultrasonic energy. As shown in Figure 7 both the amount extracted and the rate of extraction were greater for the reduced coal.

Stirring Effect: Final preliminary experiments were conducted to determine the effects of stirring on the extraction of coal in the system used. Figures 8 and 9 show comparative data for static extraction, stirred extraction and extraction with stirring and ultrasonic energy at 47° and 87°C. Stirring appears to be important in making fresh solvent available to the coal surface.

RESULTS AND DISCUSSION

Conclusions regarding the effects of ultrasonic energy on the extraction rate and yield referred to previously were confirmed. Figure 10 shows kinetic data obtained in experiments with and without the influence of ultrasonic energy.

It was found that most of the data could be fit very well to a second order equation of the form:

$$\frac{dx}{dt} = k_2 (a-x)^2 \quad (1)$$

where k_2 = reaction rate constant

a = maximum fraction of the coal which would dissolve at the temperature studied

x = fraction of the coal extracted after any reaction time, t

Integration of the above equation with the lower limit of $x = 0$ when $t = 0$ leads to:

$$\frac{x}{a(a-x)} = k_2 t \quad (2)$$

A plot of $\frac{x}{a(a-x)}$ versus t should yield straight lines with the slope k_2 for each temperature if equation (1) adequately describes the reaction kinetics. Figure 11 shows the second order plot to be in agreement with the above conditions.

The second order equation was very adequate to describe the first hour of reaction at each of the temperatures studied from 47° to 87°C. However, after 60 minutes the data no longer fit the second order curves. Table II shows the extent of the second order reaction at the temperatures studied.

TABLE II
EXTENT OF SECOND ORDER REACTION

Temperature °C	Time at End of Second Order (min.)	Maximum Potential Yield (a)	"X" at End of Second Order	Percent of "a" During Second Order
47	60	0.1782	0.1221	69
57	60	0.1899	0.1473	80
67	60	0.1985	0.1663	84
77	60	0.2098	0.1863	89
87	60	0.2240	0.2077	94

The data after 60 minutes were found to be simple first order for the remainder of the extraction reaction. The first order equation to describe the portion of the reaction taking place after 60 minutes was:

$$\frac{dx}{dt} = k_1 (a-x) \quad (3)$$

Integration and setting the limits as for equation (2)

$$\ln \frac{a}{a-x} = k_1 t \quad (4)$$

The data for this portion of the reaction are plotted in Figure 12 to show the agreement of equation (4) to the data obtained.

Applying the absolute reaction rate theory to the second order and first order portions of the extraction process the rate constant, k' (or k_2 and k_1) would be of the form:

$$k' = \kappa \frac{kT}{h} e^{-\Delta F^\ddagger/RT} \quad (5)$$

where κ = transmission coefficient (usually = 1.0)

k = Boltzman's constant

h = Planck's constant

T = absolute temperature ($^\circ\text{K}$)

R = universal gas constant

ΔF^\ddagger = activation free energy (also can be expressed as $= \Delta H^\ddagger - T\Delta S^\ddagger$)

The rate constants were expressed by the expression

$$k' = \frac{kT}{h} e^{-\Delta H^\ddagger/RT} e^{\Delta S^\ddagger/R} \quad (6)$$

and plots of equation (6) are shown in Figure 13 and 14. Since $\ln \frac{k'}{T}$ is plotted against $1/T$ the slope is then $-\frac{\Delta H^\ddagger}{R}$ and the activation entropy ΔS^\ddagger can be obtained from the intercept. The values for the activation enthalpy and apparent activation entropy for the two portions of the reaction were:

	ΔH^\ddagger	ΔS^\ddagger
2nd order	8.7 kcal/mole	-44 e.u.
1st order	2.5 kcal/mole	-70 e.u.

With the values of the activation enthalpies obtained the extraction process appears to be under essentially physical control. Forces being affected if this is the case would include van der Waals or hydrogen bonding forces which are generally of the order of 1-10 kcal/mole. Freundlich and Gillings have demonstrated the breaking of the loose gel network of van der Waals bonds in gelatin-water¹² by ultrasonic waves. However, many other degradation and depolymerization reactions have also been effected by ultrasonic energy when the bonds involved were chemical bonds of 50-100 kcal/mole. Some polymers which have been depolymerized by ultrasonic waves are polystyrene¹³, polyvinyl acetate, polyacrylates and nitrocellulose¹⁴, and rubber¹⁵.

An interesting and quite plausible explanation for the depolymerization of polystyrene solutions has been proposed by Crawford¹⁶. According to his calculations ultrasonic waves of 300 kc/s at 10 watts/cm² could easily furnish sufficient energy to break the C-C or C-O bonds. Forces from ultrasonic waves could be set up simply as friction between a polymer molecule and the surrounding liquid. In the case of polystyrene in toluene only 5 bonds in 1000 were broken at 70°C.

The structure of coal is, at best, very complex and the bonding forces are not well defined at present. There are, however, some general facts concerning the products of coal extraction, pyrolysis and hydrogenation which can be of great assistance in determining the types and magnitude of some of the important bonding forces in coal. Coal pyrolysis and coal

dissolution (solvent extraction) have been visualized by Wiser as similar processes, with similar reaction kinetics (second order) and activation enthalpies (35.6 kcal/mole and 28.8 kcal/mole respectively)¹⁷. The products resulting from coal pyrolysis and dissolution are high in aromatics, exhibiting even higher aromaticity than the original coal. From this and other work on the structure of coal the strongest bonds in the "coal macromolecule" appear to be aromatic carbon-carbon bonds. Aliphatic C-C bonds, C-O, C-H, and C-S bonding are also present and important in the coal structure¹⁸. Weaker forces such as van der Waals forces and hydrogen bonding would naturally be expected since coal can be considered as a polymer and other polymers containing C, H, S, N and O are at least partially held together by such bonding forces^{19,20}. Pimental and McClellan²⁰ give values of hydrogen bond strengths of 3.0 to 7.7 kcal/mole.

The results of any kinetic study on a complex substance such as coal will indicate only average values of the activation enthalpies and entropies involved in the process being studied.

Since the value of "a", the maximum part of the coal extractable, varies systematically with temperature it appears that at any particular temperature the quantity (a-x) represents a potential in the form of a concentration. The rate at any particular time, t, depends only upon this concentration. As "x" approaches "a" the rate approaches zero. The value of "a" is much smaller when ultrasonic energy is not used in the extraction. From this study and others the effect of this energy appears to be the actual breaking of bonds in the coal structure which cannot be broken by the solvent. The breaking of these bonds then results in fragments from the coal which are soluble in the solvent liquid. Another possible effect of the ultrasonic energy is the transfer of kinetic energy

to the coal structure in such a way that would be the same as raising the "effective" temperature of the coal to some value much higher than the temperature measured by a thermometer or thermocouple in the solvent. According to Dognon and Simonot^{21,22} the temperature of dispersed particles in an ultrasonic field is raised several degrees above the average temperature of the solution or suspension. The cavitation taking place in liquids subjected to ultrasonic waves (formation and violent collapse of small bubbles in the liquid due to pressure changes) has been credited with practically all observed chemical effects in liquid systems⁹. The violent collapse of cavitation bubbles may generate local pressures of thousands of atmospheres and/or local temperatures of hundreds of degrees above that of the environment²³. The intensity of ultrasonic energy used in this study was several times that required to produce cavitation.

The results of this study may be interpreted in two different ways based on the above information:

(1) The extraction of coal with ultrasonic energy results in the dissolving of species present in the pores of the coal structure. Extraction also takes place by breaking van der Waals and hydrogen bonds in the coal structure. The extraction yield is higher with ultrasonic energy because these weak bonding forces are severed by the energy of the ultrasonic waves. The rate controlling step in the second order portion of the reaction is the reaction between the solvent molecules and the available van der Waals or hydrogen bonds in the coal. The activation enthalpy for this second order reaction is 8.7 kcal/mole. The second order dependence is most likely due to a rate controlling step involving both a solvent molecule and a van der Waals or hydrogen bond. When most of the extraction has taken place the slow step becomes solution diffusion

either of solvent molecules to the soluble species in the coal matrix or of dissolved extraction products from the coal into the bulk solution. This part of the reaction is first order and has an activation enthalpy of 2.5 kcal/mole.

(2) Assuming that the ultrasonic effect to the coal-tetralin system is to raise the "effective temperature" of the reacting species to some higher value leads to some very interesting conclusions. To obtain the "effective temperature" (T_e) corresponding to the measured temperatures of 47°, 57°, 67°, 77° and 87°C used in this study is not difficult if "a" values at these temperatures is used to obtain the temperature necessary for the same yield in a coal-tetralin system without ultrasonic energy. In previous work by Charlot²⁴ tetralin was used to extract Spring Canyon coal without ultrasonic energy. T_e values corresponding to 47, 57, 67, 77 and 87°C are found to be 258°, 261°, 263°, 267° and 269°C. Values of the activation enthalpies for the second order and first order portions of the reaction became 31.5 and 9.1 kcal/mole respectively. With these values the second order portion of the reaction would undoubtedly involve the same type of bond rupture that occurs with pyrolysis and dissolution as previously referred¹⁷. The first order portion of the reaction would then appear to be controlled by either the breaking of van der Waals and/or hydrogen bonds or possibly solution diffusion.

CONCLUSIONS

Kinetic data of solvent extraction with tetralin and ultrasonic energy over the temperature range 47-87°C have been obtained. The kinetic data indicate that the rate determining step for most of the process is a second order reaction probably involving tetralin molecules and van der Waals or hydrogen bonds in the coal. The activation enthalpy for this

second order reaction is 8.7 kcal/mole with an activation entropy of -44 e.u. The second order reaction is followed by a first order reaction with an activation enthalpy of 2.5 kcal/mole and entropy of -70 e.u. The rate controlling step for the first order portion of the reaction is probably solution diffusion. The high negative values for the activation entropies obtained are not surprising since similar results have been obtained by others working with complex reactants such as coal, coal tar, petroleum, and some pure aromatic compounds^{25,26}. Such values are usually obtained when the number of reaction sites changes with the amount of reaction as would be the case for extraction²⁷.

No exact mechanism for the reactions taking place can be concluded. The interaction of the ultrasonic energy, tetralin, coal and environment cannot be completely understood until much more is known about such phenomena as the exact effects of ultrasonic waves upon organic solvents and suspended solids and extraction of coal; in particular how each type of bonding in coal is affected by the solvent molecules.

This work was supported by the Office of Coal Research, U. S. Department of Interior and by the University of Utah (Contract # 14-01-0001-271).

REFERENCES

1. De Marsilly, C., "Solvent Extraction of Coal," *Ann. Chem. et. Phys.*, 3, 66 (1862).
2. Dryden, I. G. C., "Behaviour of Bituminous Coal Towards Solvents," I-II, *Fuel* 29, 197-221 (1950).
3. Berkowitz, N., "Dispersibility of Coal in Supersonic Field," *Nature*, 163, 809 (1949).
4. Littlewood, K., "The Application of Ultrasonic Irradiation to Solid-Liquid Systems with Particular Reference to the Extraction of Coals with Pyridine," *Fuel Soc. J., Univ. Sheffield* 27-30 (1960).
5. Dryden, I. G. C., "Chemistry of Coal Utilization," Supplementary Volume, ed. by H. H. Lowry, John Wiley and Sons Inc., New York, N. Y., Chap. 6, 232 (1963).
6. Ching, V. C. C. et. al., "Kinetic Study of Coal Extraction by Tetralin With and Without Ultrasonic Irradiation," U. S. Dept. of Interior, Office of Coal Research Technical Report, June (1967).
7. Kirby, W. A., J. R. A. Lakey, and R. J. Sarjant, "A Study of Coal Extraction by Infrared Spectroscopy," *Fuel* 33, 480, (1954).
8. Brown, J. K. and S. M. Rybica, private communication (1960).
9. Weissler, A. E., "Ultrasound Chemical Effects on Pure Organic Liquids," *Science* 150, No. 3701, 1288-9 (1965).
10. Kessler, T., A. G. Sharkey Jr. and R. A. Friedel, "Reactions Produced by Exposing Coal Derivatives to Ultrasonic Energy," U. S. Bureau of Mines Report of Investigations 7027 (1967).
11. Anbar, M. and I. Pecht, *J. Phys. Chem.* 68, 1460-2, (1964).
12. Freundlich, H. and D. W. Gillings, *Trans. Faraday Soc.* 34, 649 (1938).
13. Prudhomme, R. O., and P. Grabar, *J. Chim. Phys.* 46, 667 (1949).
14. Schmid, G. and O. Rommel, *Z. Physik. Chem.*, 185A, 97 (1939).
15. Shibata, K., Repts. *Tokyo Imp. Ind. Research Inst. Lab.* 35, No. 31, 1 and 9 (1940).
16. Crawford, A. E., Ultrasonic Engineering, Butterworths, London (1955).
17. Wiser, W. H., "A Kinetic Comparison of Coal Pyrolysis and Coal Dissolution," Presented at SME Division, A.I.M.E., Minneapolis, Minn., Sept. (1968).

18. Hill, G. R. and L. B. Lyon, "A New Chemical Structure for Coal," *Ind. and Eng. Chem.* 54, 36 (1962).
19. Howsmon, J. A. and W. A. Sisson, High Polymers, Chap. 4B, Part I, 5, Interscience, New York (1954).
20. Pimentel, G. C. and A. L. McClellan, The Hydrogen Bond, Chap. 7, W. H. Freeman and Company, San Francisco (1960).
21. Dognon, A. and Y. Simonot, *Compt. Rend.*, 228, 230 (1949).
22. Dognon, A. and Y. Simonot, *Compt. Rend.*, 228, 990 (1949).
23. Lord Raleigh, *Phil. Mag.*, 34, 94 (1917).
24. Charlot, L. A., "The Kinetics of Thermal Dissolution of a Utah Bituminous Coal Using 1,2,3,4 Tetrahydronaphthalene," Thesis, University of Utah (1963).
25. Badawy, M. L. et. al, private communication (1969).
26. Wiser, W. H., S. Singh, S. A. Qader, and G. R. Hill, "Catalytic Hydrogenation of Multiring Aromatic Coal Tar Constituents," *Ind. and Eng. Chem., Process Des. and Dev.* 9, No. 2, April (1970).
27. Hill, G. R., "Experimental Energies and Entropies of Activation - Their Significance in Reaction Mechanism and Rate Prediction for Bituminous Coal Dissolution," *Fuel*, 45, 329 (1966).

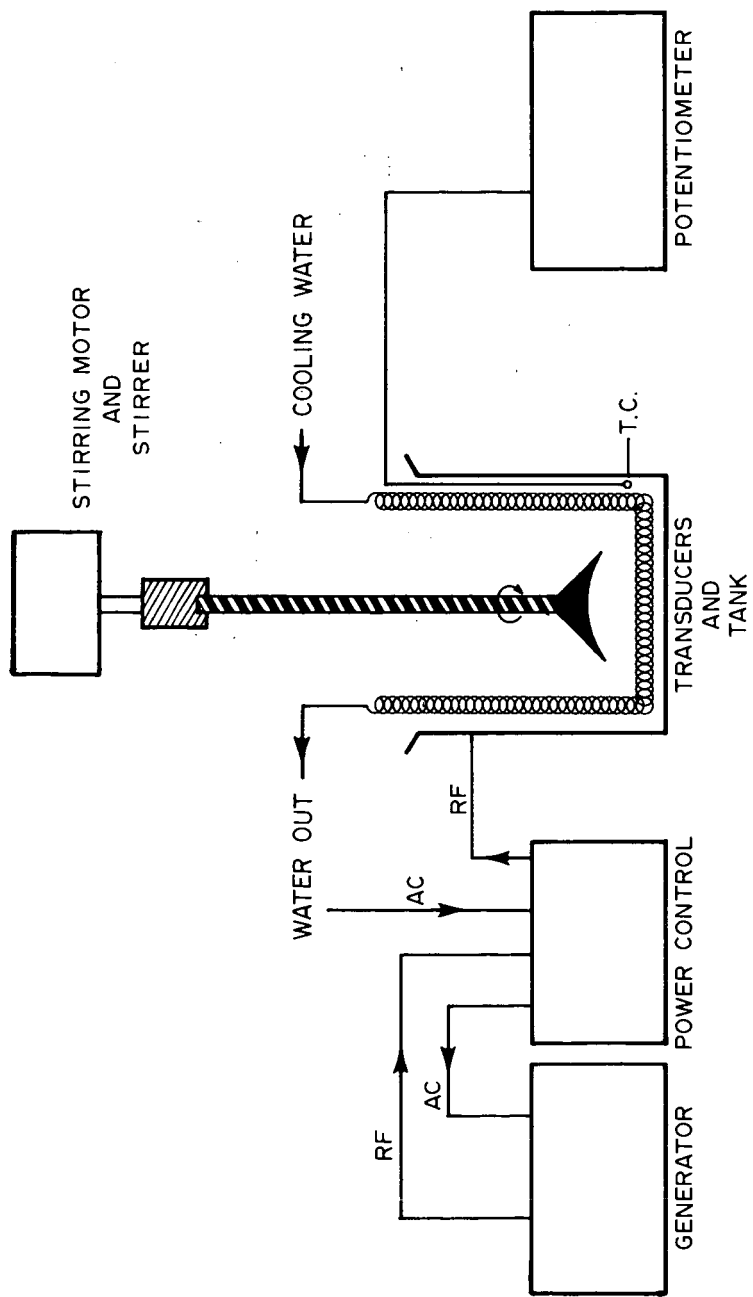


Figure 1. Schematic drawing of ultrasonic extraction apparatus.

Pure Tetralin

Column 8 ft. Carbowax

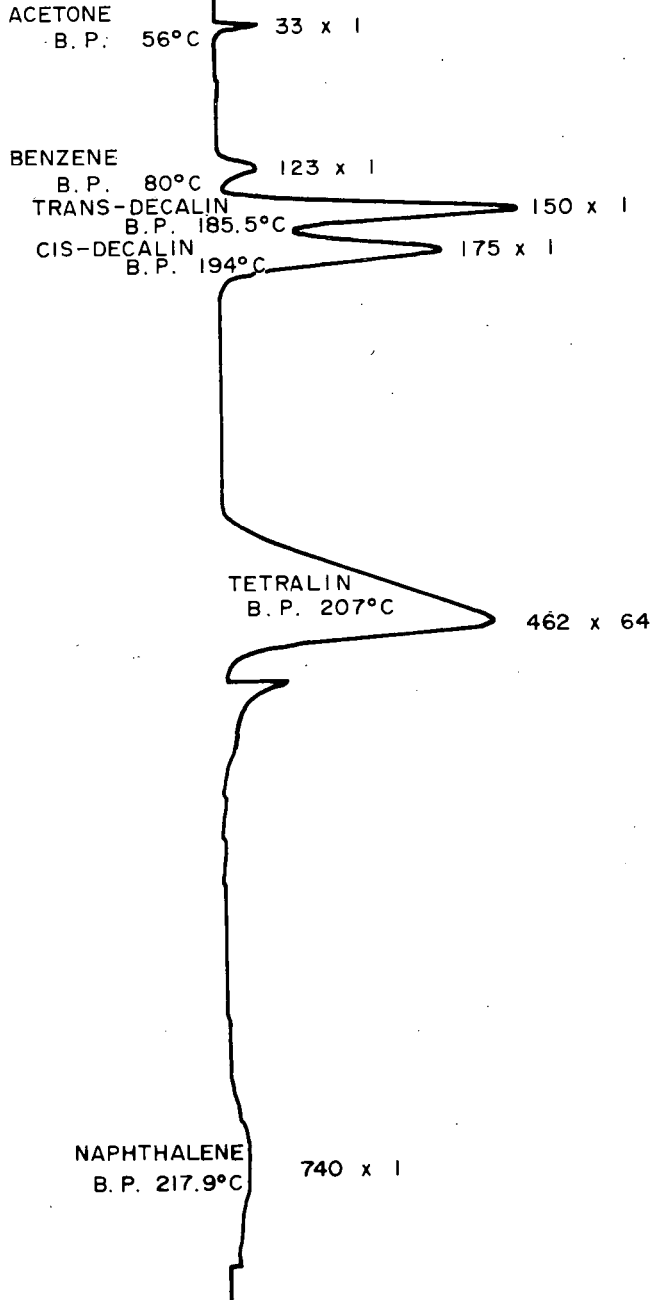


Figure 2. Chromatogram of Tetralin.

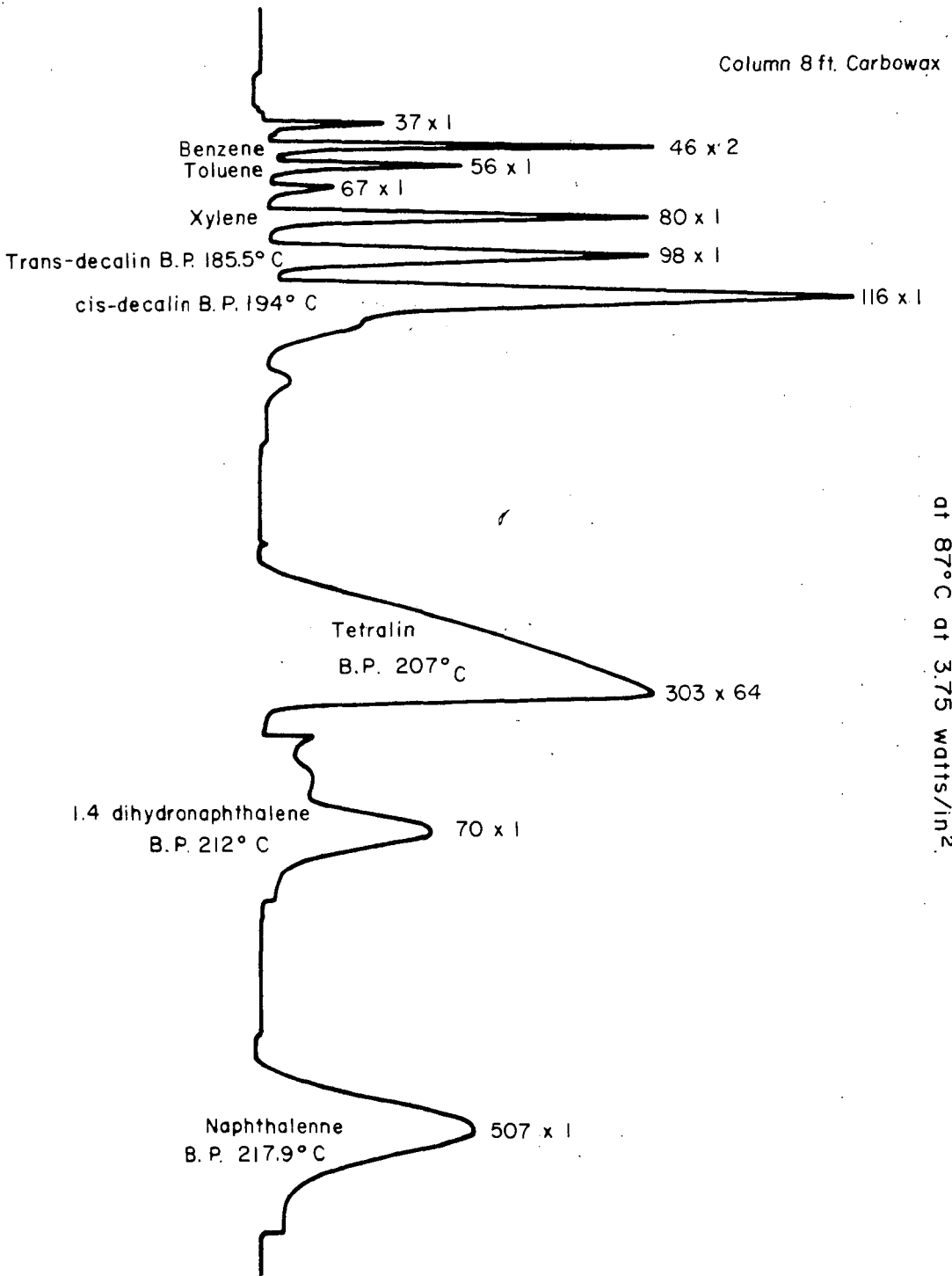


Fig. 3 Chromatogram of Tetralin Irradiated for 24 hours at 87° C at 3.75 watts/in².

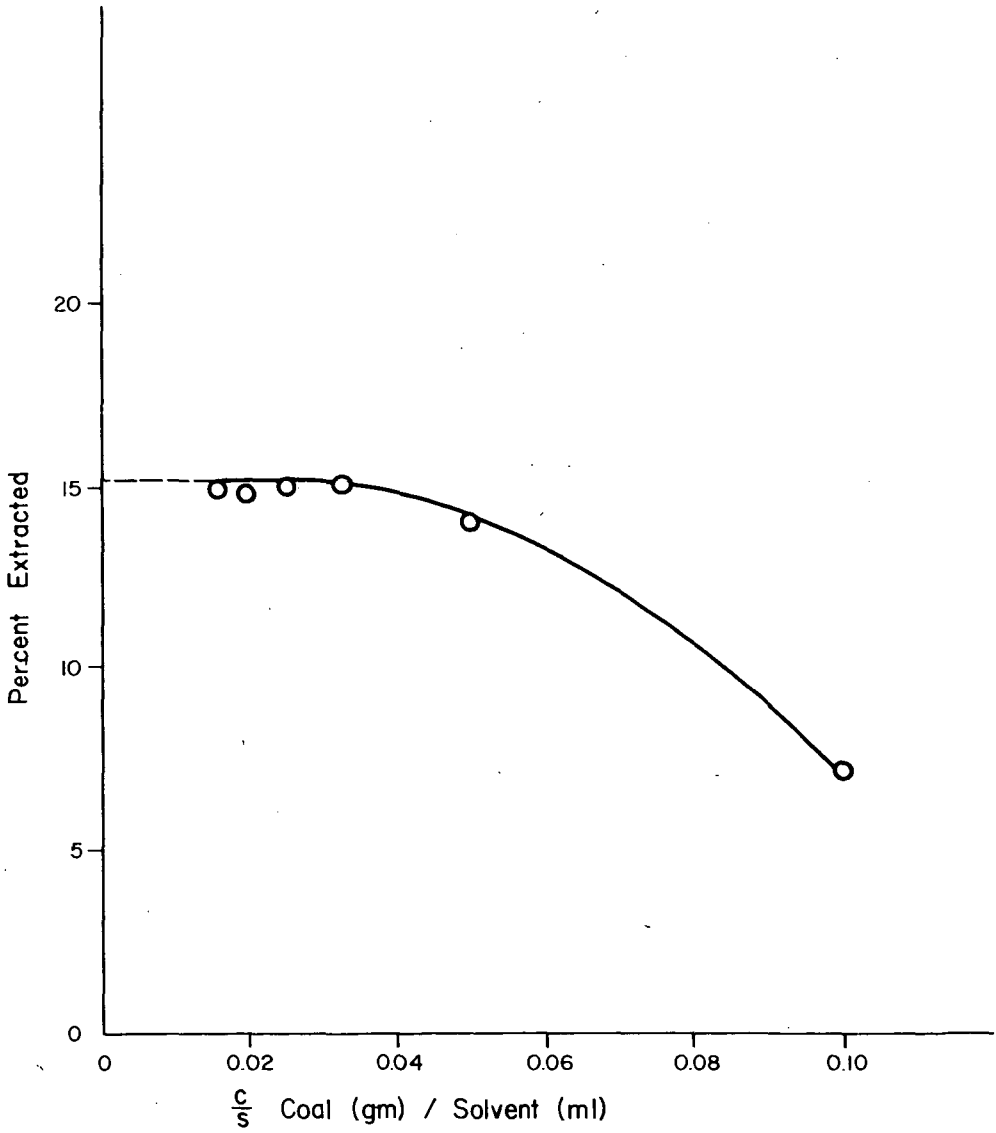


Fig. 4 Percent of extracted vs. $\frac{\text{coal}}{\text{solvent}}$ ratio
Temperature = 47°C; Time = 3 hours;
Coal size = -200 + 270 mesh
Solvent = tetralin

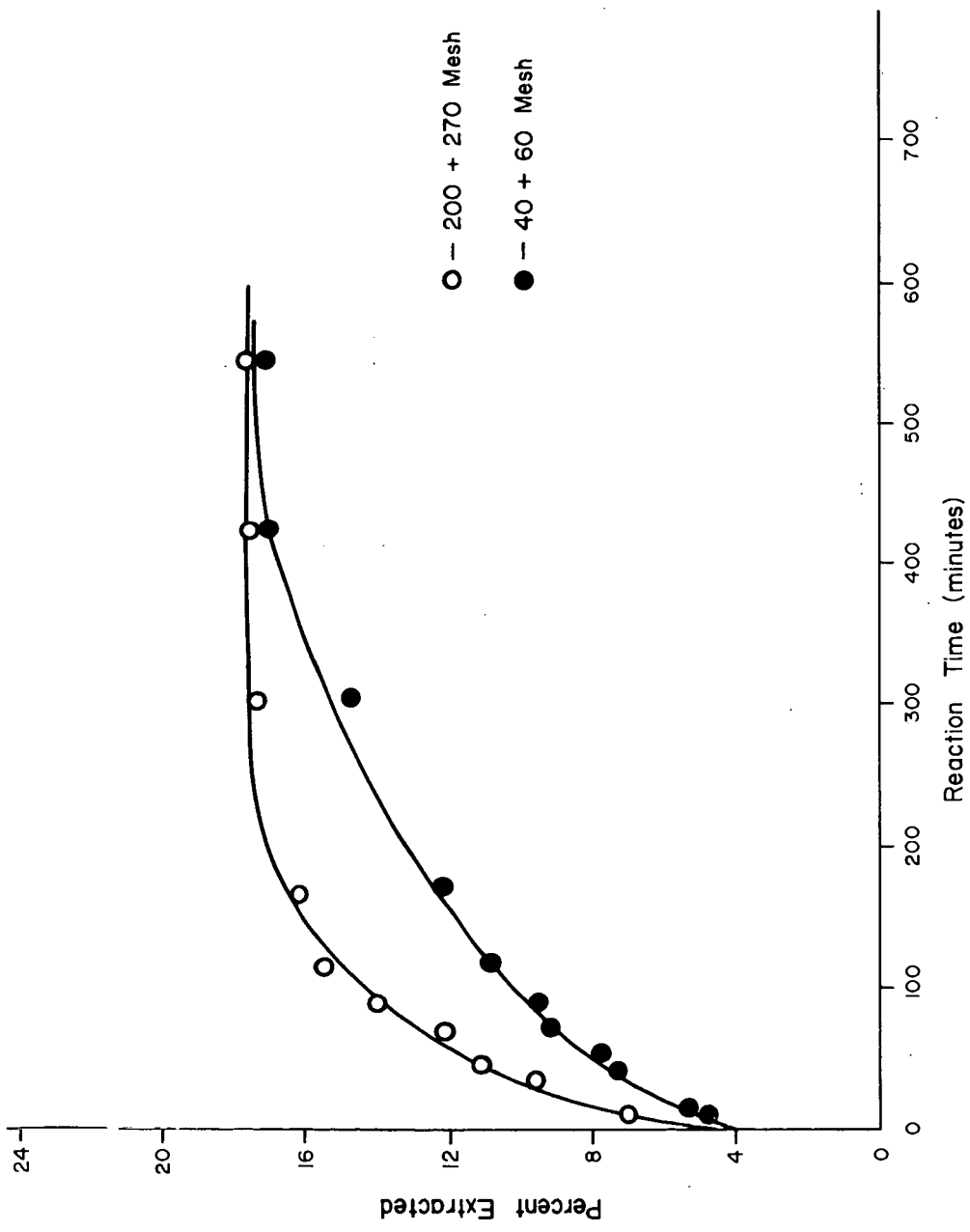


Fig. 5 - 40 + 60 and -200 + 270 mesh coals. Effect of coal particle size on ultrasonic extraction with tetralin.

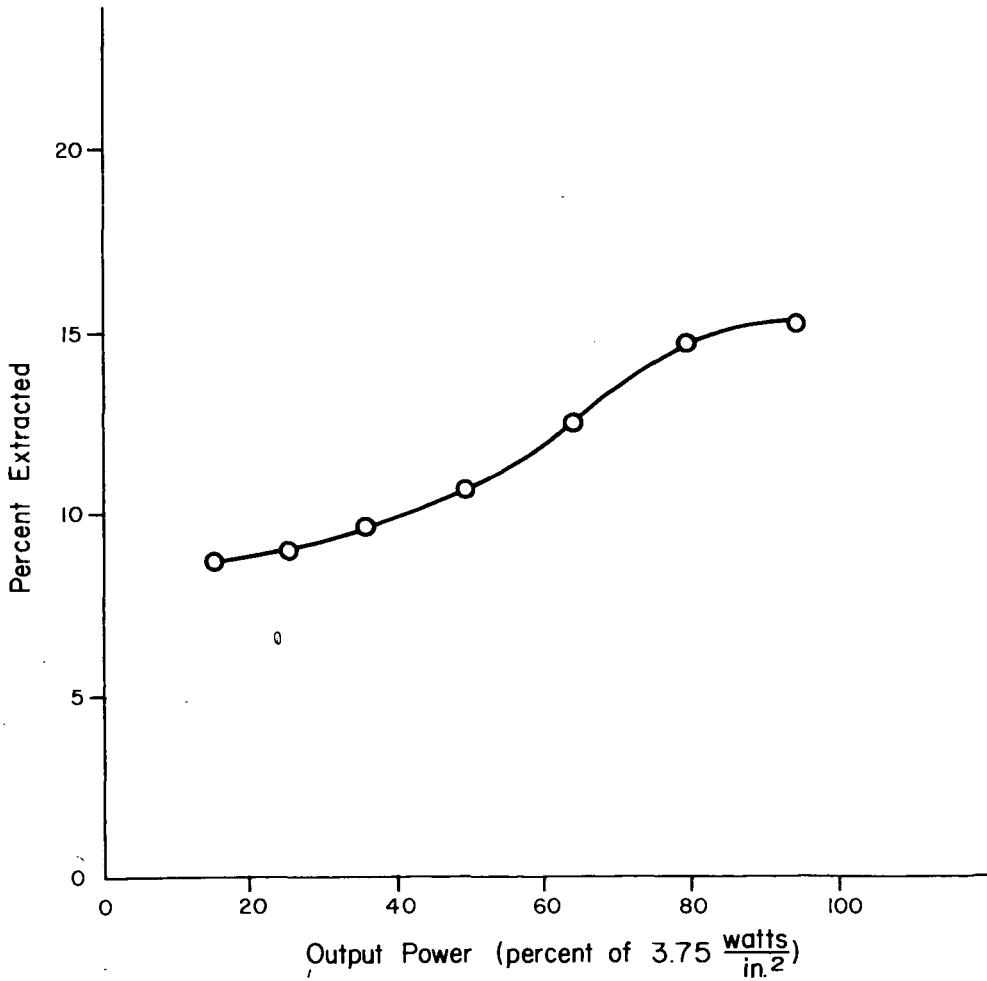


Fig. 6 Output vs. percent extracted at 47°C, and 3 hours reaction time in tetralin. Coal size = -200+270 mesh.

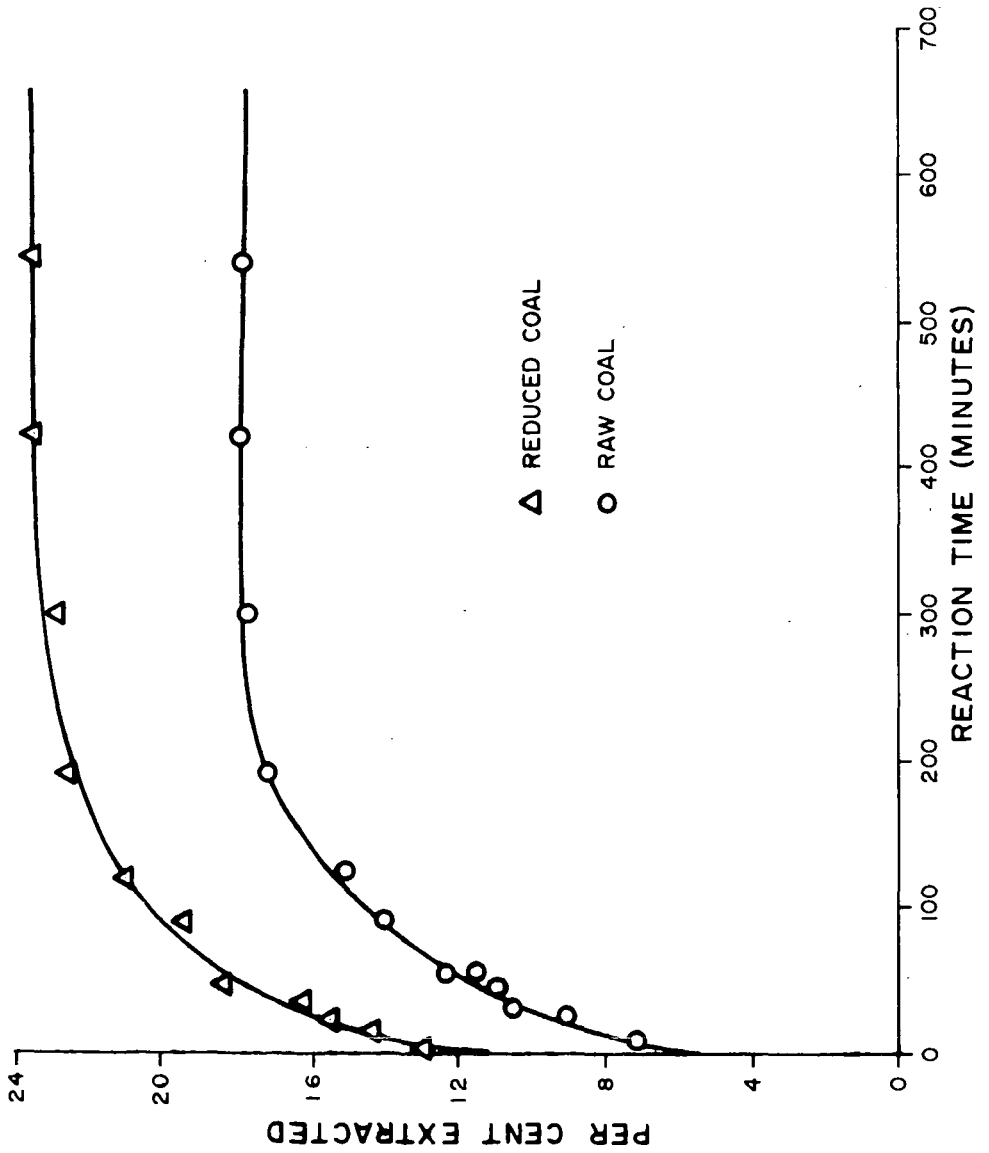


Fig. 7 Percent extracted versus time for raw and reduced coal.

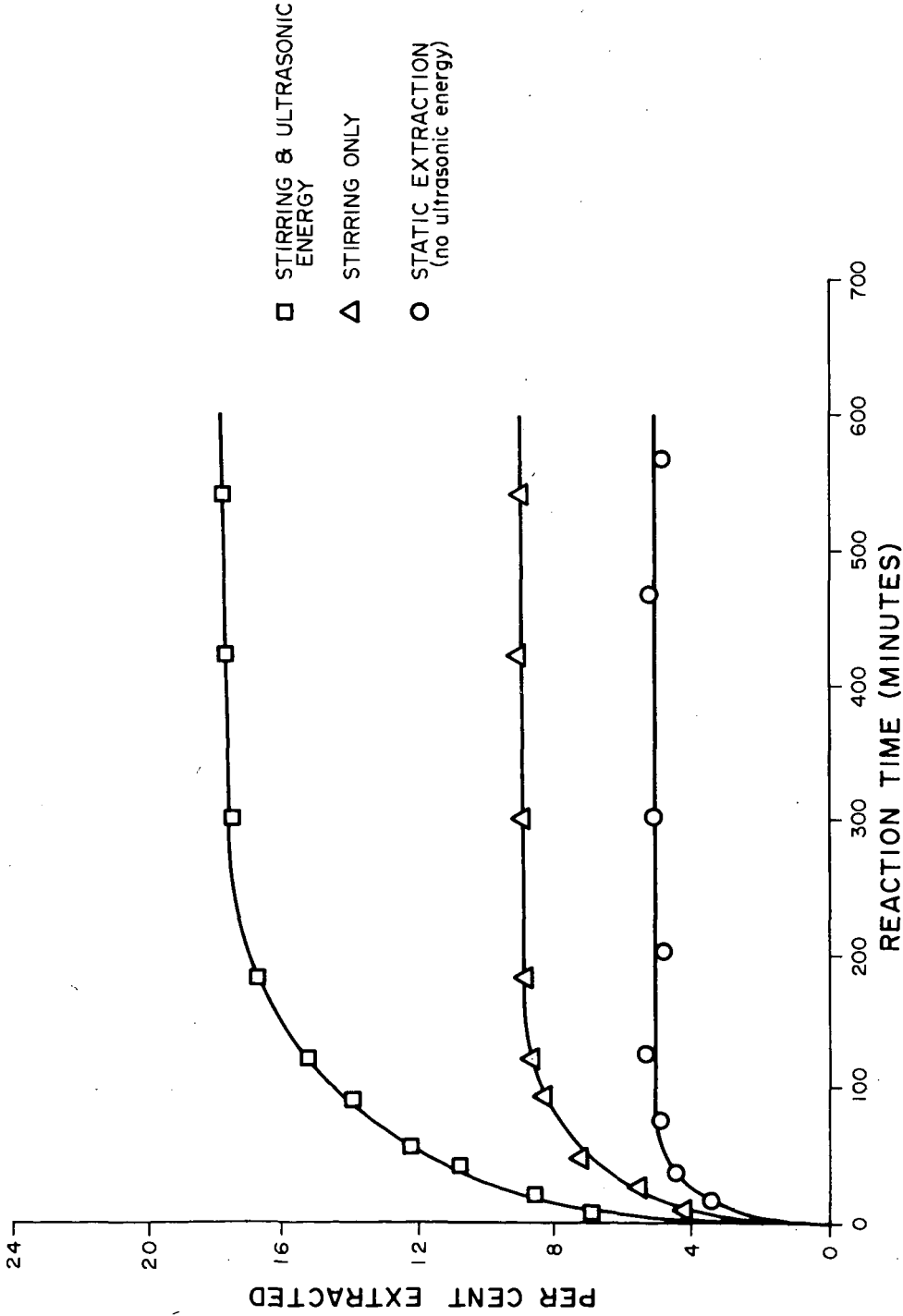


Figure 8. Percent extracted versus time at 47°C. Solvent = Tetralin, Power output = $\frac{3.75 \text{ watts}}{\text{in.}^2}$, Coal size = -200 + 270 mesh.

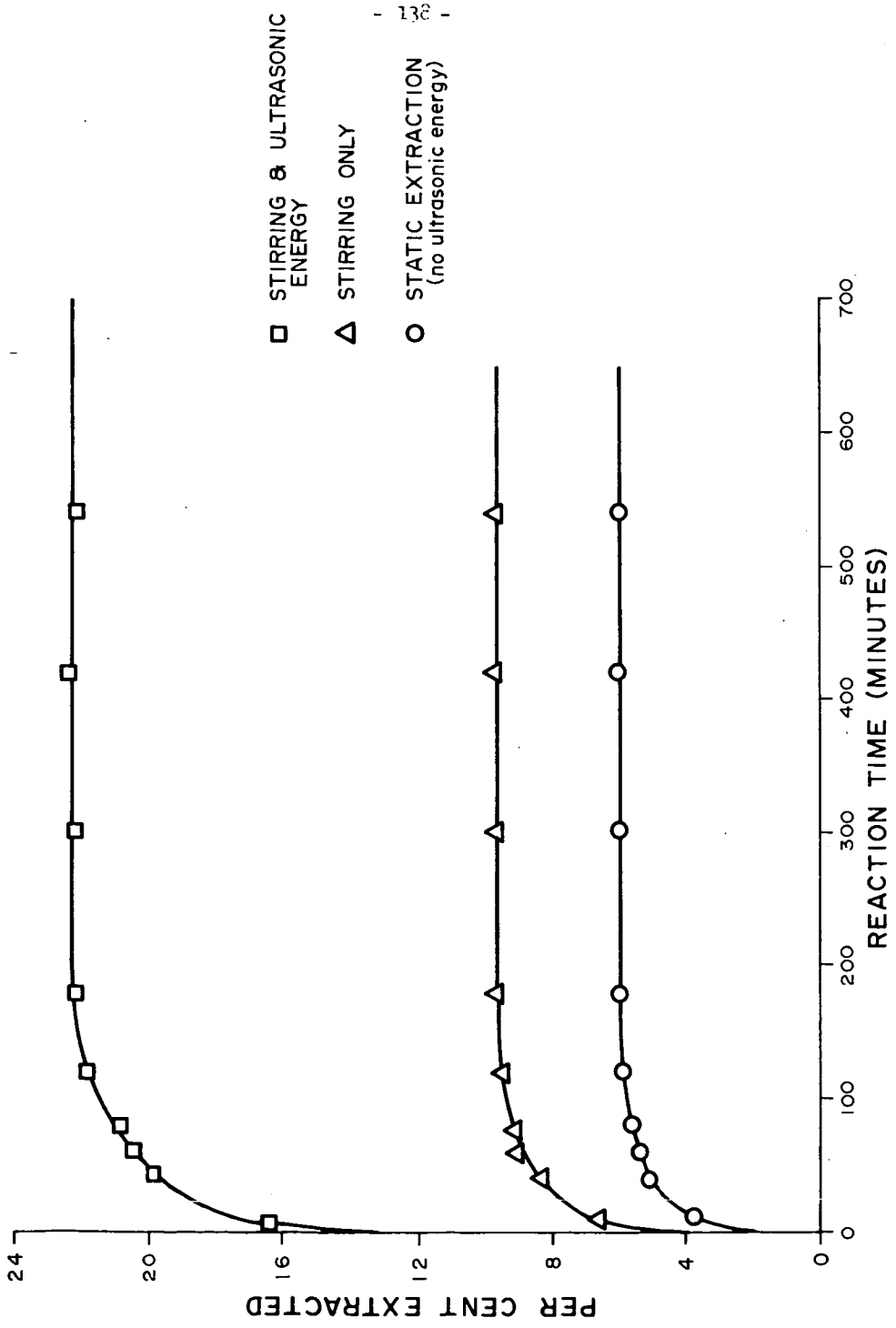


Figure 9. Percent extracted versus time at 87°C. Solvent = Tetralin, Power output = $\frac{3.75 \text{ watts}}{\text{inch}^2}$, Coal size = -200 + 270 mesh.

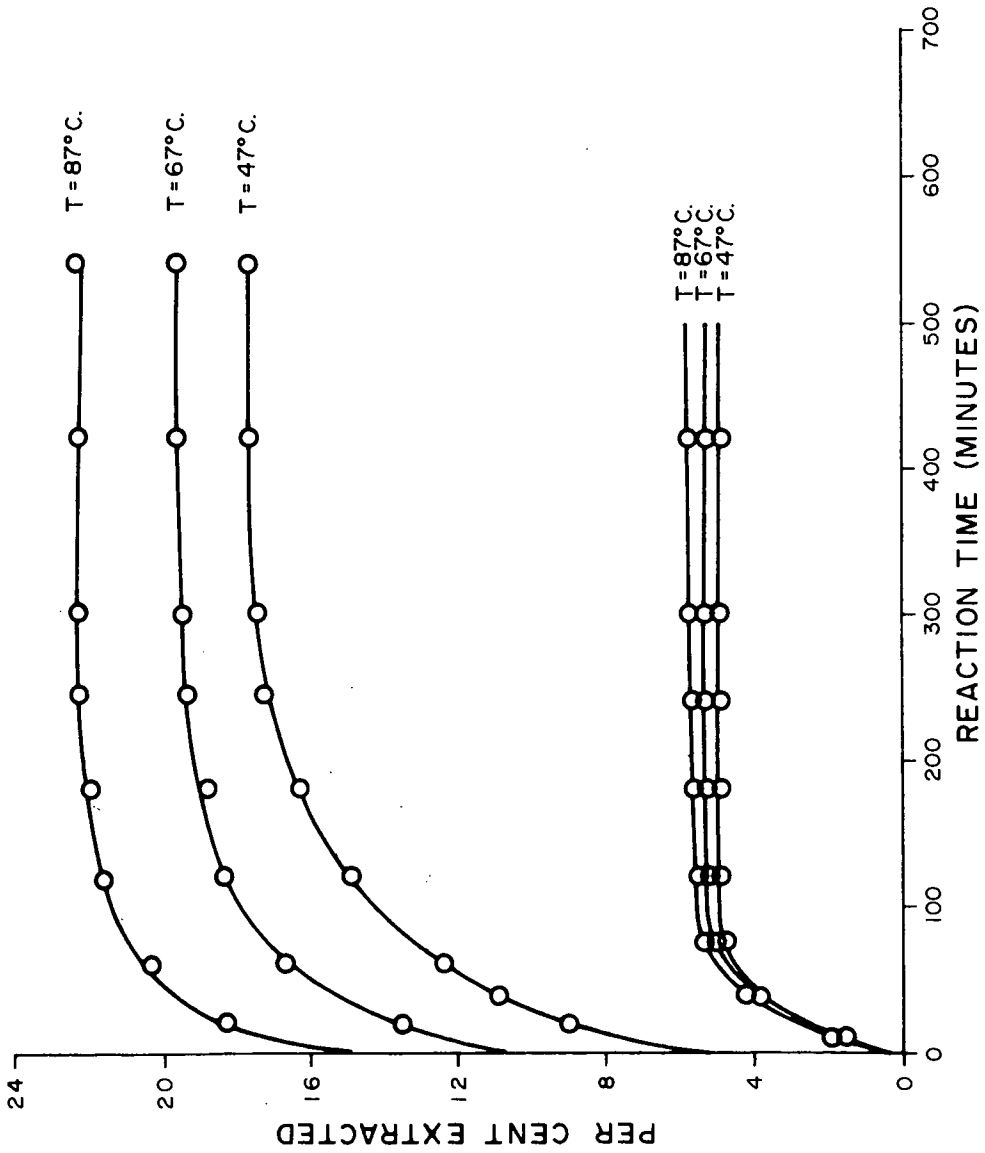


Figure 10. Kinetics of coal extraction with Tetralin.

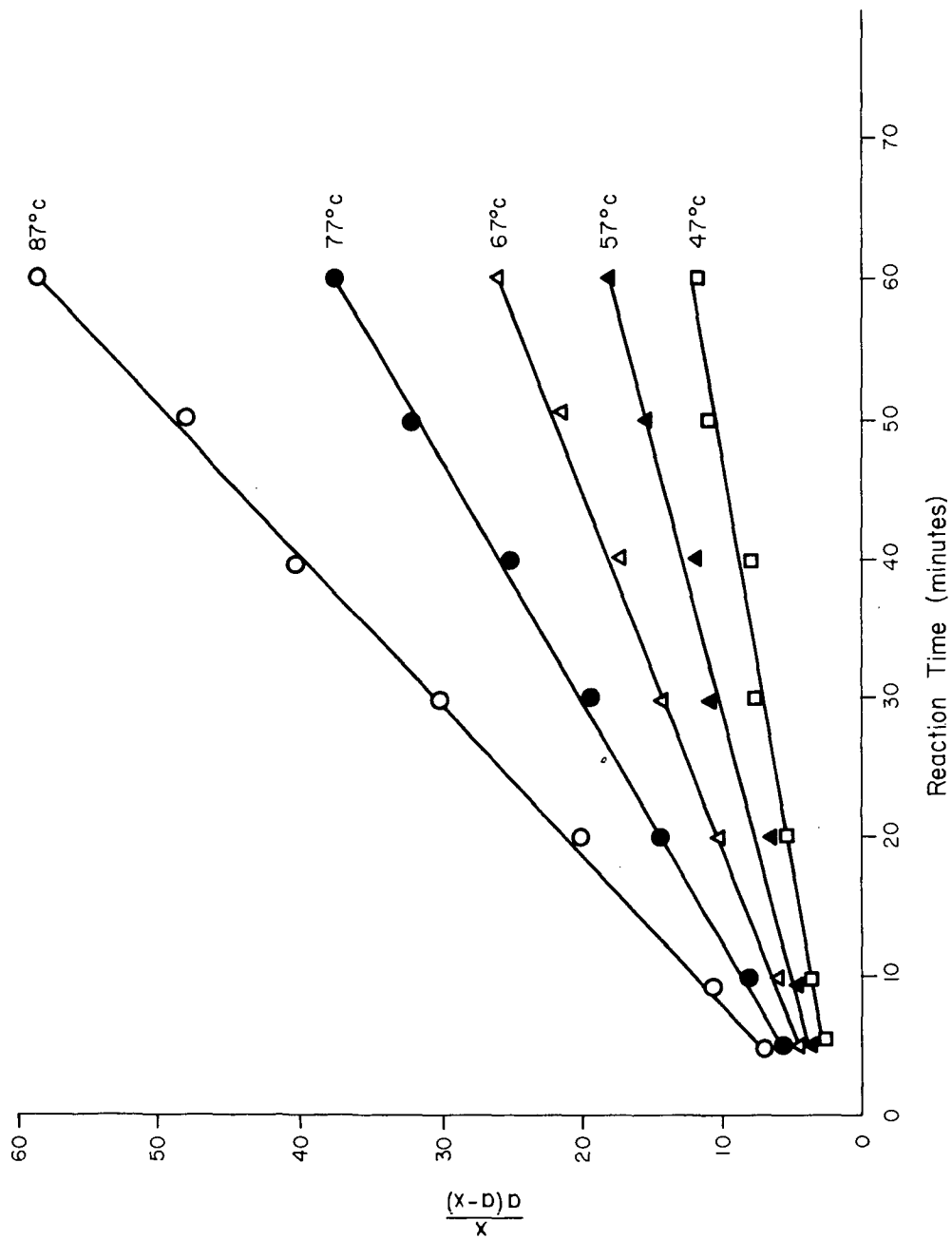


Fig. 11 Plot of $\frac{x}{a(a-x)}$ vs. time for second order reaction

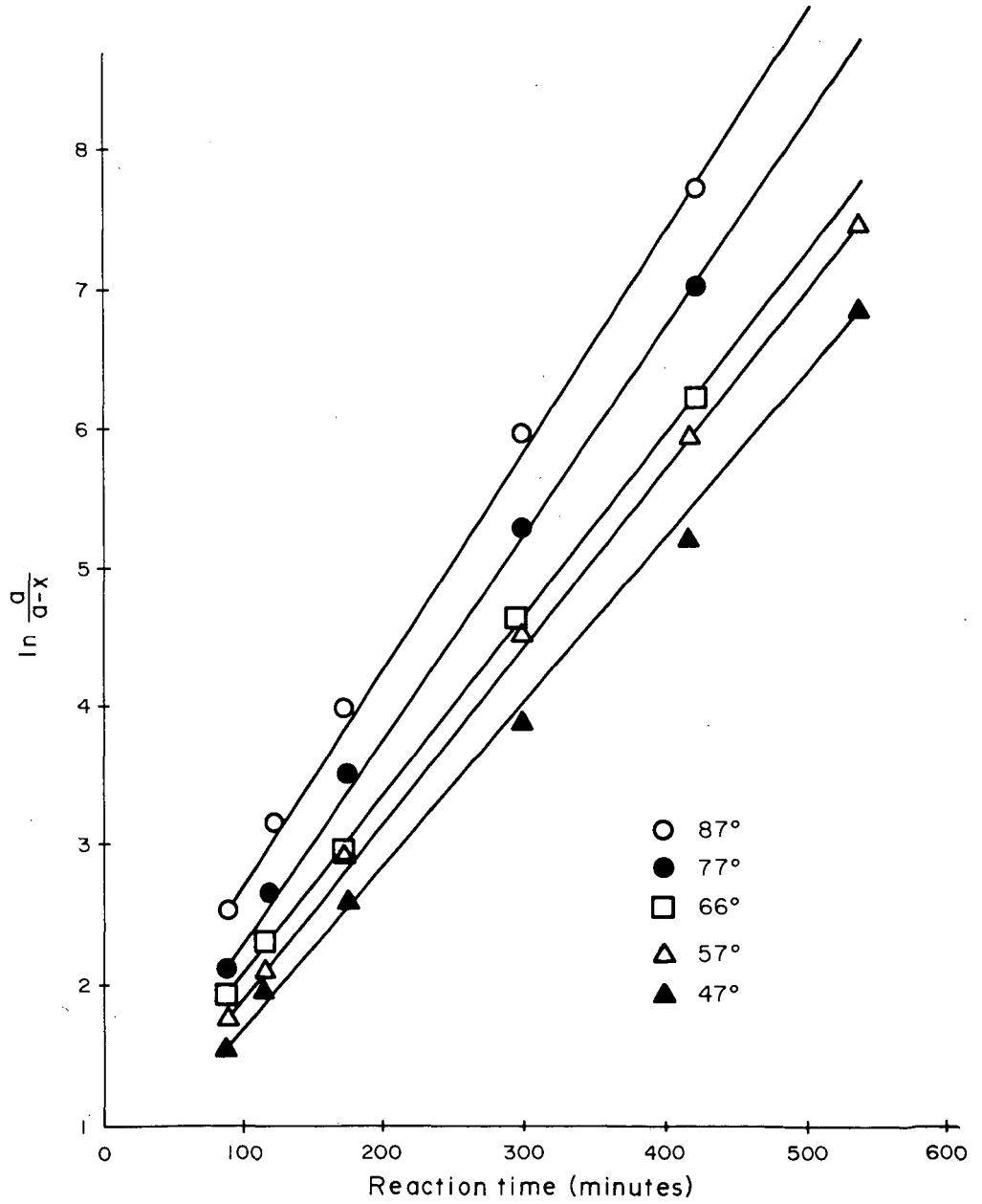


Fig.12 $\ln \frac{a}{a-x}$ versus time for first order reaction.

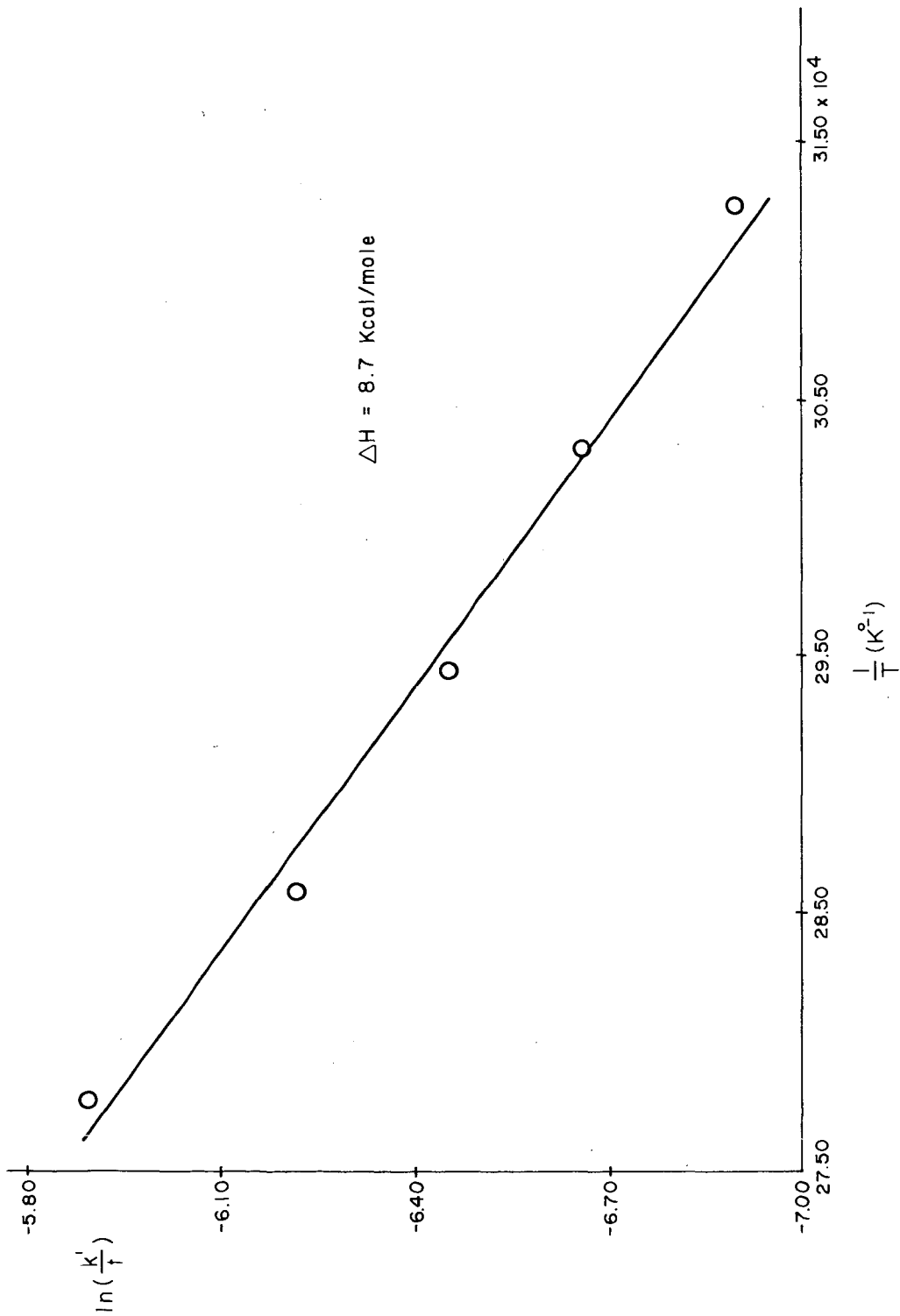


Fig. 13 $\ln \frac{k'}{T}$ versus $\frac{1}{T}$ for evaluation of the activation enthalpy and entropy for second order portion of reaction.

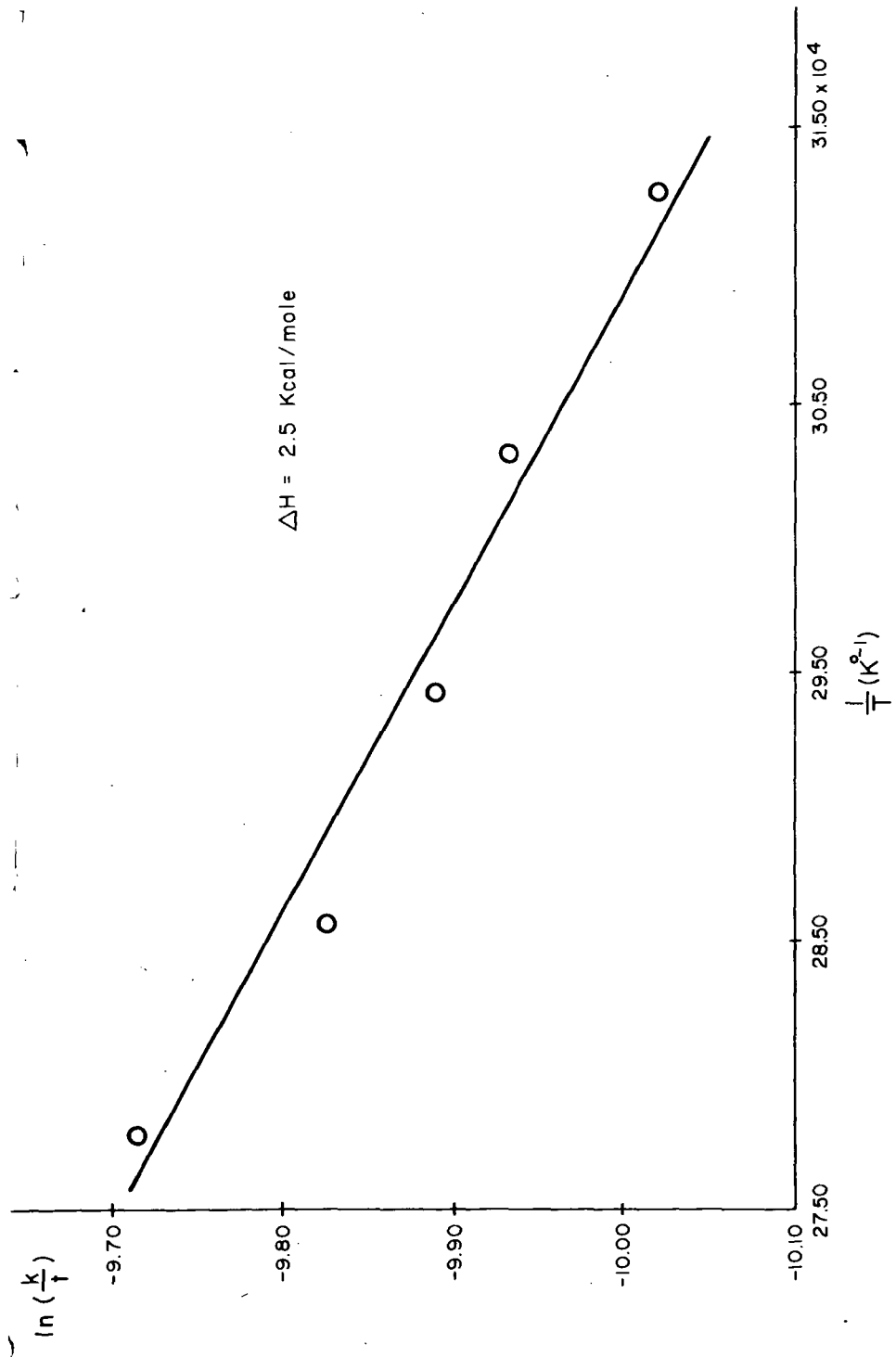


Fig. 14 $\ln \frac{k}{T}$ versus $\frac{1}{T}$ for evaluation of the activation enthalpy and entropy
(first order reaction)